

TYPE-2 FUZZY CLUSTERING FOR FUZZY MODELING APPLICATIONS

by

Ayşe Çisel Aras

B.S., Electrical Engineering, Yıldız Technical University, 2005

M.S., Electrical-Electronics Engineering, Boğaziçi University, 2008

Submitted to the Institute for Graduate Studies in
Science and Engineering in partial fulfillment of
the requirements for the degree of
Doctor of Philosophy

Graduate Program in Electrical-Electronics Engineering
Boğaziçi University

2014

TYPE-2 FUZZY CLUSTERING FOR FUZZY MODELING APPLICATIONS

APPROVED BY:

Prof. Okyay Kaynak
(Thesis Supervisor)

Assoc. Prof. Mehmet Akar

Prof. Kemal Ciliz

Prof. Fikret Gürgen

Prof. Hakan Temeltaş

DATE OF APPROVAL: 09.06.2014

ACKNOWLEDGEMENTS

I would like to express my deep and sincere gratitude to my thesis supervisor, Prof. Okyay Kaynak, for his invaluable guidance and help during this thesis. I owe him immense gratitude for having me shown this research area. His wide knowledge, practical solutions to problems, strong intuition and experience have provided a good basis for this thesis and have been of great value for me. In addition, he was always accessible and ready to help. This thesis would be impossible without him.

I would like to express my sincere gratitude to the thesis committee members Prof. Kemal Cılız and Prof. Fikret Gürgen. I deeply appreciate their patience and insightful comments on this thesis. Their direction and suggestions are very precious in the progress of this thesis. I would like to thank to my jury members Assoc. Prof. Mehmet Akar and Prof. Hakan Temeltaş for their invaluable comments. I would like to thank to Prof. Rahib Abiyev for his valuable guidance and helpful suggestions. I would like to give special thanks to Can Kurtuluş, Serkan İmram and Umut Genç of AVL Turkey for their encouragement and understanding in the process of writing my dissertation.

I consider myself very lucky to have made great friends during my years at Bogaziçi University. I would like to express my sincere thanks to my numerous friends; Yeşim Öviz, İpek Şen, Erinç Dikici, Yasin Çitkaya, Doğaç Başaran, Artun Oyman, Mehmet Yamaç, Can Altay, and Hakan Karaoğuz who endured this long process with me. They have been always helpful and supportive in the progress of this work. Their friendship is invaluable for me. I would like to give my special thanks to Leyla Çeken and Aynur İşler for their valuable and warm support.

Last but not least, I would like to express my sincere thanks to my family for their love and invaluable support. I deeply appreciate their patience and emotional support during this painstaking process. They encouraged me and took care of me while I was writing and working on this thesis.

This thesis has been supported by Bogazici University Scientific Research Project
Grant No: D 6511.

ABSTRACT

TYPE-2 FUZZY CLUSTERING FOR FUZZY MODELING APPLICATIONS

In this study, a novel approach is described to the design of an interval type-2 fuzzy neural system (IT2 FNS). It differs from the classical IT2 FNS in its use of parameterized conjunctors. In the optimization of the IT2 FNS, the membership functions are kept fixed and only the parameters of the conjunctors and the parameters in the consequent are tuned. In this study, the gradient based learning algorithm is used. The approach is tested for the modeling of a benchmark nonlinear function and for the wheel slip control of a quarter car model (QCM). In the stated applications, in the absence of any expert knowledge, some knowledge about the system is gained by the use of the interval type-2 fuzzy c-means (IT2 FCM) clustering algorithm. However, this requires the number of classes to be known beforehand. To alleviate this problem, some validity indices that have been suggested in the literature and a novel validity index that carries less computational burden are considered to determine the number of classes and the number of fuzzy rules. Another contribution to the existing literature is that in the design of an IT2 FNS, recursive FCM clustering algorithm is used and the designed algorithm is applied in control applications. The center and the standard deviation values of the interval type-2 Gaussian membership functions at the antecedent part of the Takagi-Sugeno-Kang type fuzzy rules are determined by the use of the recursive FCM clustering algorithm. The parameters at the consequent parts are tuned based on the gradient descent approach. The effectiveness of the designed algorithm is tested by simulation studies on a 2-DOF helicopter system and by experimental studies on a real-time servo system. The performance of the proposed method is compared with a traditional neuro-fuzzy structure adopted from the literature. In addition, IT2 FNS with recursive fuzzy c-means clustering is used with elliptical membership functions.

ÖZET

BULANIK MODELLEME UYGULAMALARI İÇİN TİP-2 BULANIK KÜMELEME

Bu çalışmanın özgün değerlerinden bir tanesi aralık değerli tip-2 nöro-bulanık sistemlerinin tasarımında parametrelili t-normlar kullanılmasıdır. Aralık değerli tip-2 nöro-bulanık sistemlerinin optimizasyonunda öncül kısımdaki üyelik fonksiyonlarının parametreleri sabit tutulmuş ve parametrelili t-normların parametreleri ile bulanık kural- ların soncul kısmındaki parametreler adapte edilmiştir. Bu çalışmada gradyan tabanlı öğrenme algoritması kullanılmıştır. Önerilen yaklaşım doğrusal olmayan fonksiyon modellenmesi ve çeyrek araç modelinin kayma değeri kontrolünde kullanılmıştır. Uz- man bilgisinin eksik olduğu bu uygulamalarda sistem hakkındaki bilgi aralık değerli tip-2 bulanık c-ortalamlar kümeleme algoritması ile elde edilmiştir. Bu kümeleme al- goritmasında küme sayısı önceden verilmelidir; fakat, küme sayıları her zaman önceden bilinemez. Bu sorunu gidermek için literatürde bilinen ve ayrıca bu çalışmada önerilen doğruluk indeksleri nöro-bulanık sistemlerin kural sayısını belirlemede kullanılmıştır. Bu çalışmanın diğer bir özgün değeri ise, aralık değerli tip-2 nöro-bulanık sistemler, tekrarlamalı bulanık c-ortalamlar kümeleme algoritması ile birlikte kontrol uygula- malarında kullanılmasıdır. Takagi-Sugeno-Kang (TSK) kural yapısının öncül kısmında bulunan Gauss üyelik fonksiyonlarının merkez ve standart sapma değerleri tekrarla- malı bulanık c-ortalamlar kümeleme algoritması ile, soncul kısmındaki polinom kat- sayıları ise gradyan tabanlı öğrenme algoritması ile bulunmuştur. Önerilen yaklaşım simülasyon tabanlı olarak iki serbestlik dereceli helikopter ve gerçek zamanlı olarak servo sistemine uygulanmış ve geleneksel nöro-bulanık sistem ile karşılaştırılmıştır. Ayrıca önerilen yaklaşım eliptik üyelik fonksiyonları ile de kullanılmış ve iki serbestlik dereceli helikopter üzerinde simülasyon tabanlı olarak test edilmiştir.

TABLE OF CONTENTS

ACKNOWLEDGEMENTS	iii
ABSTRACT	v
ÖZET	vi
LIST OF FIGURES	x
LIST OF TABLES	xvi
LIST OF SYMBOLS	xviii
LIST OF ACRONYMS/ABBREVIATIONS	xx
1. INTRODUCTION	1
1.1. The Aim of This Study	6
1.2. The Organization of the Thesis	7
2. TYPE-2 FUZZY LOGIC SYSTEMS	9
2.1. The Structure of the Type-2 Fuzzy Logic Systems	12
2.1.1. Fuzzification	13
2.1.2. Fuzzy Inference System and Rule Base	14
2.1.3. Type-Reduction	15
2.1.4. Defuzzification	15
2.2. Interval Type-2 Takagi-Sugeno-Kang Fuzzy Logic Systems (IT2 TSK FLSs)	16
2.2.1. Model 1	16
2.2.2. Model 2	16
2.2.3. Model 3	17
3. FUZZY CLUSTERING ALGORITHMS	18
3.1. Fuzzy C-Means (FCM) Clustering Algorithm	18
3.2. Interval Type-2 Fuzzy C-Means (IT2 FCM) Clustering Algorithm	19
4. FUZZY MODELING WITH PARAMETERIZED CONJUNCTORS	23
4.1. Type-1 Fuzzy Modeling with Parameterized Conjunctors	23
4.2. Interval Type-2 Takagi-Sugeno-Kang (IT2 TSK) Model with Parame- terized Conjunctors	25
4.3. Modeling Application	26

4.3.1.	Nonlinear Function Approximation by Using Parameterized Con- junctors	28
4.3.2.	Nonlinear Function Approximation by Using Interval Type-2 TSK Fuzzy Logic Systems with Parameterized Conjunctors . . .	30
4.3.3.	Modeling Application with Noisy Measurement	32
4.4.	Conclusion	34
5.	VALIDITY INDICES	37
5.1.	Partition Coefficient (PC)	38
5.2.	Partition Entropy (PE)	38
5.3.	Xie and Beni (XB) Validity Index	39
5.4.	Fukuyama Sugeno (FS) Validity Index	39
5.5.	PBM Validity Index	39
5.6.	Proposed Validity Index	40
5.7.	Clustering Application	41
6.	INTERVAL TYPE-2 FUZZY NEURAL SYSTEM WITH PARAMETERIZED CONJUNCTORS	44
6.1.	The Training of the Interval Type-2 FNS with Parameterized Conjunctors	46
6.2.	Modeling and Control Applications	49
6.2.1.	Modeling of a Nonlinear System	50
6.2.2.	Control Application	54
6.2.3.	The Simulation Results	56
6.3.	Conclusion	59
7.	RECURSIVE INTERVAL TYPE-2 FUZZY NEURAL SYSTEM	63
7.1.	Parameter Learning	66
7.2.	Description of the 2-DOF Helicopter System	68
7.2.1.	Simulation Studies	70
7.3.	Description of the Servo System	74
7.3.1.	Experimental Studies	77
7.4.	Conclusion	78
7.5.	Recursive Interval Type-2 Neuro Fuzzy System with Elliptical Member- ship Functions	83

7.5.1. Parameter Learning	86
7.5.2. Simulation Results	90
7.5.3. Conclusion	93
8. CONCLUSION	95
APPENDIX A: LABORATORY SETUP: SERVO SYSTEM	97
APPENDIX B: PUBLICATIONS RELATED TO THE THESIS	100
REFERENCES	102

LIST OF FIGURES

Figure 2.1.	A type-1 Gaussian membership function.	10
Figure 2.2.	An interval type-2 Gaussian membership function with uncertain standard deviation whose secondary membership grade is zero. . .	11
Figure 2.3.	An interval type-2 Gaussian membership function with uncertain standard deviation whose secondary membership grade is one. . .	11
Figure 2.4.	Block Diagram of Type-1 Fuzzy Logic Systems (T1 FLSs).	13
Figure 2.5.	Block Diagram of Type-2 Fuzzy Logic Systems (T2 FLSs).	13
Figure 4.1.	The Sinc function approximated.	27
Figure 4.2.	Rosenbrock's banana function approximated.	27
Figure 4.3.	The input membership functions obtained by using FCM algorithm in the modeling application of Sinc function without noise.	28
Figure 4.4.	The result of Sinc function approximation by using type-1 fuzzy algorithm (a) and the RMSE curve obtained by tuning the parameters of the parameterized conjunctive operators (b).	30
Figure 4.5.	The result of Rosenbrock's Banana function approximation by using type-1 fuzzy algorithm (a) and the RMSE curve obtained by tuning the parameters of the parameterized conjunctive operators (b).	30

Figure 4.6.	The input membership functions obtained by using IT2-FCM algorithm for Sinc function approximation without noise.	31
Figure 4.7.	The result of Sinc function approximation by using IT2 TSK fuzzy algorithm (a) and the RMSE curve obtained by tuning the parameters of the parameterized conjunctor operators (b).	32
Figure 4.8.	The result of Rosenbrock's Banana function approximation by using IT2 TSK fuzzy algorithm (a) and the RMSE curve obtained by tuning the parameters of the parameterized conjunctor operators (b).	32
Figure 4.9.	The Sinc function (30 dB noise added to the input signal).	33
Figure 4.10.	Rosenbrock's banana function (30 dB noise is added to the input signal).	33
Figure 4.11.	The result of Sinc function approximation by using type-1 fuzzy algorithm (a) and the RMSE curve obtained by tuning the parameters of the parameterized conjunctor operators (b).	34
Figure 4.12.	The result of Rosenbrock's Banana function approximation by using type-1 fuzzy algorithm (a) and the RMSE curve obtained by tuning the parameters of the parameterized conjunctor operators (b).	34
Figure 4.13.	The result of Sinc function approximation by using IT2 TSK fuzzy algorithm (a) and the RMSE curve obtained by tuning the parameters of the parameterized conjunctors (b).	35

Figure 4.14.	The result of Rosenbrock's Banana function approximation by using IT2 TSK fuzzy algorithm (a) and the RMSE curve obtained by tuning the parameters of the parameterized conjunctors (b). . . .	35
Figure 5.1.	Iris data set.	42
Figure 5.2.	Noisy Artificial data set.	43
Figure 6.1.	The structure of a Type-2 FNS.	45
Figure 6.2.	The flow-chart of the proposed approach.	50
Figure 6.3.	The knowledge obtained by the use of IT2 FCM clustering algorithm.	52
Figure 6.4.	The performance IT2 FNS with parameterized conjunctors.	53
Figure 6.5.	The RMSE value obtained.	53
Figure 6.6.	Schematic view of the Quarter Car Model (QCM).	55
Figure 6.7.	Road adhesion coefficient vs. wheel slip.	57
Figure 6.8.	The block diagram of the type-2 neuro-fuzzy system.	57
Figure 6.9.	Wheel slip of type-2 FNS with parameterized conjunctors.	59
Figure 6.10.	Velocity of the wheel and car without noisy input measurement.	59
Figure 6.11.	The noisy input measurement.	60
Figure 6.12.	Wheel slip of type-2 FNS with parameterized conjunctors with noise.	60

Figure 6.13.	Velocity of the wheel and car with noisy input measurement. . . .	61
Figure 7.1.	Symmetrical IT2 membership function-UMF is Gaussian and LMF is a scaled UMF.	64
Figure 7.2.	Simple free body diagram of 2-DOF helicopter [66].	70
Figure 7.3.	Block diagram of the neuro-fuzzy control system.	72
Figure 7.4.	Simulation 1: The results obtained for sinusoidal reference trajectory.	73
Figure 7.5.	Simulation 2: The results obtained for square wave reference trajectory.	73
Figure 7.6.	Simulation 3: The results obtained for sinusoidal reference trajectory with a sudden disturbance.	74
Figure 7.7.	The experimental setup.	76
Figure 7.8.	Block scheme of the plant.	76
Figure 7.9.	Block diagram of the constantly excited DC motor with load. . . .	77
Figure 7.10.	Block diagram of the neuro-fuzzy control system.	79
Figure 7.11.	Experiment 1: The results obtained for changing reference under sinusoidal load.	79
Figure 7.12.	Experiment 2: The results obtained for changing reference under sinusoidal load.	80

Figure 7.13. Experiment 3: The results obtained for constant reference under varying step load.	80
Figure 7.14. Control input signal for the second experiment (changing reference under sinusoidal load).	81
Figure 7.15. Sinusoidal load.	81
Figure 7.16. Experiment 1: The final membership functions of T1FNS.	82
Figure 7.17. Experiment 1: The final membership functions of RIT2FNS.	82
Figure 7.18. Interval type-2 elliptical membership function.	84
Figure 7.19. The block diagram of the system.	90
Figure 7.20. First simulation study, changing reference trajectory for the pitch axis and step reference trajectory for the yaw axis of a 2-DOF helicopter.	91
Figure 7.21. Second simulation study, step reference trajectory for the pitch axis and changing reference trajectory for the yaw axis of a 2-DOF helicopter.	91
Figure 7.22. Third simulation study, changing reference trajectory with a disturbance for both axes of a 2-DOF helicopter.	92
Figure 7.23. The final membership functions of the third simulation study for the pitch axis.	92

Figure 7.24. The final membership functions of the third simulation study for
the yaw axis. 93

Figure A.1. The schematic view of the hardware station. 97

LIST OF TABLES

Table 4.1.	Comparison of the Two Fuzzy Algorithms.	36
Table 5.1.	The optimal number of clusters for different data sets using the IT2 FCM clustering algorithm.	43
Table 6.1.	The optimal number of clusters for the data set using the IT2 FCM clustering algorithm.	51
Table 6.2.	The comparison of various structures in modeling application.	54
Table 6.3.	System Parameters.	56
Table 6.4.	System Parameters.	57
Table 6.5.	The optimal number of clusters for QCM input data using the IT2 FCM clustering algorithm.	58
Table 6.6.	The comparison of the fuzzy algorithms with and without noise in the input measurements.	61
Table 7.1.	Description of the nonlinear model parameters.	71
Table 7.2.	Comparison of obtained RMSE values of 2-DOF Helicopter.	75
Table 7.3.	The technical data of the laboratory setup.	78
Table 7.4.	Comparison of obtained RMSE values of real-time servo system.	83

Table 7.5.	The obtained RMSE values.	94
Table A.1.	The input/output features of the Humusoft MF614.	98
Table A.2.	The technical data for the actuator with signal adaption unit.	99

LIST OF SYMBOLS

A	Fuzzy set A
\tilde{A}	Type-2 fuzzy set
a_n^i	Coefficients of the z^i polynomial
B_p	Viscous damping about pitch axis
B_y	Viscous damping about yaw axis
C	Cluster number
C_i	Consequent type-1 fuzzy set
\tilde{C}_i	Consequent type-2 fuzzy set
d_{ji}	Distance between j_{th} cluster to x_i
E	Output error
F_x	Road friction force
F_z	Vertical load
g	Gravitational force
$J_{eq,p}$	Total moment of inertia about pitch axis
$J_{eq,y}$	Total moment of inertia about yaw axis
J_x	Primary membership functions
$J(U, v)$	Objective function of FCM clustering
K_M	Motor constant
K_{pp}	Thrust torque constant acting on pitch axis from pitch propeller
K_{py}	Thrust torque constant acting on pitch axis from yaw propeller
K_{yp}	Thrust torque constant acting on yaw axis from pitch propeller
K_{yy}	Thrust torque constant acting on yaw axis from yaw propeller
L_A	Armature inductance
l_{cm}	Center of mass length along helicopter body from pitch axis
m_{heli}	Total moving mass of the helicopter
M_L	Sum of all load torques

o^i	The result of i^{th} IF-THEN rule
p^{in}	The parameter of the G-conjunction operator
R_A	Armature resistance
T	T-norm
T_A	Armature time constant
T_b	Braking Torque
U_A	Armature voltage
$u_j(x_i)$	Membership value of x_i in j^{th} cluster
u_k^d	Desired output of the system
u_k	Actual output of the system
v_j	Center of the j^{th} cluster
$V_{m,p}$	Voltage apply to pitch motor
$V_{m,y}$	Voltage apply to yaw motor
x	The elements of X
X	Universe of discourse
z^i	Output of IF-THEN rule in Sugeno model
Z^i	Output of IF-THEN rule in Mamdani model
Z_{COS}	Center of sets type-reduction
z_r	Maximum value of z
z_l	Minimum value of z
ϵ	Error tolerance
$\mu(\lambda)$	Road adhesion coefficient
μ	Membership function
$\underline{\mu}$	Lower membership function
$\bar{\mu}$	Upper membership function
$\bar{\omega}_i$	Upper bound of firing strength for i^{th} IF-THEN rule
$\underline{\omega}_i$	Lower bound of firing strength for i^{th} IF-THEN rule
Ω^i	Interval of firing strength of the i^{th} rule
σ	Width of the Gaussian membership function

LIST OF ACRONYMS/ABBREVIATIONS

4Q	Four Quadrant
AQM	Active Queue Management
ASTFNC	Adaptive Self-Organizing Takagi-Sugeno-Kang Type Fuzzy Network Control
CLS	Command Line-of-Sight
CMAC	Cerebellar Model Articulation Controller
COS	Center of sets
CPU	Central Processing Unit
DOF	Degrees of Freedom
EC	Evolutionary Computation
EKF	Extended Kalman Filter
FCM	Fuzzy C-Means
FGNN	Fuzzy-Gaussian-Neural-Network
FL	Fuzzy Logic
FLCs	Fuzzy Logic Controllers
FLSs	Fuzzy Logic Systems
FNN	Fuzzy Neural Network
FNNs	Fuzzy Neural Networks
FNS	Fuzzy Neural System
FOU	Footprint of Uncertainty
FPFC	Fuzzy Predictive Functional Control
FS	Fukuyama Sugeno
FSFISC	Fuzzy-Integral Sliding Controller
G-conjunction	Generalized conjunction
IFSs	Intuitionistic Fuzzy Sets
ISMIC	Integral Sliding Mode Control
IT2 FCM	Interval Type-2 Fuzzy C-Means
IT2TFNS	Interval Type-2 Takagi-Sugeno-Kang Fuzzy Neural System
IT2 TSK FLSs	Interval Type-2 Takagi-Sugeno-Kang Fuzzy Logic Systems

LMFs	Lower Membership Functions
MCDM	Multiple Criteria Decision Making
MF	Membership Function
MIMO	Multi-Input-Multi-Output
ML	Machine Learning
MZSM	Mean of the ZMP Stability Margin
NNs	Neural Networks
NT	Nie-Tan
PBM	Pakhira–Bandyopadhyay–Maulik
PC	Partition Coefficient
PE	Partition Entropy
PD	Proportional-Derivative
PI	Proportional-Integral
PR	Probabilistic Reasoning
QCM	Quarter Car Model
RMSE	Root Mean Square Error
RIT2FNS	Recursive Interval Type-2 Fuzzy Neuro System
SC	Soft computing
SFGNN	Supervisory Fuzzy-Gaussian-Neural-Network
SISO	Single Input Single Output
SMC	Sliding Mode Control
SNR	Signal to noise ratio
SPSA	Simultaneous Perturbation Stochastic Approximation
SQP	Sequential Quadratic Programming
SRUKF	Square Root Unscented Kalman Filter
T1FLC	Type-1 Fuzzy Logic Controller
T1 FLSs	Type-1 Fuzzy Logic Systems
T1FNS	Type-1 Fuzzy Neuro System
T2FLC	Type-2 Fuzzy Logic Controller
T2 FLS	Type-2 Fuzzy Logic System
T2 FLSs	Type-2 Fuzzy Logic Systems

TCP	Transmission Control Protocol
TRMS	Twin Rotor MIMO Systems
TSK	Takagi-Sugeno-Kang
TSK-FNN	Takagi-Sugeno-Kang Fuzzy Neural Network
UMFs	Upper Membership Functions
UPFC	Unified Power Flow Controller
XB	Xie and Beni

1. INTRODUCTION

In recent decades, the systems that the control engineers have to deal with have become more and more complex and therefore difficult to handle. Conventional techniques based on hard computing [1] with precise, rigorous, and quantitative analytical models are found to be inadequate in most cases as, in the real world, most systems encounter many uncertainties and imprecise information due to the dynamics of the external environment and the inner uncertainties of the systems. Soft computing (SC) methodologies such as Fuzzy Logic (FL), Neural Networks (NNs), Probabilistic Reasoning (PR), Evolutionary Computation (EC), Machine Learning (ML), are therefore often resorted to, to alleviate the difficulties. It is to be noted that these methods are complementary rather than competitive and can be used together to achieve better results [1]. One of the fundamental constituents of soft computing is fuzzy logic and it is the focus of this study.

In the literature, Fuzzy Logic Systems (FLSs) have been used with great success for more than four decades in many different areas, ranging from decision making, modeling, identification, telecommunications to control of systems [2–12]. In [2], the aim is to order alternatives by using fuzzy multiple criteria decision making (MCDM) with a fuzzy number dominance based ranking approach. The effectiveness of the proposed approach is illustrated through a numerical problem, namely a facility location selection problem. In [3], simple parameterized conjunctions are used for nonlinear function approximation. In [4], fuzzy modeling of nonlinear systems based on improved fuzzy clustering algorithm is realized. In the study, the fuzzy clustering algorithm is improved by using a new objective function and a rule reduction is performed by using QR decomposition. In [5], a complex industrial process, the ball mill circuit of a cement mill, is controlled by a high precision sampling fuzzy logic controller with self-optimizing algorithm. The proposed controller is able to provide stability of the complex process. In [6], fuzzy logic controller based variable structure control is used in the control of an inverted pendulum. The obtained results indicate that the proposed algorithm is robust and is able to allay the chattering problem. In [7], the nonlinear dynamics of an

antenna is modeled by a Takagi-Sugeno neuro fuzzy model in which the membership function values are initialized by the fuzzy clustering algorithm. The results illustrate that Takagi-Sugeno fuzzy structures are able to model nonlinear systems with high accuracy. In [8], the series branch of the unified power flow controller (UPFC) is controlled by using recurrent fuzzy neural controllers. The proposed algorithm is used to improve the performance of the dynamic P-Q control. In [9], a relatively novel approach, termed Intuitionistic Fuzzy Sets (IFSs), is discussed in terms of its historical, theoretical and application aspects. In [10], a Takagi-Sugeno (TS) fuzzy model based integral sliding mode control (ISMC) technique is presented and the proposed approach is tested on the attitude control of a spacecraft. Its performance is compared with TS fuzzy model based sliding mode control (SMC) and it is seen that TS-SMC is more sensitive to uncertainties as compared to TS-ISMC. In [11], networks that use dynamic transmission control protocol (TCP) are modeled by a perturbed TS fuzzy system. Subsequently, based on this model, a robust fuzzy congestion controller is devised for the TCP/Active Queue Management (AQM) router. The simulation results indicate the robustness of the proposed approach with the dynamic TCP system. In [12], a self-tuning of 2 degrees of freedom (DOF) control algorithm is proposed for the control of a SISO helio-crane system and its performance is compared with fuzzy predictive functional control (FPFC). The design is based on a Type-1 fuzzy model of the system. The evolving fuzzy structure of the proposed approach uses recursive Gustafson-Kessel clustering.

In recent years, the integration of soft computing methodologies such as the combination of fuzzy logic and neural networks, i.e., fuzzy neural networks (FNNs), are commonly used in identification and control applications to benefit from the advantages of both. The usage of neural networks in fuzzy logic systems may increase the accuracy of the model due to their self-learning capabilities [13]. In [14], an adaptive fuzzy neural network with a novel monitoring controller is used in path planning of a defensive missile. The proposed approach is used with the principle of command line-of-sight (CLOS) missile guidance law and its performance is compared with the cerebellar model articulation controller (CMAC). It is concluded that the proposed approach shows more efficient tracking performance as compared to CMAC and carries less computational

burden. In [15], a fuzzy-Gaussian-neural-network (FGNN) controller is combined with a supervisory controller (SFGNN) and the proposed approach is used in mobile robots for path tracking. The strength of the method is validated through simulation results and compared with PID and FGNN controllers. It is seen that the presented approach has better tracking performance and less computation burden.

In many real world applications, most systems encounter many uncertainties and imprecise information due to the dynamical external environment and the inner uncertainties of the systems. The FNNs seen in literature generally use type-1 fuzzy sets as in the examples cited. The use of such fuzzy sets in the antecedent and/or the consequent parts of the fuzzy rules may not be able to handle the uncertainties discussed above since type-1 fuzzy membership functions are precise [16]. Type-2 fuzzy sets are preferable instead of type-1 fuzzy counterpart in cases when the level of uncertainty is relatively high, because type-2 fuzzy sets are able to represent these uncertainties in terms of their membership functions. In [17], three types of type-2 Takagi-Sugeno-Kang (TSK) fuzzy structure are presented. In the study, it is claimed that the proposed type-2 TSK Fuzzy Logic Controllers (FLCs) should be preferred in cases when linguistic uncertainties exist. In [18], the differences between type-2 and type-1 TSK FLSs are given and their modeling performance is compared with each other. Both algorithms are tested on a nonlinear function approximation and the simulation studies show that type-2 TSK FLS is more robust than its counterpart. In [19], a novel modeling approach based on type-2 FLS is developed for modeling application with uncertainties. The proposed approach is tested on modeling the characteristic of a photovoltaic array. The obtained results illustrate the effectiveness of the algorithm. In [20], solar power plant is modeled using three TSK fuzzy models; type-1 antecedents and crisp consequents, type-1 antecedents and consequents, and the last model is the interval type-2 antecedents and crisp consequents. The simulation results show that the type-2 TSK fuzzy system has better modeling performance compared to other fuzzy models even in the presence of noise in the measurements. In [21], an interval type-2 Takagi-Sugeno-Kang fuzzy neural system (IT2TFNS) with an on-line adaptive controller that uses a stable simultaneous perturbation stochastic approximation (SPSA) algorithm is suggested for the control of nonlinear systems. Its performance is tested in tracking

control of a Chua's chaotic circuit and in a real-time application, namely the temperature control of a water bath. The results obtained are compared with a type-1 Takagi-Sugeno-Kang Fuzzy Neural Network (TSK-FNN) and a traditional IT2TFNN. The simulation results show the effectiveness of the proposed approach. In [22], a type-2 Takagi-Sugeno-Kang fuzzy neural system (FNS) is presented for the identification of a dynamical plant and for the speed control of a servo system and its performance is compared with a type-1 FNS. It is observed that the T2 FNS system is able to handle the uncertainties with less transients as compared to the type-1 fuzzy structure and it has less root mean square error (RMSE). In [23], to enhance the robustness of the biped walking robots under the conditions of complex process and measurement noise, a type-2 fuzzy logic controller (T2FLC) with a state estimator that is based on the Square Root Unscented Kalman Filter (SRUKF) is suggested. The performance of the proposed approach is compared with a PID controller, a type-1 fuzzy logic controller (T1FLC), and a traditional T2FLC. The simulation results show that, especially under the conditions of strong process and measurement noise, the proposed approach has a better value for the mean of the ZMP stability margin (MZSM) as compared to some other methods from the literature. In this dissertation, interval type-2 fuzzy logic system is used with the combination of neural networks to take advantage of the both approaches.

This study presents a novel approach that uses type-2 fuzzy logic systems with parameterized conjunctors. In traditional type-1 FLSs, a sufficiently accurate fuzzy logic model cannot be obtained in most cases. Therefore, the traditional type-1 FLSs are generally used with some optimization techniques [24]. A common approach to the optimization process is the tuning of the parameters of the membership functions. However, this may lead to a distortion or loss of the expert knowledge about the system. To prevent this, the use of generalized conjunction (G-conjunction) operators are proposed in the literature [25,26]. In the approach, the optimization of the model is achieved by the adaptation of the parameter of the conjunctor. The motivation behind the study is to obtain an optimal fuzzy model without changing the parameters of the antecedent membership functions which are obtained by using an interval type-2 fuzzy c-means (IT2 FCM) clustering algorithm.

Clustering is an unsupervised classification algorithm that has been used in many interdisciplinary areas, such as data mining, image analysis, pattern recognition, bioinformatics, etc. [27–29]. For a general overview the reader may refer to the survey papers [30–32]. In this study, IT2 FCM clustering algorithm is used to determine the center values of the antecedent membership functions [33].

One major disadvantage of FCM clustering algorithm is that the number of clusters has to be fixed a priori. However, the data sets may not always be well separable. To overcome this problem, the use of a validity index is proposed. A summary of fuzzy clustering indices proposed in the literature is given in [34]. There still is the problem however that a certain validity index may not always be capable of finding the cluster numbers of all data sets [34].

In this study, Partition Coefficient (PC) [35,36], Partition Entropy (PE) [37,38], Xie and Beni [39], Fukuyama Sugeno (FS) [40], and PBM [41] validity indices are used in the determination of the optimal number of clusters in a number of real and artificial data sets. In addition, a new validity index is proposed and compared with the performances of the stated validity indices and seen to be more efficient. The proposed validity index is then used to determine the number of fuzzy rules of IT2 FNS with parameterized conjunctors and the IT2 FCM clustering algorithm is applied to determine the centers of the membership functions. The developed IT2 FNS with parameterized conjunctors is used in two applications, namely for the modeling of a benchmark nonlinear function and the wheel slip control of a Quarter Car Model (QCM).

Most systems encountered today are time varying and control or modeling of such processes should be done in a recursive manner. In this study, an interval type-2 FNS with a recursive fuzzy c-means clustering algorithm is used in tracking a specified trajectory of a 2-DOF helicopter and in the speed control application of a servo system. The main contribution of this part of the study is that the interval type-2 FNS is used with a recursive fuzzy c-means clustering algorithm [42] based on Euclidean distance and this designed algorithm is used in control applications. The recursive

fuzzy c-means clustering algorithm is used to identify the center and the standard deviation values of the interval type-2 Gaussian membership functions at the antecedent parts of the TSK-type fuzzy rules. The parameters at the consequent parts of the fuzzy rules are tuned based on gradient descent approach. The proposed approach is first tested by simulation studies for position tracking of a 2-DOF helicopter and then by experimental studies for speed control of a servo system. Subsequently, the interval type-2 neuro-fuzzy system with recursive FCM clustering algorithm is used with elliptical membership functions and is tested on trajectory tracking of a 2-DOF helicopter.

1.1. The Aim of This Study

The engineers of today encounter complex control applications due to the rapidly evolving technology. For modeling and control of such complex systems, a number of different methodologies can be used. One such methodology is the use of type-2 fuzzy logic systems (T2 FLSs) and it is the focus of this study. In this dissertation, the objectives are summarized in the following:

(i) A novel approach, interval type-2 fuzzy neural system with parameterized conjunctors is used with interval type-2 fuzzy c-means clustering algorithm. In conventional fuzzy modeling and control, to obtain an optimal fuzzy system, a commonly used approach is to tune the parameters of the membership functions. However, if the membership functions carry significant expert knowledge about the system, this may be lost or distorted during the optimization process. In the proposed approach, in order to prevent such a loss of valuable information, parameterized conjunction operators are used as the AND operator in the inference engine. During the optimization process, their parameters are tuned instead. Thus, any knowledge that is carried by the antecedent membership functions is not lost or distorted.

(ii) In the stated approach, in the absence of any expert knowledge, some knowledge about the system is gained by the use of the interval type-2 fuzzy c-means (IT2 FCM) clustering algorithm. However, this requires the number of classes to be known

beforehand and to alleviate the problem, some validity indices that are suggested in the literature and a novel validity index that carries less computational burden are considered to determine the number of classes and therefore the number of fuzzy rules.

(iii) Interval type-2 neuro-fuzzy system is used with recursive fuzzy c-means clustering algorithm. The center and the standard deviation values of the interval type-2 Gaussian membership functions at the antecedent parts of the TSK-type fuzzy rules are determined by using recursive fuzzy c-means clustering algorithm. Its contribution to the existing literature is that in the design of an interval type-2 fuzzy neural system, recursive fuzzy c-means clustering algorithm is used and the designed algorithm is applied in control applications. In addition, the designed algorithm is also used with elliptical membership functions.

The proposed algorithms are verified through modeling and control applications.

1.2. The Organization of the Thesis

In Chapter 1, the literature review in fuzzy logic and neuro-fuzzy systems are given. In sequence, the aim of the study and the organization of the thesis are briefly presented.

In the second chapter, an overview of type-2 fuzzy logic systems is given.

In Chapter 3, Fuzzy C-Means (FCM) clustering and Interval Type-2 Fuzzy C-Means (IT2 FCM) clustering algorithms are presented.

In chapter four, initially, type-1 and type-2 fuzzy logic systems are used with parameterized conjunctors for modeling applications.

In the fifth chapter, the normalization method used is explained in detail and the validity indices adopted from the literature and the newly proposed validity index are described. To show the effectiveness of the validity index proposed, IT2 FCM clustering

algorithm is tested on different data sets. An analysis of the clustering results is given.

In Chapter 6, a brief account of the theoretical and the mathematical backgrounds of IT2 FNS (Fuzzy Neural System) with parameterized conjunctors is given. The proposed approach is used; firstly for the approximation of a benchmark nonlinear function and then for the control of a QCM (Quarter Car Model). Its performance is compared with the other methods seen in the literature.

In Chapter 7, the theoretical and the mathematical background of the IT2 FNS with the recursive fuzzy c-means clustering algorithm is given in detail. The mathematical descriptions of the Quanser 2-DOF (Degrees of freedom) helicopter and the DC servo system are presented. To validate the proposed approach, it is tested in a trajectory tracking of the 2-DOF helicopter and in a speed control application of the DC servo system. The presented approach is also tested with elliptical membership functions in position tracking of a 2-DOF helicopter. Consequently, the outcomes of the applications are analyzed and further progress in this area is discussed.

2. TYPE-2 FUZZY LOGIC SYSTEMS

Type-1 fuzzy logic has been first introduced by Prof. Lotfi A. Zadeh, who is a professor of computer science at the University of California, Berkeley, in 1965 and the first industrial applications appeared in 1970s. Since then, fuzzy logic systems (FLSs) have been widely used in scientific arena more than four decades. However, traditional type-1 fuzzy sets may not represent the uncertainties in terms of membership functions since type-1 membership functions are precise. The uncertainties that can be encountered are defined as follows [43–45];

- The meaning of the words that are used in antecedent and consequent part of the rules can mean different things to different people.
- The input measurements of the system has uncertainties according to the environmental conditions (such as wind, rain, humidity etc.), and sensors that are effected by high noise levels from various sources.
- Using noisy training data stimulates uncertainties.
- Uncertainties in consequents of the system may occur due to the change of actuator characteristics.
- The uncertainties in antecedent and consequent arise due to the changing operation conditions.

As it is mentioned above, these uncertainties may not be handled by using only type-1 fuzzy logic system. To alleviate this problem, type-1 fuzzy logic systems are used with some optimization techniques to achieve required performance by enabling the adaptation of the fuzzy system. However, to achieve the desired performance with a minimum error response under these uncertainties, type-1 fuzzy logic systems may become inadequate and any type of optimization that is done becomes irrelevant [45].

In order to overcome these uncertainties, type-2 fuzzy logic was proposed by Prof. Lotfi A. Zadeh in 1975 as an extension of type-1 fuzzy sets. Type-2 fuzzy logic systems have the ability to represent the uncertainties mentioned above in terms type-2 fuzzy

membership functions.

A type-1 fuzzy set, A is defined as in the following [24]:

$$A = \{(x, \mu_A(x)) | x \in X\} \quad (2.1)$$

where x are the elements of input X , which is the universe of discourse. $\mu_A(x)$ is the membership function, which takes values in the closed interval $[0, 1]$. Every element of X maps to a membership grade taking the values between 0 and 1. In Figure 2.1, a typical example of a type-1 fuzzy membership function is given. As it is seen, the uncertainties are not taken into consideration since an input value is represented by a precise value. To handle the uncertainties mentioned above, an interval type-2 membership function can be used as an alternative. In Figure 2.2, the type-1 Gaussian membership

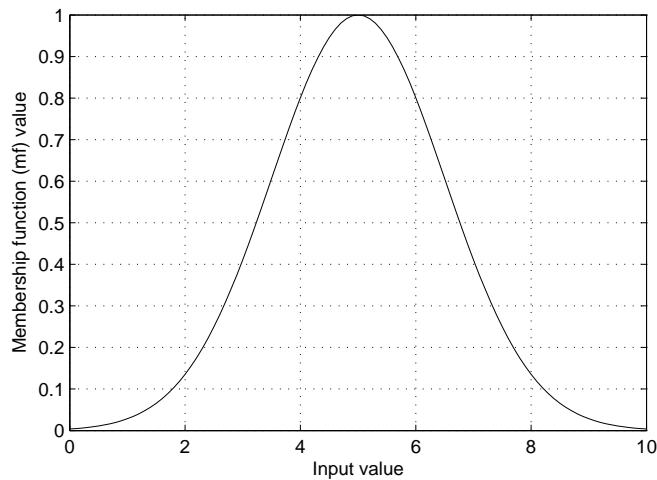


Figure 2.1. A type-1 Gaussian membership function.

function that is given in Figure 2.1 is blurred to the left and right. The obtained figure is called as the footprint of uncertainty (FOU). An input value corresponds to a closed interval. In addition, this closed interval has a secondary membership grade, which constitutes the third dimension of the type-2 membership functions. For interval type-2 membership functions, this value is either zero or one as seen in Figures 2.2 and 2.3.

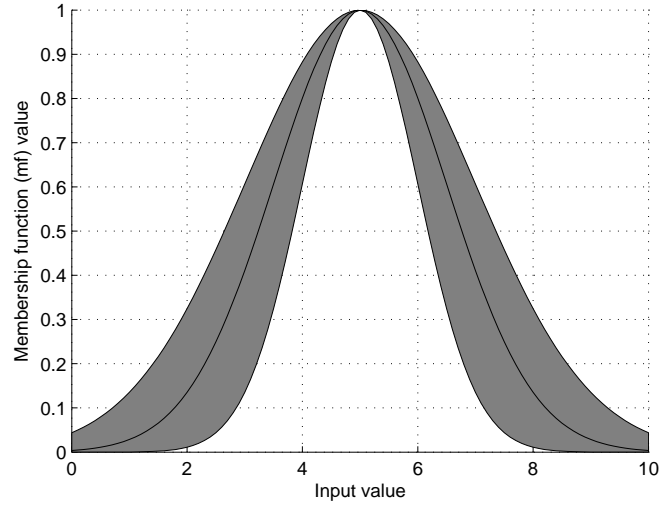


Figure 2.2. An interval type-2 Gaussian membership function with uncertain standard deviation whose secondary membership grade is zero.

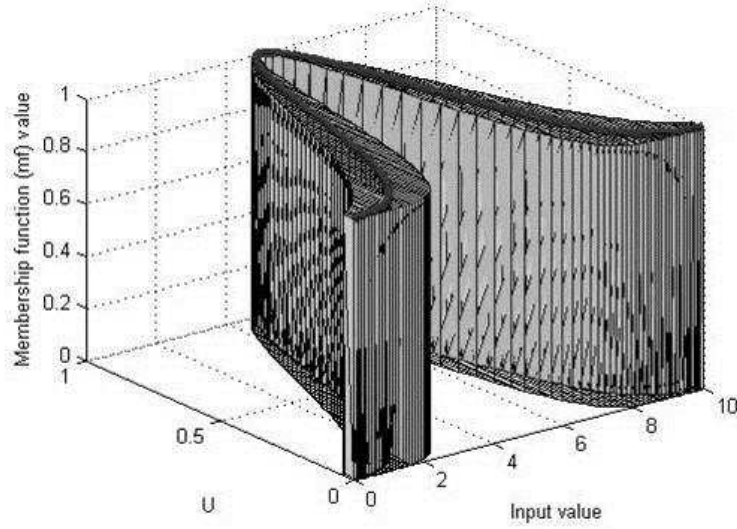


Figure 2.3. An interval type-2 Gaussian membership function with uncertain standard deviation whose secondary membership grade is one.

A type-2 fuzzy set is defined as follows [43] and [46]:

$$\tilde{A} = \int_{x \in X} \int_{u \in J_x \subseteq [0,1]} \mu_{\tilde{A}}(x, u) / (x, u) \tag{2.2}$$

An interval type-2 fuzzy set is defined as follows:

$$\tilde{A} = \int_{x \in X} \int_{u \in J_x \subseteq [0,1]} 1/(x, u) \quad (2.3)$$

where \mathbf{x} is the primary variable and X is the input domain. The secondary membership grade $\mu_{\tilde{A}}(x, u)$ is either zero or one for interval type-2 fuzzy sets. u is the secondary variable. \tilde{A} is the interval type-2 fuzzy set. J_x are the primary membership functions. The union of all primary membership functions forms the FOU [43] and [46]. As seen in Figure 2.2, FOU is bounded by the lower and the upper membership functions and these membership functions are type-1 that enable to use type-1 fuzzy arithmetic in calculations of type-2 fuzzy sets [45] and [47].

General type-2 fuzzy sets may increase the accuracy of the approximation capability of type-2 fuzzy logic systems. However, the computational burden of the general type-2 fuzzy system is high as compared to interval type-2 fuzzy logic system. Thus, interval type-2 fuzzy system is preferred by many researchers due to its computational ease in the design of a type-2 fuzzy logic system [22]. In this study, Takagi-Sugeno-Kang (TSK) type fuzzy inference engine, which is a well-known universal approximator, is used in the design of interval type-2 neuro-fuzzy system. In the subsequent sections, the structure of type-2 fuzzy logic systems are briefly given and the three types of Interval Type-2 Takagi-Sugeno-Kang Fuzzy Logic Systems (IT2 TSK FLSs) are described.

2.1. The Structure of the Type-2 Fuzzy Logic Systems

The block diagrams of T1 FLS and T2 FLS are seen in Figures 2.4 and 2.5. The main difference between the structure of type-1 and type-2 fuzzy logic is the type-reduction procedure. The main components of type-2 fuzzy logic system are listed as in the following:

- Fuzzification
- Fuzzy Inference System and Rule Base
- Type-Reduction

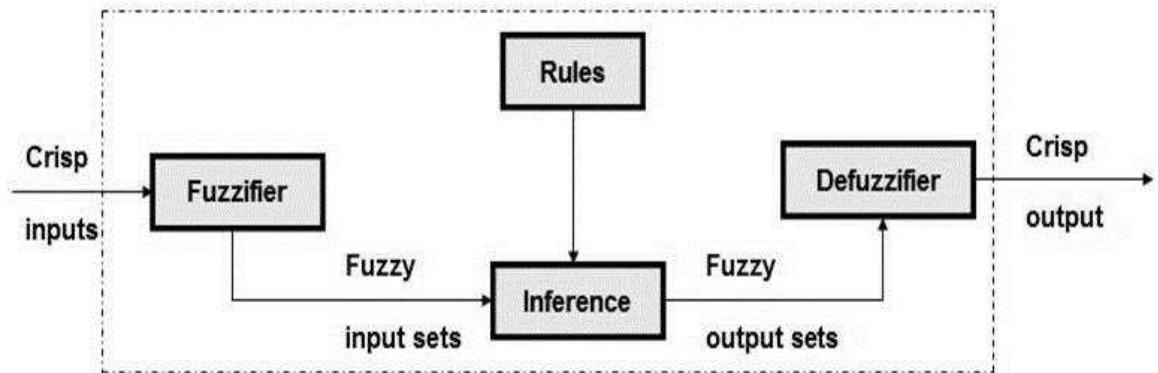


Figure 2.4. Block Diagram of Type-1 Fuzzy Logic Systems (T1 FLSs).

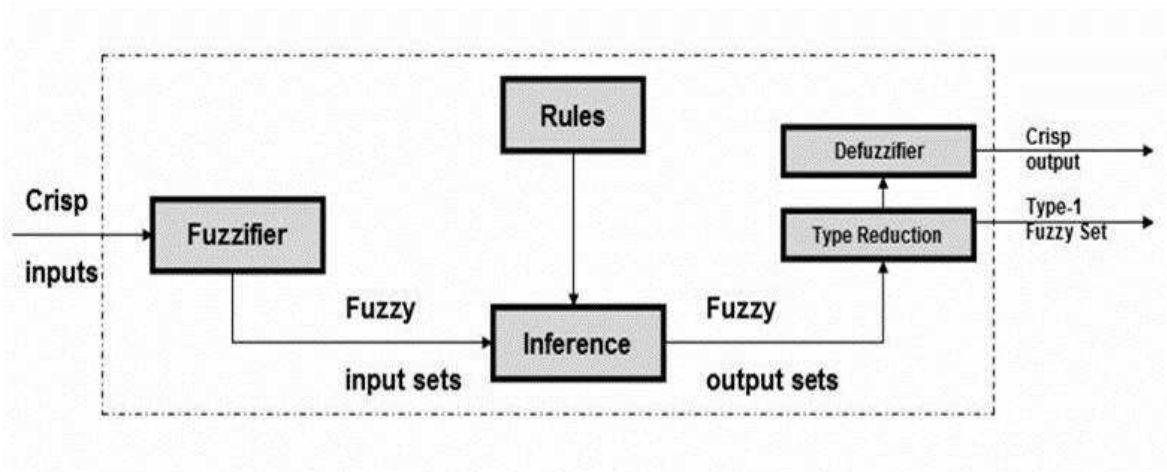


Figure 2.5. Block Diagram of Type-2 Fuzzy Logic Systems (T2 FLSs).

- Defuzzification

These components are given briefly in the following subsections.

2.1.1.1. Fuzzification

Initially, the input values are fuzzified by using membership functions. A crisp input value x is mapped to a fuzzy set value \tilde{A} ($x \in X$, $\tilde{A} \subset X$). Any fuzzy logic system that contains a type-2 fuzzy set is a type-2 fuzzy logic system.

2.1.2. Fuzzy Inference System and Rule Base

The IF-THEN fuzzy rule structure of a type-2 fuzzy logic system can be as follows:

A Mamdani Type-2 FLS:

$$\begin{aligned} R^i &= \text{IF } X_1 \text{ is } \tilde{A}_{i1} \text{ and } \dots \text{ and } X_n \text{ is } \tilde{A}_{in}, \\ &\text{THEN } Z^i = \tilde{C}_i \end{aligned}$$

where X_n are the input values and \tilde{A}_{in} are the type-2 fuzzy sets at the antecedents of the fuzzy rules. At the consequents of the fuzzy rules, Z^i is the output and \tilde{C}_i is the type-2 fuzzy sets. M indicates the number of rules ($i=1, \dots, M$) and n indicates the antecedent numbers.

A Type-2 TSK FLS:

$$\begin{aligned} R^i &= \text{IF } X_1 \text{ is } \tilde{A}_{i1} \text{ and } \dots \text{ and } X_n \text{ is } \tilde{A}_{in}, \\ &\text{THEN } z^i = a_n^i x_n + a_{n-1}^i x_{n-1} + \dots + a_0^i \end{aligned}$$

where z^i is the output of the T2 TSK type fuzzy rules.

Meet under minimum or product t-norm and join operators are used in the fuzzy inference engine and they are given in the following respectively [43];

$$\underline{\omega}^i = \underline{\mu}_{\tilde{A}_{i1}}(x_1) * \dots * \underline{\mu}_{\tilde{A}_{in}}(x_n) \quad (2.4)$$

$$\bar{\omega}^i = \bar{\mu}_{\tilde{A}_{i1}}(x_1) * \dots * \bar{\mu}_{\tilde{A}_{in}}(x_n) \quad (2.5)$$

where “*” indicates product or minimum operation for meet under product or minimum t-norm, or it indicates maximum for join operation for interval singleton type-2 fuzzy

sets.

2.1.3. Type-Reduction

In type-2 fuzzy logic systems, the output is a type-2 fuzzy set. This output is initially reduced to a type-1 fuzzy set by using a type-reduction method. In the literature, one of the most commonly used type-reduction procedure is the center of sets (COS) type-reduction and it is given as follows [43]:

$$Z_{COS}(Z^1, \dots, Z^M, \Omega^1, \dots, \Omega^M) = [z_l, z_r] = \int_{z^1} \cdots \int_{z^M} \int_{\omega^1} \cdots \int_{\omega^M} 1 / \frac{\sum_{i=1}^M \omega^i z^i}{\sum_{i=1}^M \omega^i} \quad (2.6)$$

The result of the type-reduction procedure, Z_{COS} , equals to interval set, $[z_l, z_r]$, where $z^i \in Z^i = [z_l^i, z_r^i]$ and $\omega^i \in \Omega^i = [\underline{\omega}^i, \bar{\omega}^i]$. z_l and z_r are calculated respectively as in the following:

$$z_l = \frac{\sum_{i=1}^M \omega_l^i z_l^i}{\sum_{i=1}^M \omega_l^i} \quad (2.7)$$

$$z_r = \frac{\sum_{i=1}^M \omega_r^i z_r^i}{\sum_{i=1}^M \omega_r^i} \quad (2.8)$$

2.1.4. Defuzzification

An interval set $[z_l, z_r]$ is obtained at the end of the type-reduction. The output of the system is obtained by using the defuzzification procedure, which is taking the average of the interval set and it is given as follows [43]:

$$z = \frac{z_l + z_r}{2} \quad (2.9)$$

2.2. Interval Type-2 Takagi-Sugeno-Kang Fuzzy Logic Systems (IT2 TSK FLSs)

In this study, interval type-2 Takagi-Sugeno-Kang type fuzzy logic system is used. In literature, three types of IT2 TSK FLSs are proposed depending on the types of fuzzy sets at the antecedents or consequents of fuzzy IF-THEN rules [17]. In the subsequent subsection the rule structures of these models are given in detail.

2.2.1. Model 1

The first model has the following rule structure [17]:

$$\begin{aligned} R^i &= \text{IF } X_1 \text{ is } \tilde{A}_{i1} \text{ and } \dots \text{ and } X_n \text{ is } \tilde{A}_{in}, \\ \text{THEN } Z^i &= C_{in}x_n + C_{i(n-1)}x_{n-1} + \dots + C_{i0} \end{aligned}$$

where the antecedents are interval type-2 fuzzy sets indicated with \tilde{A}_{in} and consequents are type-1 fuzzy sets C_{in} . X_n is the input and Z^i is the output of the system.

2.2.2. Model 2

The second model has the following rule structure [17]:

$$\begin{aligned} R^i &= \text{IF } X_1 \text{ is } \tilde{A}_{i1} \text{ and } \dots \text{ and } X_n \text{ is } \tilde{A}_{in}, \\ \text{THEN } z^i &= a_n^i x_n + a_{n-1}^i x_{n-1} + \dots + a_0^i \end{aligned}$$

where the antecedents are interval type-2 fuzzy sets, \tilde{A}_{in} , and the consequents are first order polynomial. a_n^i are the coefficients of the polynomial. X_n is the input of the system.

2.2.3. Model 3

The third model has the following rule structure [17]:

$$\begin{aligned}
 R^i &= \text{IF } X_1 \text{ is } A_{i1} \text{ and } \dots \text{ and } X_n \text{ is } A_{in}, \\
 \text{THEN } Z^i &= C_{in}x_n + C_{i(n-1)}x_{n-1} + \dots + C_{i0}
 \end{aligned}$$

where both the antecedents and the consequents are type-1 fuzzy sets, A_{in} and C_{in} . The fuzzy sets at the consequents represent the uncertainties. X_n and Z^i are the input and the output of the system, respectively.

In this study, the second model of IT2 TSK FLSs is used. In this rule structure, antecedents are interval type-2 fuzzy sets and consequents are first order polynomial. The center values of the antecedent membership functions are determined by using interval type-2 fuzzy c-means clustering algorithm.

3. FUZZY CLUSTERING ALGORITHMS

Clustering is an unsupervised classification algorithm and is a challenging task that has been considered in many interdisciplinary areas, such as data mining, image analysis, pattern recognition, bioinformatics, etc. by scientists. In literature, there are noteworthy studies that have used clustering algorithms as referenced in survey papers [30–32]. Most of the applications in this topic are in the area of science, technology, engineering, biochemistry and molecular biology [27–29].

In hard or crisp clustering algorithms, each data object belongs to only one cluster. It is either in the cluster or not. However, in overlapping data sets, crisp clustering algorithms cannot identify the data object to which cluster it belongs. On the contrary, in Fuzzy C-Means (FCM) clustering algorithms each data object is assigned to a cluster with a degree of membership function value. Furthermore, in interval type-2 fuzzy c-means clustering algorithm the uncertainties can be handled by using two fuzzification parameters.

3.1. Fuzzy C-Means (FCM) Clustering Algorithm

In FCM clustering, an object may belong to a cluster with a degree of membership. One of the maximum fuzzy region parameter in FCM clustering is the fuzzification parameter m , which specifies the shape of the membership functions and the width of the fuzzy boundary. For type-1 FCM clustering, the fuzzification parameter is generally set to 2 [35] and [48]. The choice of m does not make any difference if the clusters have the similar volume and density, otherwise the choice of m will effect the clustering results [33]. The algorithm is given below.

- (i) Initialize the values m , C , and ε where m is the fuzzification parameter, C is the number of clusters and ε is the error tolerance.

(ii) Update the membership matrix \mathbf{U} as follows:

$$u_j(\mathbf{x}_i) = \frac{1}{\sum_{k=1}^c \left(\frac{d_{ji}}{d_{ki}} \right)^{2/(m-1)}} \quad (3.1)$$

where d_{ji} and d_{ki} are the distances between j_{th} cluster to x_i and k_{th} cluster to x_i , respectively.

(iii) Update the centers \mathbf{v} by using:

$$\mathbf{v}_j = \frac{\sum_{i=1}^N u_j(\mathbf{x}_i)^m \mathbf{x}_i}{\sum_{i=1}^N u_j(\mathbf{x}_i)^m} \quad (3.2)$$

where N is the number of data and ($j=1, \dots, C$).

(iv) Calculate the objective function \mathbf{J} is as follows:

$$J(\mathbf{U}, \mathbf{v}) = \sum_{i=1}^N \sum_{j=1}^C u_j(\mathbf{x}_i)^m d_{ji}^2 \quad (3.3)$$

(v) If $\|J^{(k)} - J^{(k-1)}\| < \varepsilon$ stop the iteration, else go to step (ii).

3.2. Interval Type-2 Fuzzy C-Means (IT2 FCM) Clustering Algorithm

One of the most important features of type-2 fuzzy sets is its ability to incorporate uncertainties into the membership functions and this feature makes type-2 fuzzy sets preferable when there exist significant uncertainties. In interval type-2 FCM clustering, the use of the two fuzzification parameters m_1 and m_2 enables the designer to define and manage the uncertainty.

In finding the optimum cluster center, the aim is to minimize the following objective functions [33]:

$$J_{m_1}(\mathbf{U}, \mathbf{v}) = \sum_{i=1}^N \sum_{j=1}^C u_j(\mathbf{x}_i)^{m_1} d_{ji}^2 \quad (3.4)$$

$$J_{m_2}(\mathbf{U}, \mathbf{v}) = \sum_{i=1}^N \sum_{j=1}^C u_j(\mathbf{x}_i)^{m_2} d_{ji}^2 \quad (3.5)$$

where $u_j(\mathbf{x}_i)$ is the membership value and d_{ji} is the distance between j_{th} cluster to \mathbf{x}_i .

For the optimization of Equation 3.4 and 3.5, an iterative algorithm is used. Firstly, the membership and the center values are initialized. Then, the upper and the lower values of the membership values are calculated as follows [49]:

$$\begin{aligned} \text{If } \frac{1}{\sum_{k=1}^C \left(\frac{d_{ji}}{d_{ki}}\right)^{\frac{2}{(m_1-1)}}} > \frac{1}{\sum_{k=1}^C \left(\frac{d_{ji}}{d_{ki}}\right)^{\frac{2}{(m_2-1)}}}, \text{ then, } \bar{u}_j(\mathbf{x}_i) &= \frac{1}{\sum_{k=1}^C \left(\frac{d_{ji}}{d_{ki}}\right)^{\frac{2}{(m_1-1)}}} \\ \text{Otherwise, } \bar{u}_j(\mathbf{x}_i) &= \frac{1}{\sum_{k=1}^C \left(\frac{d_{ji}}{d_{ki}}\right)^{\frac{2}{(m_2-1)}}} \end{aligned}$$

$$\begin{aligned} \text{If } \frac{1}{\sum_{k=1}^C \left(\frac{d_{ji}}{d_{ki}}\right)^{\frac{2}{(m_1-1)}}} \leq \frac{1}{\sum_{k=1}^C \left(\frac{d_{ji}}{d_{ki}}\right)^{\frac{2}{(m_2-1)}}}, \text{ then, } \underline{u}_j(\mathbf{x}_i) &= \frac{1}{\sum_{k=1}^C \left(\frac{d_{ji}}{d_{ki}}\right)^{\frac{2}{(m_1-1)}}} \\ \text{Otherwise, } \underline{u}_j(\mathbf{x}_i) &= \frac{1}{\sum_{k=1}^C \left(\frac{d_{ji}}{d_{ki}}\right)^{\frac{2}{(m_2-1)}}} \end{aligned}$$

where d_{ji} and d_{ki} are the distances between j_{th} cluster to \mathbf{x}_i and k_{th} cluster to \mathbf{x}_i , respectively. Then, the membership value, u is calculated by the mean of upper and lower membership values.

In the determination of the left and the right center values, the Karnik and Mendel iterative algorithm is used. It reduces the computational burden considerably. The algorithm given below is for the right center, that for the left center can be derived in a similar manner [33]:

- (i) The cluster centers v'_{jl} are calculated for all data features by using the following

equation:

$$\mathbf{v}'_j = \frac{\sum_{i=1}^N u_j(\mathbf{x}_i)^m \mathbf{x}_i}{\sum_{i=1}^N u_j(\mathbf{x}_i)^m} \quad (3.6)$$

- (ii) The data is sorted in ascending order.
- (iii) The cluster center v'_{jl} for each feature is compared with the sorted data $x_l(k) \leq v'_{jl} \leq x_l(k+1)$ to find the index k ($1 \leq k \leq N-1$). For $i \leq k$, $u_j(x_i) = \underline{u}(x_i)$, otherwise, $u_j(x_i) = \bar{u}(\mathbf{x}_i)$.
- (iv) Then, the cluster center, v''_{jl} is calculated. If $v''_{jl} \neq v'_{jl}$, $v'_{jl} = v''_{jl}$, else stop the iteration and keep the value v''_{jl} . After calculation of all the features of center, set $v_R = v''_j$.

A crisp center for the estimated center \mathbf{v}_j can be found as follows:

$$\mathbf{v}_j = \frac{\mathbf{v}_L + \mathbf{v}_R}{2} \quad (3.7)$$

The right and left membership values are calculated as follows:

$$u_j^R(\mathbf{x}_i) = \frac{\sum_{l=1}^M u_{jl}(\mathbf{x}_i)}{M} \quad (3.8)$$

where M indicates the feature number of \mathbf{x}_i and

$$u_{jl}(\mathbf{x}_i) = \begin{cases} \bar{u}_j(\mathbf{x}_i), & \text{if } x_{il} \text{ uses } \bar{u}_j(\mathbf{x}_i) \text{ for } \mathbf{v}_j^R \\ \underline{u}_j(\mathbf{x}_i), & \text{otherwise} \end{cases}$$

$$u_j^L(\mathbf{x}_i) = \frac{\sum_{l=1}^M u_{jl}(\mathbf{x}_i)}{M} \quad (3.9)$$

where

$$u_{jl}(\mathbf{x}_i) = \begin{cases} \bar{u}_j(\mathbf{x}_i), & \text{if } x_{il} \text{ uses } \bar{u}_j(\mathbf{x}_i) \text{ for } \mathbf{v}_j^L \\ \underline{u}_j(\mathbf{x}_i), & \text{otherwise} \end{cases}$$

Then, type-reduction is applied as follows:

$$u_j(\mathbf{x}_i) = \frac{u_j^L(\mathbf{x}_i) + u_j^R(\mathbf{x}_i)}{2} \quad (3.10)$$

Hard-partitioning can be done as follows:

If $u_j(\mathbf{x}_i) > u_k(\mathbf{x}_i)$ for $k = 1, \dots, C$ and $j \neq k$, Then \mathbf{x}_i is in j th cluster.

The clustering algorithms mentioned above are used in the neuro-fuzzy structures to determine the center values of the membership functions at the antecedents of the fuzzy IF-THEN rules.

In the next chapter, these clustering algorithms are used with type-1 and type-2 TSK fuzzy logic systems with parameterized conjunctors. The performances of the designed fuzzy algorithms are compared in modeling of benchmark nonlinear functions.

4. FUZZY MODELING WITH PARAMETERIZED CONJUNCTORS

4.1. Type-1 Fuzzy Modeling with Parameterized Conjunctors

In fuzzy modeling applications to obtain an optimal fuzzy model, one of the most commonly used approaches is to tune the parameters of the membership functions. This kind of adaptation is undesirable in applications where the expert knowledge is vital. To overcome this drawback, parametric conjunction or disjunction operators are used as the fuzzy operators, thus the parameters of the operators can be tuned while keeping the expert knowledge of the system. However, these operators may mean complications in the optimization of the structure and in hardware realizations. In [25] and [26] the authors tune a number of simple generalized parametric conjunction operators to obtain an optimal fuzzy model.

A conjunctor (generalized conjunction operation) is defined in [26] as a function $T: [0,1] \times [0,1] \rightarrow [0,1]$ satisfying the properties of binary conjunction operation:

$$\begin{aligned} T(0, 0) = T(0, 1) = T(1, 0) &= 0, \\ T(1, 1) &= 1 \end{aligned} \tag{4.1}$$

and monotonicity condition on $[0,1]$:

$$T(x, y) \leq T(u, v) \text{ if } x \leq u \text{ and } y \leq v. \tag{4.2}$$

These operators are not required to have the associativity and the commutativity properties. As a result, the simplest conjunctors proposed in [26] have the following mathematical representations:

$$T(x, y) = x^p y^q \tag{4.3}$$

$$T(x, y) = \min(x^p, y^q) \quad (4.4)$$

where $p, q \geq 0$. In this study, the expert knowledge about the system is obtained by using fuzzy c-means (FCM) clustering algorithm [35] and [48].

In the application for nonlinear function modeling, a first order type Takagi-Sugeno-Kang (TSK) fuzzy logic system (FLS) is used and has the following IF-THEN rule structure:

$$\begin{aligned} R^i &= \text{IF } X_1 \text{ is } A_{i1} \text{ and } \dots \text{ and } X_n \text{ is } A_{in}, \\ \text{THEN } z^i &= a_n^i x_n + a_{n-1}^i x_{n-1} + \dots + a_0^i \end{aligned}$$

where i ($i = 1, 2, \dots, M$) indicates the number of rules and n is the number of the antecedent parameters. In this rule structure, X_n 's ($i=1, \dots, n$) are the inputs of the system, A_{in} 's ($i=1, \dots, n$) are the fuzzy sets, and z^i is the output of the each rule. a_n^i 's are the coefficients of the consequent part of the rule, which is a first order polynomial.

The firing strengths of the rules are calculated by using one of the parameterized conjunctive operators in Equations 4.3 and 4.4. In the simulations, the first parameterized conjunctive operator is used as an AND operator and defined as follows:

$$\begin{aligned} \omega^i &= T(\mu_{A_{i1}}(x_1), \dots, \mu_{A_{in}}(x_n)) \\ &= \mu_{A_{i1}}(x_1)^{p_{i1}} \dots \mu_{A_{in}}(x_n)^{p_{in}} \end{aligned} \quad (4.5)$$

where i ($i = 1, 2, \dots, M$) indicates the number of rules. ω^i is the firing strength of each rule. $\mu_{A_{in}}(x_n)$ is the membership function value of the fuzzy set A_{in} and p_{in} is the parameter of the parameterized conjunctive operator.

After computing the firing strengths, the implication method is applied to find out the result of each rule. The most commonly used implication methods are product

and minimum operations, given respectively in Equations 4.6-4.7.

$$o^i = \omega^i z^i \quad (4.6)$$

$$o^i = \min(\omega^i, z^i) \quad (4.7)$$

In this study, to find the result of each rule, the product implication method, which involves multiplying the firing strength with the consequent part of the rules, is used. The output of the fuzzy system is calculated as follows [24]:

$$u = \frac{\sum_{i=1}^M \omega^i z^i}{\sum_{i=1}^M \omega^i} \quad (4.8)$$

M is the number of rules ($i = 1, 2, \dots, M$) and u is the output of the system.

4.2. Interval Type-2 Takagi-Sugeno-Kang (IT2 TSK) Model with Parameterized Conjunctors

The second modeling approach used in this study is the interval type-2 TSK fuzzy logic system with parameterized conjunctors. The rule structure has the following form [16, 17], and [50]:

$$\begin{aligned} R^i &= \text{IF } X_1 \text{ is } \tilde{A}_{i1} \text{ and } \dots \text{ and } X_n \text{ is } \tilde{A}_{in}, \\ \text{THEN } z^i &= a_n^i x_n + a_{n-1}^i x_{n-1} + \dots + a_0^i \end{aligned}$$

In the antecedent part of the rules, the interval type-2 fuzzy sets are used and are indicated with tildes. The consequent part of the rule is a first order polynomial. The centers of the antecedent membership functions are obtained by using interval type-2 fuzzy c-means clustering algorithm, in which the uncertainty can be represented by using two fuzzification parameters m_1 and m_2 [33].

In the calculations of the firing strength of each rule, parameterized conjunctive operators are used as the AND operator. To calculate the lower and the upper firing strengths of the rules, the mathematical representations of these operators are given in the following:

$$\underline{\omega}^i = \underline{\mu}_{\tilde{A}_{i1}}(x_1)^{p_{i11}} \cdots \underline{\mu}_{\tilde{A}_{in}}(x_n)^{p_{in}} \quad (4.9)$$

$$\bar{\omega}^i = \bar{\mu}_{\tilde{A}_{i1}}(x_1)^{p_{iu1}} \cdots \bar{\mu}_{\tilde{A}_{in}}(x_n)^{p_{iun}} \quad (4.10)$$

The output of the system is calculated by using the inference engine in [51] as follows:

$$u = r \frac{\sum_{i=1}^M \underline{\omega}^i z^i}{\sum_{i=1}^M \underline{\omega}^i} + (1 - r) \frac{\sum_{i=1}^M \bar{\omega}^i z^i}{\sum_{i=1}^M \bar{\omega}^i} \quad (4.11)$$

where r is chosen as 0.5.

4.3. Modeling Application

The two methods which are explained above are tested in the approximation of nonlinear functions to compare their performances [52]. In Figure 4.1, the first nonlinear function is depicted, the mathematical representation of which is:

$$u^d = f(x_1, x_2) = \frac{\sin(5\pi x_1 x_2)}{5\pi x_1 x_2}, \quad x_1, x_2 \in [-1, 1] \quad (4.12)$$

For each one of the methods, the same input range $[-1, 1]$ ($x_1, x_2 \in [-1, 1]$) is used. The input space is equally partitioned into 27x27 which leads to 729 values of functions that are calculated. To enhance the validation of the simulation results, the two fuzzy algorithms are tested on the Rosenbrock's banana function seen in Figure 4.2. It is one of the benchmark nonlinear function, which is nontrivial to approximate. The

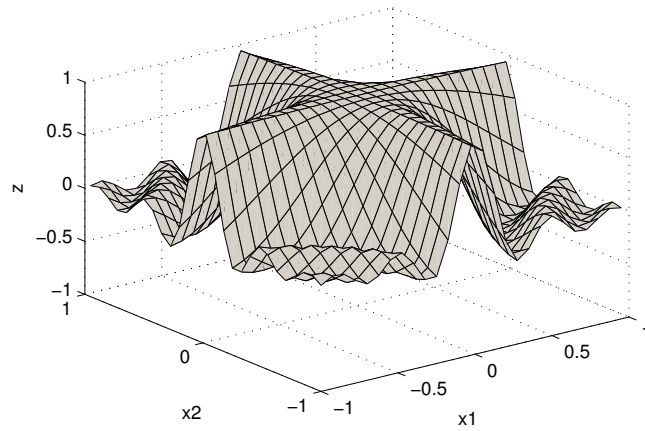


Figure 4.1. The Sinc function approximated.

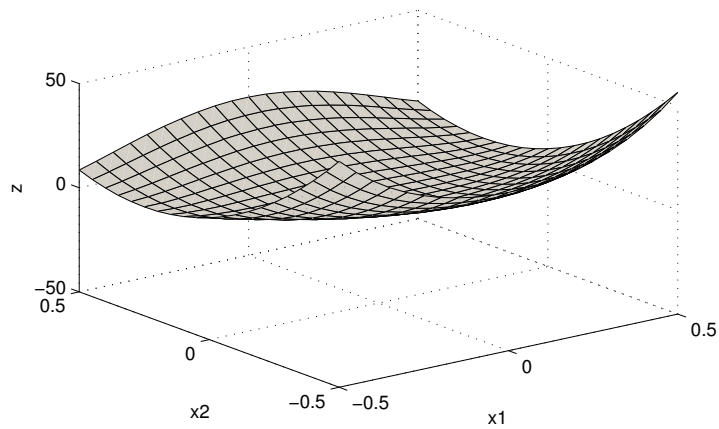


Figure 4.2. Rosenbrock's banana function approximated.

mathematical description of this function is as follows:

$$u^d = f(x_1, x_2) = (1 - x_1)^2 + 100(x_2 - x_1^2)^2 \quad (4.13)$$

The input range is between $[-0.5, 0.5]$ ($x_1, x_2 \in [-0.5, 0.5]$) and 441 (21x21) values of the function are calculated. In order to obtain the optimal fuzzy model, the RMSE value is used as the objective function which is given in the following:

$$F_{obj} = \sqrt{\frac{\sum_{k=1}^N (u_k^d - u_k)^2}{N}} \quad (4.14)$$

where u_k^d is the desired output and u_k is the actual output of the system where $k=1,2,\dots,N$.

4.3.1. Nonlinear Function Approximation by Using Parameterized Conjunctors

In this algorithm in the modeling application of the two nonlinear functions, for each input, x_1 and x_2 , four Gaussian membership functions are used, which leads to a total of 8 membership functions. They are mathematically defined as follows:

$$\text{Gaussian membership function} = e^{-\frac{1}{2}\left(\frac{x-v}{\sigma}\right)^2} \quad (4.15)$$

The most significant feature of this algorithm is that the parameters of the parameterized conjunctors are tuned instead of the parameters of the membership functions. The input membership functions that are carrying the linguistic information about the system are determined by using the FCM algorithm. In the application of the FCM algorithm, the fuzzification parameter m is chosen as 2. The input membership functions used in the modeling application of Sinc function are given in Figure 4.3. The

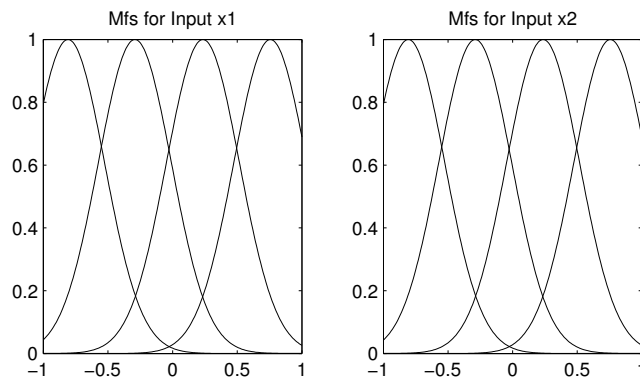


Figure 4.3. The input membership functions obtained by using FCM algorithm in the modeling application of Sinc function without noise.

rule base is composed of 16 rules and the rule structure is:

$$R^i = \text{IF } x_1 \text{ is } A_{i1} \text{ and } x_2 \text{ is } A_{i2},$$

$$\text{THEN } z^i = a_2^i x_2 + a_1^i x_1 + a_0^i$$

In this structure, at the antecedent part of the rules, x_1 and x_2 are the inputs, and A_{i1} and A_{i2} are the type-1 fuzzy sets where i indicates the number of rules ($i=1,2,\dots,16$). In the consequent part of the rule, z^i is the output of the each rule and a_2^i , a_1^i , and a_0^i are the coefficients of the first order polynomial. In this algorithm, not to lose or distort the linguistic information about the system, the parameters of the parameterized conjunctors are tuned instead of tuning the membership function parameters. These operators are used as the AND operator to calculate the firing strengths of each rule as follows:

$$\omega^i = T(\mu_{A_{i1}}(x_1), \mu_{A_{i2}}(x_2)) = \mu_{A_{i1}}(x_1)^{p_i} \cdot \mu_{A_{i2}}(x_2)^{q_i} \quad (4.16)$$

where $\mu_{A_{in}}$'s are the membership functions, p_i and q_i are the parameters of the parameterized conjunctors. The actual output of the system is calculated by using Equation 4.8. As it is stated above, in this algorithm the parameters of operators, p_i and q_i and the parameters of the polynomial at the consequent part of the rules, a_2^i , a_1^i , and a_0^i are tuned by using the Sequential Quadratic Programming (SQP) method. For the left sides of the rules a total of 32 parameters are tuned ($16 \times 2 = 32$) and for the right sides of the rules a total of 48 parameters ($16 \times 3 = 48$) are tuned together to minimize the root-mean-squared-error (RMSE), and the bound constraints for these parameters are chosen as $-50 \leq a_2^i, a_1^i, a_0^i \leq 50$ and $0.1 \leq p_i, q_i \leq 50$. The main objective is to obtain a minimum RMSE response by tuning these parameters. The approximated fuzzy model and the RMSE curve are given in Figure 4.4a-b and Figure 4.5a-b for Sinc and Rosenbrock's Banana functions, respectively. In this algorithm, the obtained RMSE values for the Sinc and Rosenbrock's Banana functions are 0.0777 and 0.0675, respectively.

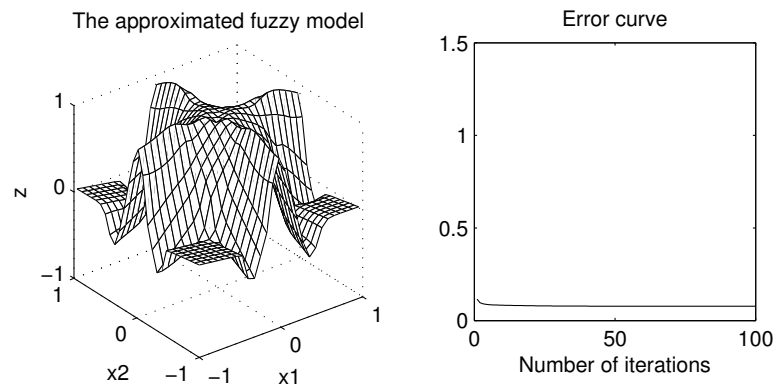


Figure 4.4. The result of Sinc function approximation by using type-1 fuzzy algorithm (a) and the RMSE curve obtained by tuning the parameters of the parameterized conjunctive operators (b).

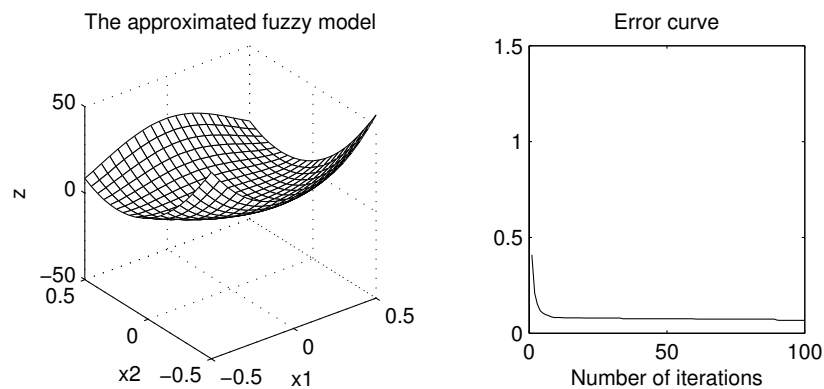


Figure 4.5. The result of Rosenbrock's Banana function approximation by using type-1 fuzzy algorithm (a) and the RMSE curve obtained by tuning the parameters of the parameterized conjunctive operators (b).

4.3.2. Nonlinear Function Approximation by Using Interval Type-2 TSK Fuzzy Logic Systems with Parameterized Conjunctors

In this approach, four Gaussian primary membership functions with uncertain mean are used for each input, and these membership functions are kept fixed as they are, since they are supposed to carry the linguistic information about the system. The center of these membership functions are determined by using IT2 FCM algorithm and the fuzzification parameters m_1 and m_2 are chosen as 1.8 and 2.3, respectively. The input membership functions used in the modeling application of Sinc function are given

in Figure 4.6. The i^{th} rule structure of the system is given as:

$$R^i = \text{IF } X_1 \text{ is } \tilde{A}_{i1} \text{ and } X_2 \text{ is } \tilde{A}_{i2},$$

$$\text{THEN } z^i = a_2^i x_2 + a_1^i x_1 + a_0^i$$

To calculate the firing strength of each rule, parameterized conjunctors are used as in the following:

$$\underline{\omega}^i = \underline{\mu}_{\tilde{A}_{i1}}(x_1)^{p_{il}} \cdot \underline{\mu}_{\tilde{A}_{i2}}(x_2)^{q_{il}} \quad (4.17)$$

$$\overline{\omega}^i = \overline{\mu}_{\tilde{A}_{i1}}(x_1)^{p_{iu}} \cdot \overline{\mu}_{\tilde{A}_{i2}}(x_2)^{q_{iu}} \quad (4.18)$$

where p_i and q_i are the parameters of the parameterized conjunctors and i indicates the number of rules ($i=1,2,\dots,16$). After the calculation of the firing strengths, the actual output of the system is calculated by using Equation 4.11. To tune the design parameters of the system, SQP optimization method is used. The parameters of the operators (16x4) are tuned in the interval of $0.1 \leq p_i, q_i \leq 50$, together with the coefficients of the right sides of the rules (16x3) in the interval of $-50 \leq a_2^i, a_1^i, a_0^i \leq 50$. The output of the model and the RMSE curve are given in Figure 4.7a-b and Figure 4.8a-b for Sinc and Rosenbrock's Banana functions, respectively. In this algorithm, the obtained RMSE values for the Sinc and Rosenbrock's Banana functions are 0.0531 and

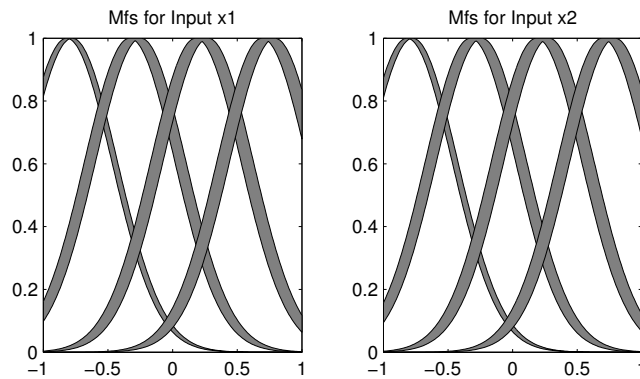


Figure 4.6. The input membership functions obtained by using IT2-FCM algorithm for Sinc function approximation without noise.

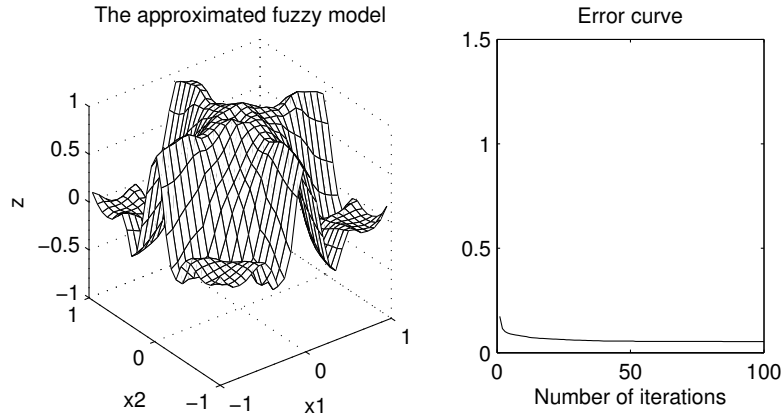


Figure 4.7. The result of Sinc function approximation by using IT2 TSK fuzzy algorithm (a) and the RMSE curve obtained by tuning the parameters of the parameterized conjunctor operators (b).

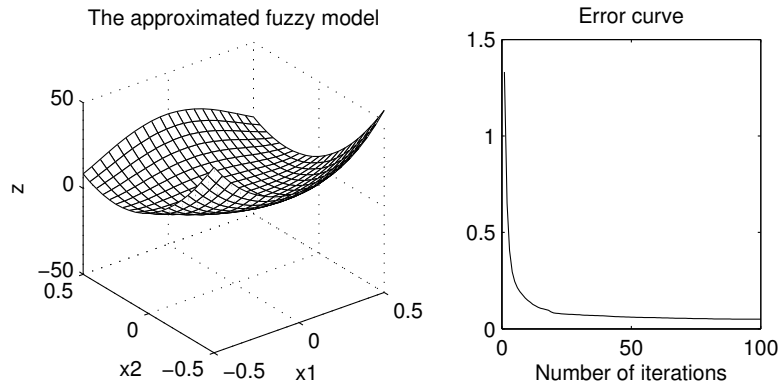


Figure 4.8. The result of Rosenbrock's Banana function approximation by using IT2 TSK fuzzy algorithm (a) and the RMSE curve obtained by tuning the parameters of the parameterized conjunctor operators (b).

0.0502, respectively.

4.3.3. Modeling Application with Noisy Measurement

In real world applications, noise is an inevitable event that should be considered in most of the applications. The modeling studies described above are repeated with the input values, x_1 and x_2 , being corrupted by noise. The uncertainty is represented by white noise. It is randomly generated. The mathematical description of the signal

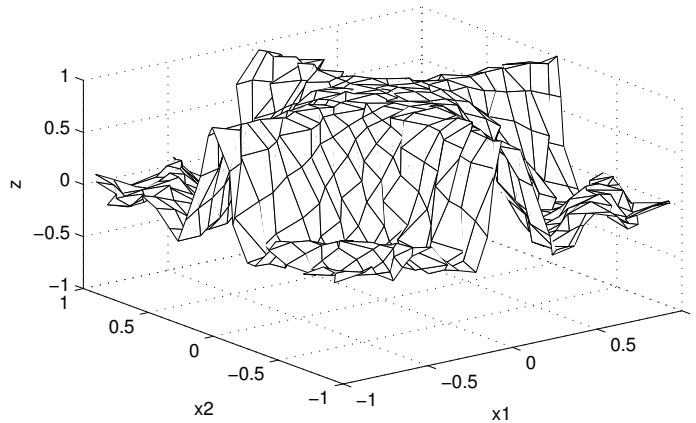


Figure 4.9. The Sinc function (30 dB noise added to the input signal).

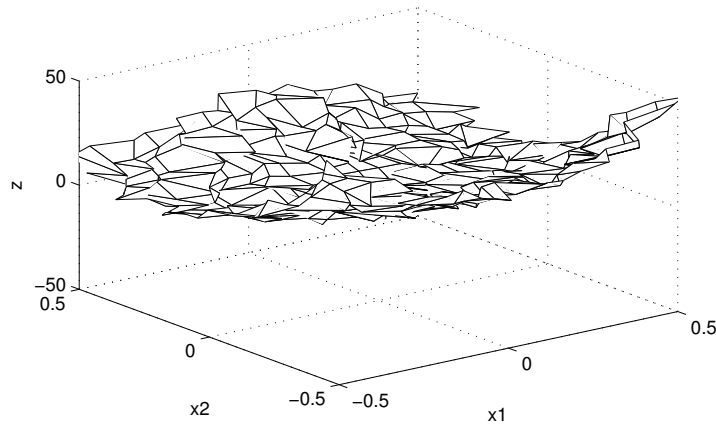


Figure 4.10. Rosenbrock's banana function (30 dB noise is added to the input signal).

to noise ratio (SNR) is given as follows:

$$n_{SNR} = 10 \log_{10} \frac{P_{Signal}}{P_{Noise}} \quad (4.19)$$

30 dB noise is added to the input signals. The corrupted nonlinear functions are given in Figures 4.9 and 4.10. To make a fair comparison, the same number and type of membership functions, and the same optimization method are used in modeling applications. The fuzzy methods that are described above are applied and the output of the model and the RMSE curve are given in Figures 4.11a-b through Figure 4.14a-b for Sinc and Rosenbrock's Banana functions, respectively. The resulting RMSE values are given in Table 4.1.

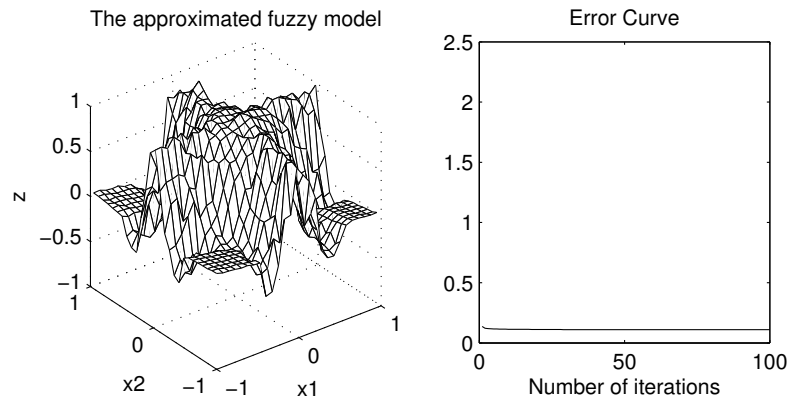


Figure 4.11. The result of Sinc function approximation by using type-1 fuzzy algorithm (a) and the RMSE curve obtained by tuning the parameters of the parameterized conjunctor operators (b).

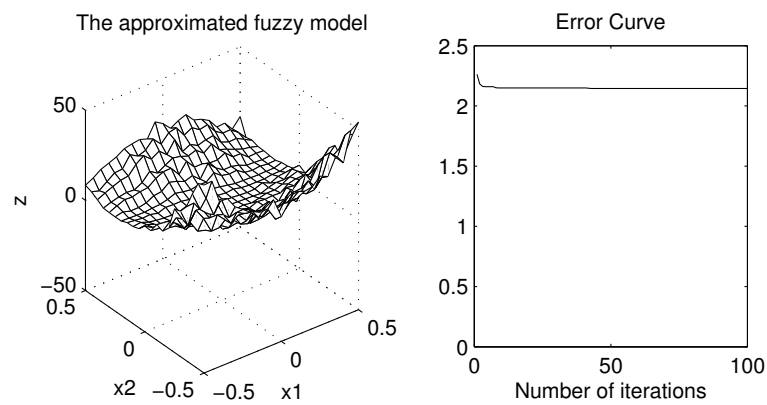


Figure 4.12. The result of Rosenbrock's Banana function approximation by using type-1 fuzzy algorithm (a) and the RMSE curve obtained by tuning the parameters of the parameterized conjunctor operators (b).

4.4. Conclusion

In this study, two fuzzy modeling methods are tested on the benchmark nonlinear functions; Sinc and Rosenbrock's banana functions with and without noisy input measurements. In both of the fuzzy approaches, the parameters of the parameterized conjunctors are tuned instead of antecedent membership function parameters and additionally the parameters of the consequent part of the rules are tuned.

The advantage of these algorithms is that the linguistic information of the system is not lost or distorted. When the results are examined in detail, it is seen that the

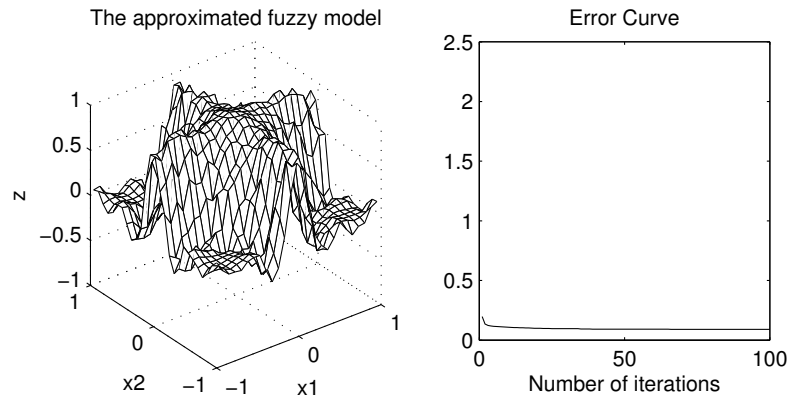


Figure 4.13. The result of Sinc function approximation by using IT2 TSK fuzzy algorithm (a) and the RMSE curve obtained by tuning the parameters of the parameterized conjunctors (b).

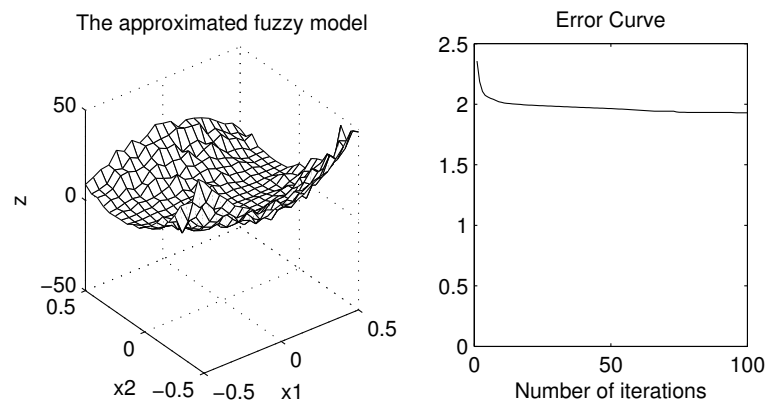


Figure 4.14. The result of Rosenbrock's Banana function approximation by using IT2 TSK fuzzy algorithm (a) and the RMSE curve obtained by tuning the parameters of the parameterized conjunctors (b).

use of interval type-2 fuzzy systems gives better RMSE value comparing to type-1 fuzzy algorithm. In addition, interval type-2 fuzzy algorithms are able to handle the uncertainties caused by the noisy input measurements. The results are consistent that interval type-2 fuzzy logic systems give better results when applied to systems having a large amount of uncertainty. The next step of this work will be applying and modifying these algorithms for real time control applications.

Table 4.1. Comparison of the Two Fuzzy Algorithms.

	Type-1 Fuzzy Algorithm	Type-2 Fuzzy Algorithm
RMSE for Sinc function	0.0777	0.0531
RMSE for Banana function	0.0675	0.0502
RMSE for Sinc function with noise	0.1094	0.0896
RMSE for Banana function with noise	2.1443	1.9292
Number of parameters	80	112
Optimization method	SQP	SQP
Iteration no	100	100

5. VALIDITY INDICES

In FCM clustering algorithms, the number of clusters is determined before the iteration procedure. However, the data sets in real life applications may not always be well separable. In literature, to overcome this problem, several validity indices are proposed. [34] represents a summary of fuzzy clustering indices in the literature.

In data mining applications, one important preprocessing is the normalization of data set. The reason for this is that a particular feature of data may be very large as compared to others and this can influence the accuracy of the clustering algorithm, especially in distance based algorithms. Additionally, normalization can have a positive effect on the computational time of the clustering algorithm. Data set can be scaled into a specific range by using one of the normalization procedures suggested in literature [53]. In this study, min-max normalization is used to scale the data sets into [0,1] range. It has the following form

$$\mathbf{x}_i = \frac{\mathbf{x}_i - \min(\mathbf{X})}{\max(\mathbf{X}) - \min(\mathbf{X})} \quad (5.1)$$

where \mathbf{x}_i is the data set ($i=1,\dots,N$).

In fuzzy clustering algorithms, one of the most significant problems is that the number of clusters has to be specified at the beginning of the algorithm. However, in real world applications, the data sets encountered are not always well-separable and therefore the number of clusters to be used may not be very obvious. To overcome this difficulty, a validity index can be used and there are many of these proposed in literature. In this study, a novel validity index is proposed and to illustrate the effectiveness of the proposed validity index, its performance is compared with some of the well-known validity indices; Partition Coefficient (PC) [35,36], Partition Entropy (PE) [37,38], Xie and Beni (XB) [39], Fukuyama and Sugeno (FS) [40] and PBM [41] on real and artificial data sets with an IT2 FCM clustering algorithm that uses Euclidean distance. The algorithm is iterated in the range of $C = 2, \dots, \sqrt{N}$ [34]. Depending on

the definition of the validity index measure, the minimum or maximum value of the measure gives the optimal number of clusters.

In below, an overview of the validity indices that are commonly used in literature is given together with the description of the proposed validity index.

5.1. Partition Coefficient (PC)

Bezdek has suggested the use of the following, named as Partition Coefficient, as a measure of the amount of overlap between the clusters [35, 36]:

$$V_{PC} = \frac{1}{N} \sum_{j=1}^C \sum_{i=1}^N u_{ji}^2 \quad (5.2)$$

In above u_{ji} is the membership value, C is the number of clusters and N is the sample number of the data set ($j=1, \dots, C$ and $i=1, \dots, N$). The maximum value of Partition Coefficient gives the optimal number of clusters.

5.2. Partition Entropy (PE)

Another validity index that Bezdek has proposed is Partition Entropy (PE) and has the following form [37, 38]:

$$V_{PE} = -\frac{1}{N} \sum_{j=1}^C \sum_{i=1}^N u_{ji} \log_a u_{ji} \quad (5.3)$$

The minimum value of Partition Entropy gives the optimal number of clusters.

5.3. Xie and Beni (XB) Validity Index

Xie and Beni [39], proposed the following validity index:

$$V_{XB} = \frac{\sum_{j=1}^C \sum_{i=1}^N u_{ji}^m \|\mathbf{x}_i - \mathbf{v}_j\|^2}{N \min_{j,i} \|\mathbf{v}_j - \mathbf{v}_i\|^2} \quad (5.4)$$

where the numerator and the denominator indicate the compactness and the separation of the clusters respectively. The compactness is the closeness of the clusters and the separation is the furthest distance between the clusters [34]. This validity index uses both inter and intra cluster distances. The minimum value of the validity index gives the optimal number of clusters.

5.4. Fukuyama Sugeno (FS) Validity Index

Fukuyama and Sugeno [40], proposed the following validity index:

$$V_{FS} = \sum_{j=1}^C \sum_{i=1}^N u_{ji}^m \|\mathbf{x}_i - \mathbf{v}_j\|^2 - \sum_{j=1}^C \sum_{i=1}^N u_{ji}^m \|\mathbf{v}_j - \bar{\mathbf{v}}\|^2 \quad (5.5)$$

where $\bar{\mathbf{v}} = \sum_j^C \mathbf{v}_j / C$. Compactness of the clusters is calculated at the first part of the validity index. At the second part, the distance between the j_{th} cluster center to the mean of the clusters centers are multiplied by the each row of the membership value \mathbf{U} . The minimum value of the validity index gives the optimal number of cluster.

5.5. PBM Validity Index

PBM index is proposed by Pakhira et al. [41], which is used with crisp and fuzzy clustering algorithms. In this study, the index that is used in FCM algorithms is considered.

$$V_{PBM} = \left(\frac{1}{C} \times \frac{E_1}{E_C} \times D_C \right)^2 \quad (5.6)$$

$$E_C = \sum_{j=1}^C \sum_{i=1}^N u_{ji}^m \|\mathbf{x}_i - \mathbf{v}_j\| \quad (5.7)$$

$$E_1 = \sum_{i=1}^N u_{ji} \|\mathbf{x}_i - \mathbf{v}\| \quad (5.8)$$

$$D_C = \max_{j,i=1}^C \|\mathbf{v}_j - \mathbf{v}_i\| \quad (5.9)$$

This validity index is composed of three factors. The first one is $1/C$ which is the inverse proportion of the number of clusters. The second factor is the ratio between E_1 and E_C . E_1 is a constant value and E_C decreases while the number of clusters is increasing. The last factor is D_C which is the maximum separation between the clusters and increases as the number of clusters increase. The choice of the fuzzification parameter m is also significant. The optimal number of clusters in a data set is achieved when the validity index reaches to its maximum value.

5.6. Proposed Validity Index

The novel validity index proposed in this study is based on the separation of the clusters and the closeness of the data objects in one cluster to the cluster center [54]. The separation is obtained by using the following:

$$V_{separation} = \max_{j,i=1}^C \|\mathbf{v}_j - \mathbf{v}_i\| \quad (5.10)$$

where \mathbf{v}_i is the center value of each cluster ($j,i=1,\dots,C$ and $j \neq i$). The larger the value of Equation 5.10 is, the more separated the cluster centers are.

The compactness of a cluster is obtained by using:

$$V_{compactness} = \frac{\sum_{i=1}^N \max_j(u_{ji})}{\sum_{i=1}^N \min_j(u_{ji})} \quad (5.11)$$

where u_{ji} is the membership value ($j=1, \dots, C$ and $i=1, \dots, N$). The larger this value is, the closer are the data objects of the cluster to the cluster center. In the following the proposed validity index is given.

$$V_p = \frac{1}{C^2} \frac{\max_{j,i=1}^C \|\mathbf{v}_j - \mathbf{v}_i\| \sum_{i=1}^N \max_j(u_{ji})}{\sum_{i=1}^N \min_j(u_{ji})} \quad (5.12)$$

When the number of clusters increases, both the separation and the compactness values increase, resulting in a large increase in the validity index. The $1/C^2$ term in the index allays this tendency. The optimal number of clusters is obtained when the value of this validity index reaches a maximum. It is to be noted that the main difference of the proposed validity index as compared to PBM-index is that the proposed validity index uses only the inter cluster distance and the membership value and therefore is simpler. Additionally, it is not sensitive to the choice of the fuzzification parameter m .

5.7. Clustering Application

In the first part of this study, the validity indices explained above and the proposed new validity index are tested on real and artificial data sets [54]. The Iris data set given in [55] has 150 samples and 4 features, sepal length, sepal width, petal length, and petal width in centimeters. The data set has three classes, Setosa, Versicolour, and Virginica; among these classes two are not linearly separable while the other one is. The optimal cluster number is three. The Breast Cancer data set given in [55] has 683 samples and 9 features. The data set has two clusters. The Wine data set in [55] has 178 samples and 13 features. The data set has three types of wine each from different cultivators in Italy, and it is defined by chemical analysis of these wines. The artificial data has six clusters and the clusters are close to each other. In the application of IT2 FCM clustering, first of all, all of the sets are normalized. Several simulation studies

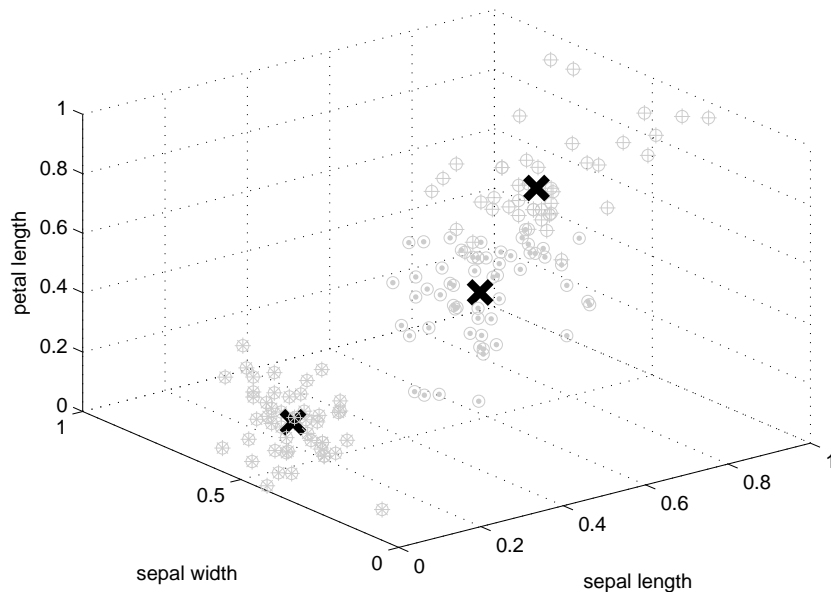


Figure 5.1. Iris data set.

then are carried out, in which C is taken as $C = 2, \dots, \sqrt{N}$ where N is the sample number of the data set. The fuzzification parameters m , m_1 , and m_2 are chosen as 2, 1.8, and 2.3, respectively. The results of the validity indices are given in Table 5.1. Additionally, the centers of the Iris data and the noisy artificial data are indicated in Figure 5.1 and 5.2, respectively. When the results are examined in detail, it is seen that the proposed validity index is able to determine the correct number of clusters for all data sets. Although the cluster numbers obtained by the PBM-index are the same except for the artificial data set; it should not be forgotten that the computational burden of the proposed index is lower because it uses only inter cluster distance and membership value. In the second part of the study, the proposed validity index is used to determine the number of fuzzy rules in the IT2 FNS with parameterized conjunctors used for modeling and control purposes.

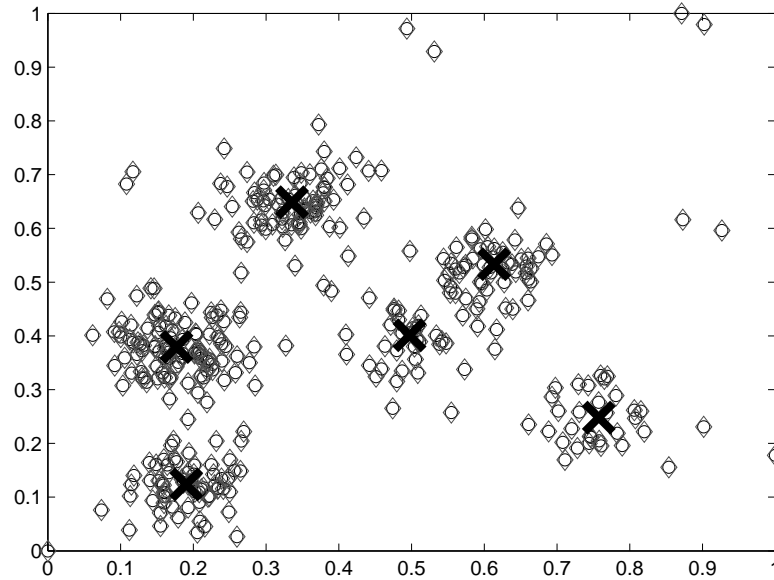


Figure 5.2. Noisy Artificial data set.

Table 5.1. The optimal number of clusters for different data sets using the IT2 FCM clustering algorithm.

Data Set	Iris	Breast Cancer	Wine	Artificial
Cluster No	3	2	3	6
PC	2	2	2	2
PE	2	2	2	2
XB	2	2	3	5
FS	4	4	2	6
PBM	3	2	3	5
Proposed	3	2	3	6

6. INTERVAL TYPE-2 FUZZY NEURAL SYSTEM WITH PARAMETERIZED CONJUNCTORS

Type-2 fuzzy systems are capable of handling uncertain and imprecise information. In this study, a TSK type fuzzy structure, which is commonly used for modeling benchmark nonlinear systems, is used. Interval type-2 TSK FLSs are divided into three models, depending on the types of membership functions used in the antecedents and the consequents of the fuzzy IF-THEN rules [17]. In this study, to reduce the computational burden of the type-2 fuzzy system, the second model is used, in which the fuzzy sets in the antecedent are of type-2 and the consequent is a first order polynomial [17]. The i^{th} rule structure for M rules and n antecedents is

$$\begin{aligned} R^i &= \text{IF } x_1 \text{ is } \tilde{A}_{i1} \text{ and } \dots \text{ and } x_n \text{ is } \tilde{A}_{in}, \\ \text{THEN } z^i &= a_n^i x_n + a_{n-1}^i x_{n-1} + \dots + a_0^i \end{aligned}$$

where z^i is the output of the system and is a first order polynomial. a_n^i are the coefficients of the polynomial. x_n is the input and \tilde{A}_{in} are the interval type-2 fuzzy sets.

The structure of the interval type-2 Fuzzy Neural System (IT2 FNS) used in this study is as given in Figure 6.1 [22]. In this structure, the input is given at the first layer. In the second layer, the input space is interpreted by Gaussian membership functions with uncertain means that have the following form:

The upper membership function is

$$\bar{\mu}_{\tilde{A}_{in}}(x) = \begin{cases} e^{-\frac{1}{2}\left(\frac{x-v_1}{\sigma}\right)^2}, & x < v_1 \\ 1, & v_1 \leq x \leq v_2 \\ e^{-\frac{1}{2}\left(\frac{x-v_2}{\sigma}\right)^2}, & x > v_2 \end{cases} \quad (6.1)$$

The lower membership function is

$$\underline{\mu}_{\tilde{A}_{in}}(x) = \begin{cases} e^{-\frac{1}{2}\left(\frac{x-v_2}{\sigma}\right)^2}, & x \leq \frac{v_1+v_2}{2} \\ e^{-\frac{1}{2}\left(\frac{x-v_1}{\sigma}\right)^2}, & x > \frac{v_1+v_2}{2} \end{cases} \quad (6.2)$$

where v_1 and v_2 are the centers and σ is the standard deviation of the membership functions. i indicates the number of rules ($i=1,\dots,M$) and n is the number of antecedents. The centers of these membership functions are determined by the interval type-2 FCM clustering algorithm given in [33]. The aim is to find the optimum center and the membership value by minimizing Equations 3.4 and 3.5. Then, it is assumed that these membership functions carry a degree of expert knowledge about the system. The IT2 FNS design approach described in this study has the goal of preserving this expert knowledge about the system. Therefore, in the proposed structure, parameterized conjunctors (t-norms) are used and, instead of tuning the parameters of the membership functions, the parameters of the parameterized conjunctors are tuned. At the third layer, the firing strength of each rule is calculated using “meet under the product t-norm” [16]. In the calculations of interval type-2 fuzzy sets, the upper and the lower membership functions are used and they are type-1 fuzzy sets. Thus, type-1 fuzzy arithmetic can be used in calculations of interval type-2 fuzzy sets. A general

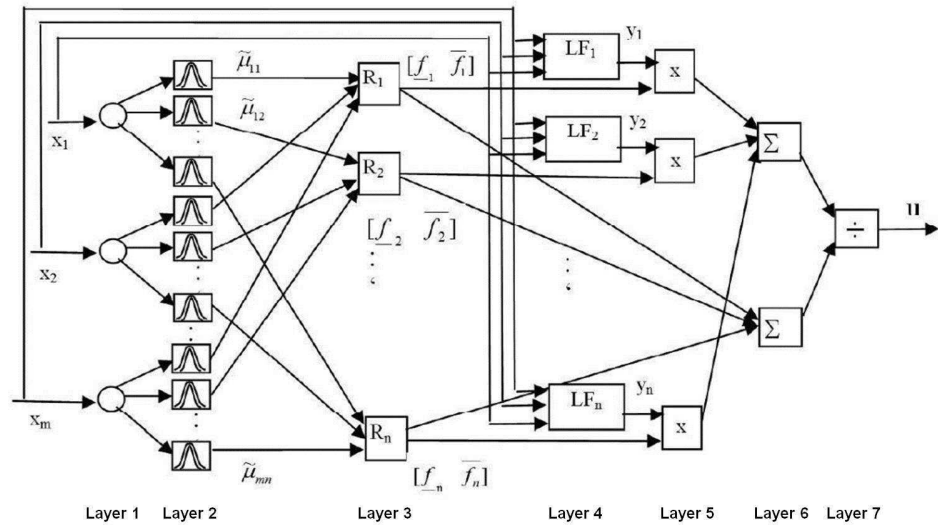


Figure 6.1. The structure of a Type-2 FNS.

formulation of the meet of interval type-2 fuzzy sets is

$$\prod_{j=1}^n A_j = [\underline{\omega}^i, \bar{\omega}^i] \quad (6.3)$$

where n indicates the antecedent number ($j = 1, 2, \dots, n$) and i indicates the rule number. A_j is the interval type-1 fuzzy set [16]. The meet of interval type-2 fuzzy sets under product t-norm is computed basically via the lower and the upper membership functions. In the proposed algorithm, for the calculation of the lower and the upper bounds of the firing strength, a parameterized product t-norm is used as follows:

$$\bar{\omega}^i = \bar{\mu}_{\bar{A}_{1i}}(x_1)^{\bar{p}_{1i}} \cdots \bar{\mu}_{\bar{A}_{ni}}(x_n)^{\bar{p}_{ni}} \quad (6.4)$$

$$\underline{\omega}^i = \underline{\mu}_{\bar{A}_{1i}}(x_1)^{p_{1i}} \cdots \underline{\mu}_{\bar{A}_{ni}}(x_n)^{p_{ni}} \quad (6.5)$$

The output of the consequent part of each rule is determined at the fourth layer. At the fifth, sixth, and seventh layers of the neuro-fuzzy structure, the type reduction and the defuzzification procedures are realized and the output of the system is determined by the inference engine proposed in [51], and the output has the following form:

$$u = r \frac{\sum_{i=1}^M \underline{\omega}^i z^i}{\sum_{i=1}^M \underline{\omega}^i} + q \frac{\sum_{i=1}^M \bar{\omega}^i z^i}{\sum_{i=1}^M \bar{\omega}^i} \quad (6.6)$$

where $\underline{\omega}^i$ and $\bar{\omega}^i$ are the lower and upper firing strength of each rule, respectively. r and q are the design parameters that weight the lower and upper part of the output of the neuro-fuzzy system, M is the number of rules.

6.1. The Training of the Interval Type-2 FNS with Parameterized Conjunctors

In the design of the interval type-2 FNS with parameterized conjunctors, the design parameters are the parameters of the parameterized conjunctors at the antecedent

of the rules, the coefficients of the first order polynomial at the consequent of the rules, and the r and q values of Equation 6.6. These values are tuned using the gradient descent algorithm. The output error is calculated as in the following:

$$E = \frac{1}{2} \sum_{i=1}^O (u_i^d - u_i)^2 \quad (6.7)$$

where u_i^d and u_i are the desired and the actual output of the network, respectively, and O is the number of outputs. The coefficients at the consequent of the rules, a_{ij} , a_{0j} and the parameters of the parameterized conjunctors, \bar{p}_{ij} , \underline{p}_{ij} are tuned using gradient descent algorithm as follows:

$$a_{ij}(t+1) = a_{ij}(t) - \lambda \frac{\partial E}{\partial a_{ij}} \quad (6.8)$$

$$a_{0j}(t+1) = a_{0j}(t) - \lambda \frac{\partial E}{\partial a_{0j}} \quad (6.9)$$

$$\bar{p}_{ij}(t+1) = \bar{p}_{ij}(t) - \lambda \frac{\partial E}{\partial \bar{p}_{ij}} \quad (6.10)$$

$$\underline{p}_{ij}(t+1) = \underline{p}_{ij}(t) - \lambda \frac{\partial E}{\partial \underline{p}_{ij}} \quad (6.11)$$

where λ is the learning rate. The derivatives in Equations 6.8-6.11 are determined as follows:

$$\frac{\partial E}{\partial a_{ij}} = \frac{\partial E}{\partial u} \frac{\partial u}{\partial z_j} \frac{\partial z_j}{\partial a_{ij}} \quad (6.12)$$

$$\frac{\partial E}{\partial a_{0j}} = \frac{\partial E}{\partial u} \frac{\partial u}{\partial z_j} \frac{\partial z_j}{\partial a_{0j}} \quad (6.13)$$

$$\frac{\partial E}{\partial \bar{p}_{ij}} = \frac{\partial E}{\partial u} \frac{\partial u}{\partial \bar{\omega}_j} \frac{\partial \bar{\omega}_j}{\partial \bar{\mu}_{ij}} \frac{\partial \bar{\mu}_{ij}}{\partial \bar{p}_{ij}} \quad (6.14)$$

$$\frac{\partial E}{\partial \underline{p}_{ij}} = \frac{\partial E}{\partial u} \frac{\partial u}{\partial \underline{\omega}_j} \frac{\partial \underline{\omega}_j}{\partial \underline{\mu}_{ij}} \frac{\partial \underline{\mu}_{ij}}{\partial \underline{p}_{ij}} \quad (6.15)$$

where

$$\frac{\partial E}{\partial u} = u(t) - u^d(t); \quad (6.16)$$

$$\frac{\partial u}{\partial \underline{\omega}_j} = r \frac{z_j - \underline{u}}{\sum_{j=1}^n \underline{\omega}_j}; \quad \frac{\partial u}{\partial \bar{\omega}_j} = q \frac{z_j - \bar{u}}{\sum_{j=1}^n \bar{\omega}_j}$$

$$\underline{u} = \frac{\sum_{j=1}^n \underline{\omega}_j z_j}{\sum_{j=1}^n \underline{\omega}_j}; \quad \bar{u} = \frac{\sum_{j=1}^n \bar{\omega}_j z_j}{\sum_{j=1}^n \bar{\omega}_j} \quad (6.17)$$

t-norm *prod* operator has the following form:

$$\frac{\partial \bar{\omega}_j}{\partial \bar{\mu}_{ij}} = \bar{p}_{ij} \bar{\mu}_{ij}^{(\bar{p}_{ij}-1)} \prod_{\substack{k=1 \\ k \neq i}}^{N_1} \bar{\mu}_{kj}^{\bar{p}_{kj}} \quad (6.18)$$

$$\frac{\partial \underline{\omega}_j}{\partial \underline{\mu}_{ij}} = \underline{p}_{ij} \underline{\mu}_{ij}^{(\underline{p}_{ij}-1)} \prod_{\substack{k=1 \\ k \neq i}}^{N_1} \underline{\mu}_{kj}^{\underline{p}_{kj}} \quad (6.19)$$

where $i = 1, \dots, N_1, k = 1, \dots, N_1$, and $j = 1, \dots, N_2$.

$$\frac{\partial \bar{\mu}_{ij}}{\partial \bar{p}_{kj}} = \prod_{i=1}^{N_1} \bar{\mu}_{ij}^{\bar{p}_{ij}} \ln(\bar{\mu}_{kj}) \quad (6.20)$$

$$\frac{\partial \underline{\mu}_{ij}}{\partial \underline{p}_{kj}} = \prod_{i=1}^{N_1} \underline{\mu}_{ij}^{\underline{p}_{ij}} \ln(\underline{\mu}_{kj}) \quad (6.21)$$

The parameters r and q enable us to adjust the lower and upper portions of the final output in Equation 6.6. The initial value for both parameters is chosen as 0.5, and the optimization algorithm for these parameters is given in the following:

$$r(t+1) = r(t) - \gamma \frac{\partial E}{\partial r} \quad (6.22)$$

$$q(t+1) = q(t) - \gamma \frac{\partial E}{\partial q} \quad (6.23)$$

where

$$\frac{\partial E}{\partial r} = (u - u^d) \frac{\omega_j}{\sum_{j=1}^n \omega_j} \quad (6.24)$$

$$\frac{\partial E}{\partial q} = (u - u^d) \frac{\bar{\omega}_j}{\sum_{j=1}^n \bar{\omega}_j} \quad (6.25)$$

6.2. Modeling and Control Applications

As has been stated earlier, this study suggests the use of parameterized conjunctions in an IT2 FNS. Additionally, the use of a novel validity index is suggested for the optimal partitioning of the input space. The flow of the approach is depicted in Figure 6.2. The first aim is to determine some meaningful knowledge about the system and

not to lose or distort this knowledge subsequently. For this purpose, first of all, the interval type-2 fuzzy c-means clustering algorithm is applied to the input data set. In order to set the number of clusters (as required by the algorithm), a validity index measure is used. It is a common problem that one or more features of the given input data set may outweigh others. To alleviate this problem, the data is normalized at the beginning of the procedure. After acquiring some knowledge about the system in this way, IT2 FNS with parameterized conjunctors is used for modeling and control purposes as described in the subsequent subsections in detail.

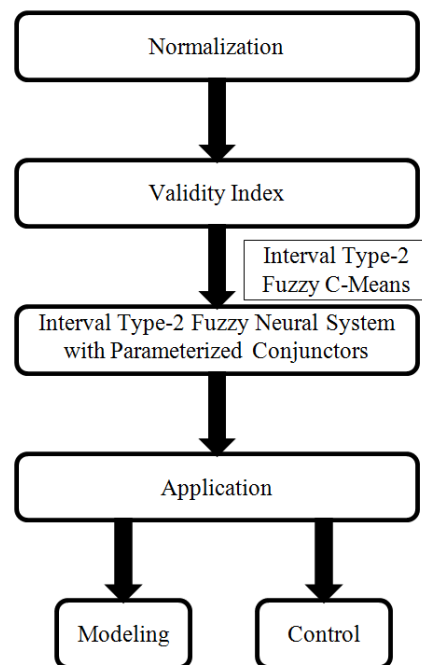


Figure 6.2. The flow-chart of the proposed approach.

6.2.1. Modeling of a Nonlinear System

System modeling is an important area in engineering. In this study, the interval type-2 fuzzy neural system with parameterized conjunctors is used to estimate the fuzzy model parameters using the measured input and output data [54]. The algorithm is tested for the modeling of a nonlinear, benchmark single input single output (SISO) dynamic system, which is characterized by the following equation [56]:

$$y(k+1) = f(y(k), y(k-1), y(k-2), u(k), u(k-1)) =$$

$$\frac{y(k)y(k-1)y(k-2)u(k-1)(y(k-2)-1) + u(k)}{1 + (y(k-2))^2 + (y(k-1))^2}$$

Here, the $y(k)$ is the current output of the system. $u(k)$ is the current excitation signal given as follows:

$$u(k) = \begin{cases} \sin(\frac{\pi k}{25}), & k < 250 \\ 1, & 250 \leq k < 500 \\ -1, & 500 \leq k < 750 \\ 0.3\sin(\frac{\pi k}{25}) + 0.1\sin(\frac{\pi k}{32}) + 0.6\sin(\frac{\pi k}{10}), & 750 \leq k < 1000 \end{cases}$$

The excitation signal $u(k)$ and the current output of the system $y(k)$ are used as the inputs of the IT2 FNS structure, and $y(k+1)$ is the output of the system. The input data is clustered using the IT2 FCM clustering algorithm. The validity indices are used to determine the number of fuzzy rules to be used in IT2 FNS with parameterized conjunctors. The results of the validity indices are given in Table 6.1. The value of the fuzzification parameter m is taken as 2, m_1 and m_2 values are chosen as 1.8 and 2.8, respectively. For the determination of the number of the fuzzy rules, the result of the proposed validity index is used. Therefore, three Gaussian membership functions for each input are used for the interpretation of the input space, as shown in Figure 6.3. A number of simulation studies are carried out. During the training, gradient descent

Table 6.1. The optimal number of clusters for the data set using the IT2 FCM clustering algorithm.

	PC	PE	XB	FS	PBM	Proposed
Number of classes	2	2	2	6	4	3

is applied as the learning algorithm. This is used to determine the coefficients at the consequent of the fuzzy rules; the parameterized conjunctive values; and the parameter values, r and q , which specify the upper and the lower portion of the output of the fuzzy system. The learning rate is chosen as 0.03. The initial values of the coefficients at the consequent of the fuzzy rules are selected randomly, the initial values for the parameterized conjunctors are chosen as 1 and for the parameters r and q , as 0.5. The parameterized conjunctors are tuned in the closed interval of $[0.1, 100]$. The final values of the parameterized conjunctors are given as follows: $\underline{p}_{ni} = [0.9914, 0.8766, 0.6522; 1.5260, 1.1859, 1.0438]$ and $\bar{p}_{ni} = [0.9694, 0.9943, 0.8270; 1.2116, 1.1704, 1.0972]$. The output and the RMSE (root mean square error) value are indicated in Figure 6.4 and 6.5, respectively. The obtained training RMSE is 0.0304 and the testing error is 0.0363. In Table 6.2, the RMSE values, the number of design parameters, and the CPU (central processing unit) time in seconds for training are compared with type-1 fuzzy neural system (T1 FNS) and IT2 FNS (with non-parameterized t-norms) [22]. The initial membership functions for T1 FNS are distributed equally onto the input domain. In IT2 FNS, the membership functions that are obtained by the proposed approach are used as the initial membership functions. During the optimization process of these

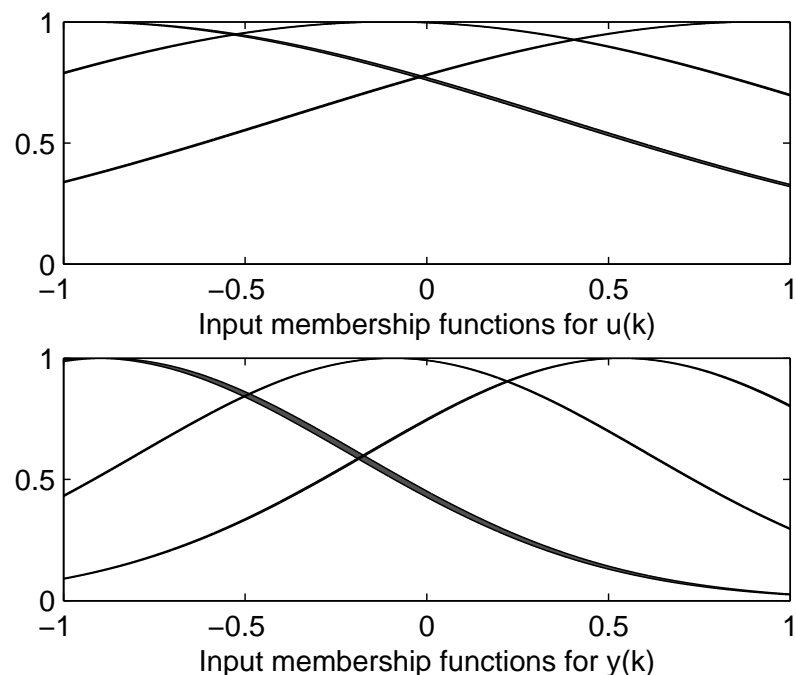


Figure 6.3. The knowledge obtained by the use of IT2 FCM clustering algorithm.

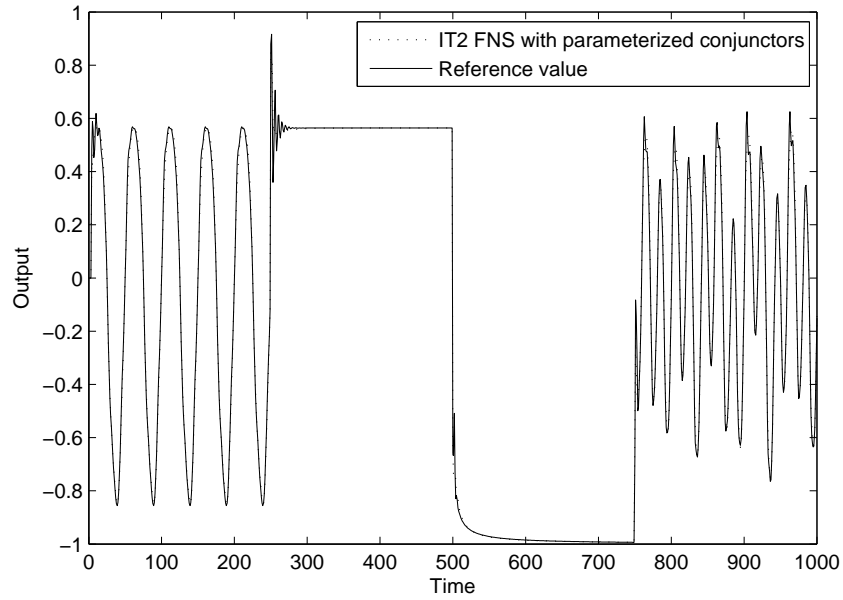


Figure 6.4. The performance IT2 FNS with parameterized conjunctors.

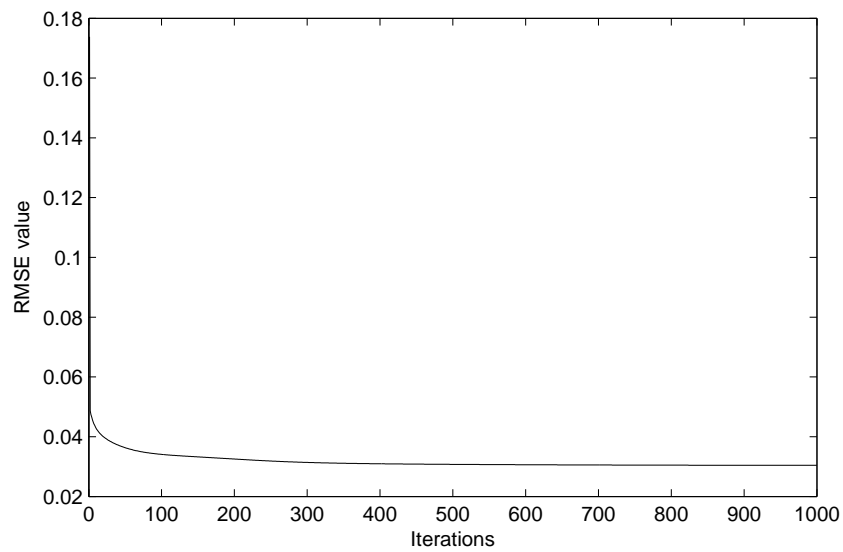


Figure 6.5. The RMSE value obtained.

Table 6.2. The comparison of various structures in modeling application.

Methods	RMSE (Training)	RMSE (Testing)	No. of Parameters	CPU Time
T1 FNS	0.0392	0.0454	21	141.8
IT2 FNS [22]	0.0318	0.0374	29	325.9
IT2 FNS with parameterized conjunctors	0.0304	0.0363	23	253.4

FNS structures, whatever information that is in these membership functions may be lost or distorted. However, in the proposed approach the parameters of these membership functions are kept fixed and the parameters of the parameterized conjunctors are tuned instead. Additionally, in T1 and IT2 FNS, the number of fuzzy rules is determined heuristically. In the proposed approach, however, the number of fuzzy rules is determined by a validity index measure. To make a fair comparison, the same number of fuzzy rules are used in all the fuzzy approaches. The results obtained illustrate that type-2 fuzzy algorithms have less RMSE value as compared to T1 FNS algorithm; however, they require more computational time.

6.2.2. Control Application

The proposed approach [54] is also tested for the control of a Quarter Car Model (QCM) in Figure 6.6. The model has a single wheel with a mass. The car is assumed to move with a velocity, v . Road friction force F_x is generated between the wheel and the road in the opposite direction of car's motion. T_b is the braking torque, which causes the wheel to slow down. The mathematical model of the quarter car is given by the following dynamic equations [57, 58]:

$$\dot{\omega} = \frac{R}{J}F_x - \frac{\text{sign}(\omega)}{J}T_b \quad (6.26)$$

$$\dot{v} = -\frac{F_x}{m} \quad (6.27)$$

In these equations F_x and F_z can be expressed as:

$$F_x = F_z \mu(\lambda) \quad (6.28)$$

$$F_z = mg \quad (6.29)$$

During driving, the speed of the vehicle and the rotational velocity of the wheel have matching values. However, during braking, a braking torque is generated at the interface between the wheel and road surface, which causes the wheel speed to decrease. Consequently, the wheel speed will tend to be lower than the vehicle speed. The parameter used to specify this difference is called wheel slip and denoted by λ .

$$\lambda = \frac{v - \omega r}{v} \quad (6.30)$$

A zero wheel slip means that the wheel velocity is equal to the speed of the car, whereas a ratio of one indicates that the wheel is not rotating, but the car is still moving, *i.e.* the wheels are skidding on the road and the vehicle is no longer steerable.

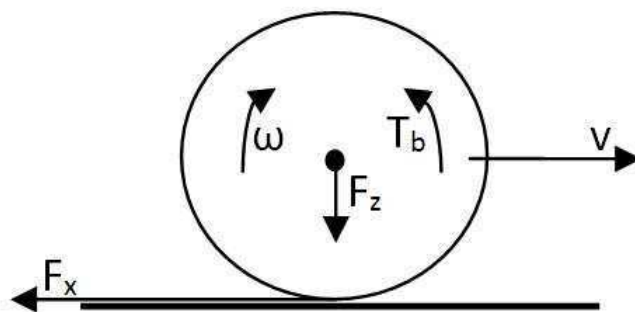


Figure 6.6. Schematic view of the Quarter Car Model (QCM).

The road adhesion coefficient is a nonlinear function that depends on slip value and some parameters. In this study, the Burckhardt formula [59] is used, which is defined as:

$$\mu(\lambda) = c_1(1 - e^{-c_2\lambda}) - c_3\lambda \quad (6.31)$$

where c_1 , c_2 , and c_3 represent the road surface condition and λ is the slip value. The relation between road adhesion coefficient and slip value is given in Figure 6.7. In this study, the reference slip value is chosen as 0.2 and it is assumed that the car is moving on dry asphalt. The numerical values used in the simulations are given in Tables 6.3 and 6.4, respectively.

6.2.3. The Simulation Results

The proposed approach is used on the quarter car model, and the block diagram of the control system being used is as given in Figure 6.8, where e , the error and Δe , the derivative of the error, are the inputs to the system, g is the reference signal, u

Table 6.3. System Parameters.

ω	Angular velocity of the wheel (rad/s)
v	Velocity of the car (m/s)
r	Radius of the wheel (m)
J	Inertia of the wheel (kgm^2)
F_x	Road friction force (kgm/s^2)
F_z	Vertical load (kgm/s^2)
T_b	Braking Torque (kgm^2/s^2)
m	Mass of the vehicle (kg)
g	Gravitational force (m/s^2)
$\mu(\lambda)$	Road adhesion coefficient
λ	Wheel slip

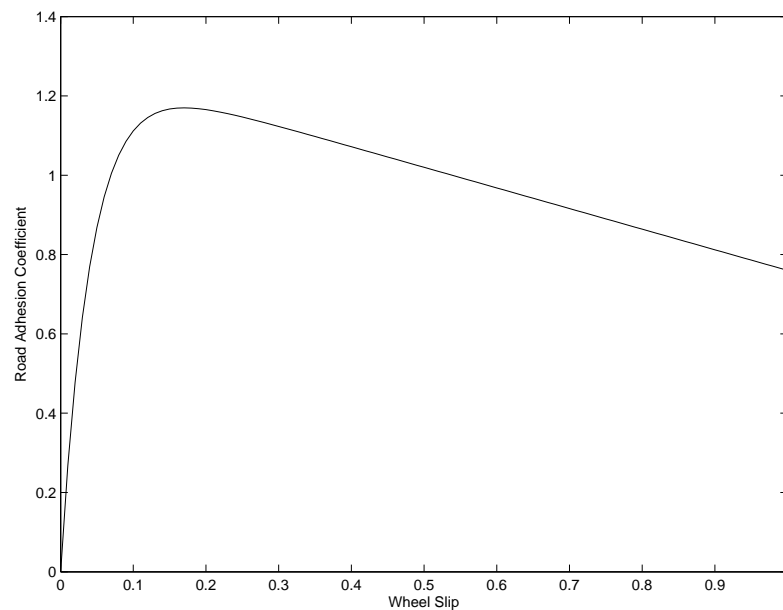


Figure 6.7. Road adhesion coefficient vs. wheel slip.

Table 6.4. System Parameters.

$v_0 = 25(m/s)$	$r = 0.32(m)$	$J = 1(kgm^2)$
$g = 9.81(m/s^2)$	$m = 350(kg)$	$m_0 = 350(kg)$
$c_1 = 1.28$	$c_2 = 23.99$	$c_3 = 0.52$

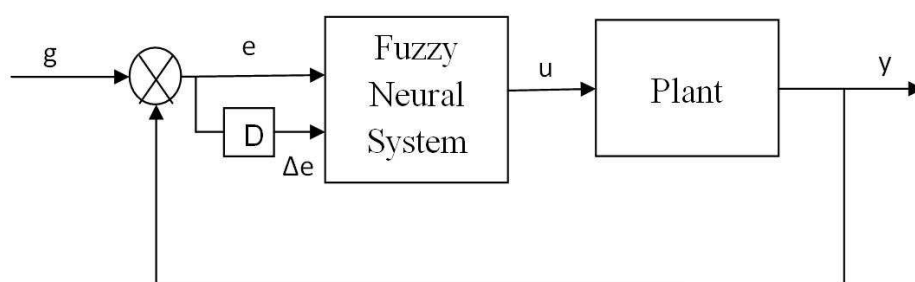


Figure 6.8. The block diagram of the type-2 neuro-fuzzy system.

is the control input signal, and y is the output of the system [54]. First of all, the expert knowledge about the system is generated by the IT2 FCM clustering algorithm. For this purpose, the quarter car model is controlled by an IT2 FNS. The obtained error and the derivative of the error values are used in the application of the IT2 FCM clustering algorithm. The fuzzification parameters m , m_1 , and m_2 are taken as 2, 1.8, and 2.3, respectively. The proposed validity index is used to determine the

Table 6.5. The optimal number of clusters for QCM input data using the IT2 FCM clustering algorithm.

	PC	PE	XB	FS	PBM	Proposed
Number of classes	2	2	2	9	7	5

fuzzy rules of the fuzzy structure. The results of the validity indices are given in Table 6.5. A number of simulations are realized with the sampling time set to $1ms$. The initial velocity of the car is chosen as $25 (m/s)$ before the braking operation. The reference wheel slip is set to 0.2, which corresponds to the peak value of $\mu - \lambda$. The proposed approach is tested both without and with noisy input measurement, and the results are given in Figures 6.9 and 6.12. The applied noise is depicted in Figure 6.11. The signal-to-noise ratio (SNR) is about 30dB. The parameterized conjunctors are initially set to 1 and are tuned in the interval of $[0.1, 100]$. The obtained values of \underline{p}_{ni} and \bar{p}_{ni} without and with noise in the input measurements are given as follows; $\underline{p}_{ni} = [1.6257, 1.0945, 1.0337, 0.5976, 0.8641; 1.6648, 1.1258, 0.9350, 0.1083, 1.1495]$, $\bar{p}_{ni} = [0.1073, 1.2394, 1.2330, 1.2766, 1.3410; 0.1010, 1.2979, 1.2935, 1.3893, 1.5449]$ and $\underline{p}_{ni} = [3.2031, 2.7929, 3.8361, 0.1100, 2.3736; 3.1848, 2.7146, 3.6040, 0.1100, 2.0082]$, $\bar{p}_{ni} = [3.8713, 3.8991, 0.1100, 3.6123, 3.4932; 3.7843, 3.8427, 0.1007, 3.5607, 3.3997]$, respectively. The velocity of the wheel and the car without and with noisy input measurements is given in Figure 6.10 and 6.13, respectively. The RMSE values of T1 FNS, IT2 FNS, and the proposed approach without and with noisy input measurements is given in Table 6.6. The fuzzy approaches have similar RMSE values without noise in the input measurements, which is as expected. When noise is added into the input measurements, the type-2 fuzzy approaches are able to handle the uncertainties and have less RMSE value as compared to their type-1 counterpart. The main characteristic of the proposed approach is that it has fewer design parameters than IT2 FNS.

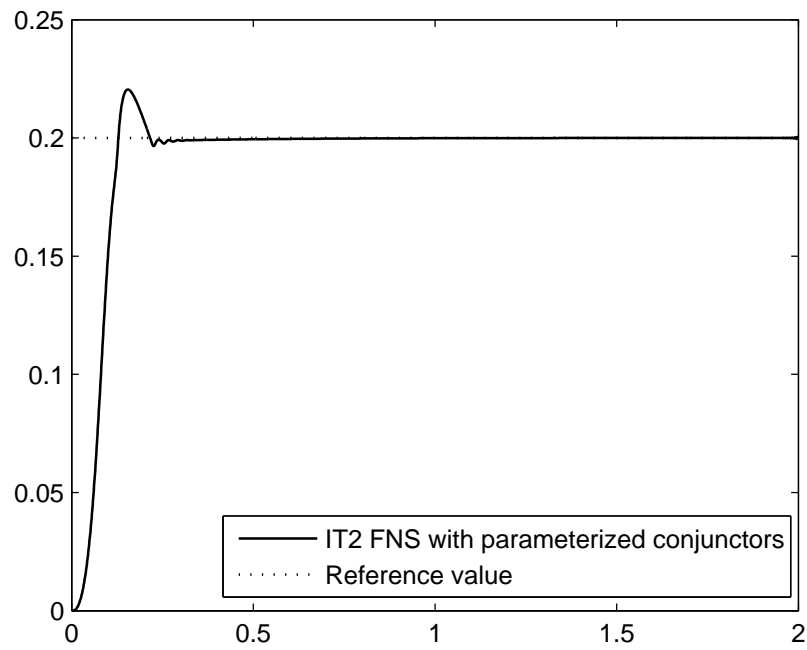


Figure 6.9. Wheel slip of type-2 FNS with parameterized conjunctors.

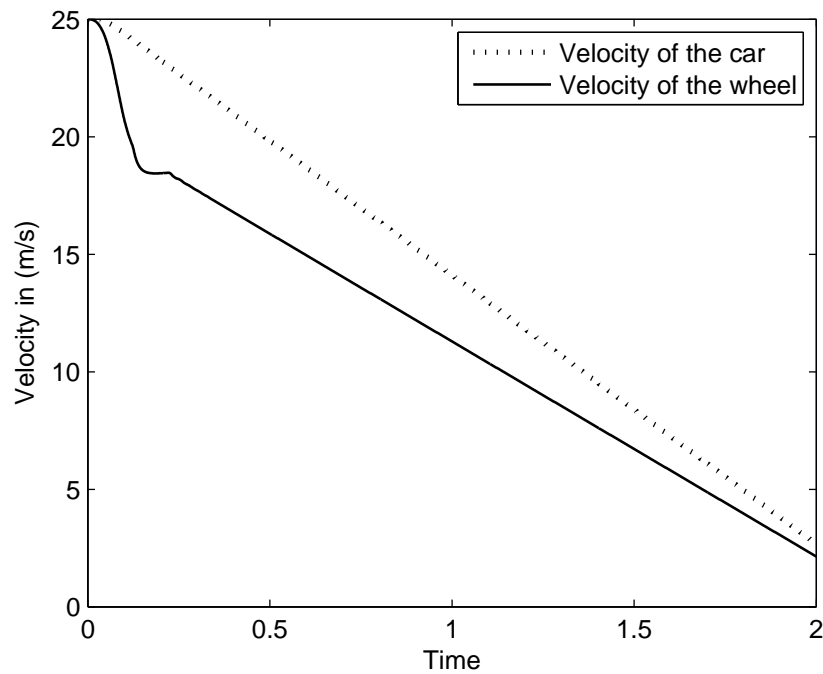


Figure 6.10. Velocity of the wheel and car without noisy input measurement.

6.3. Conclusion

In this study, a novel approach to the use of neuro-fuzzy structures is proposed for modeling and control purposes. In this approach, on the assumption that no expert

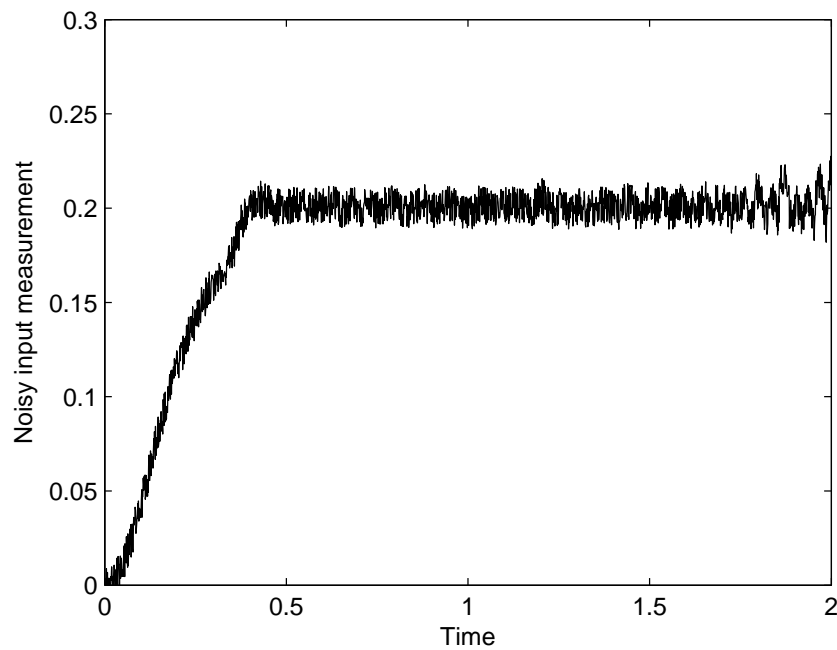


Figure 6.11. The noisy input measurement.

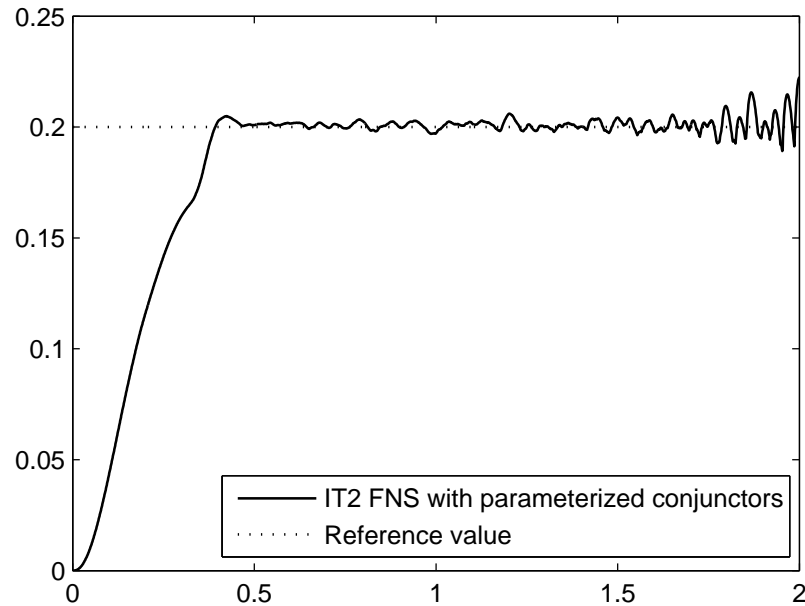


Figure 6.12. Wheel slip of type-2 FNS with parameterized conjunctors with noise.

knowledge is available about the system, the first thing that is done is to acquire some knowledge about the system. This is done by the use an IT2 FCM clustering algorithm. For the determination of the number of classes to be used in this algorithm, a novel validity index is used. This is another contribution of the study. The design parameters

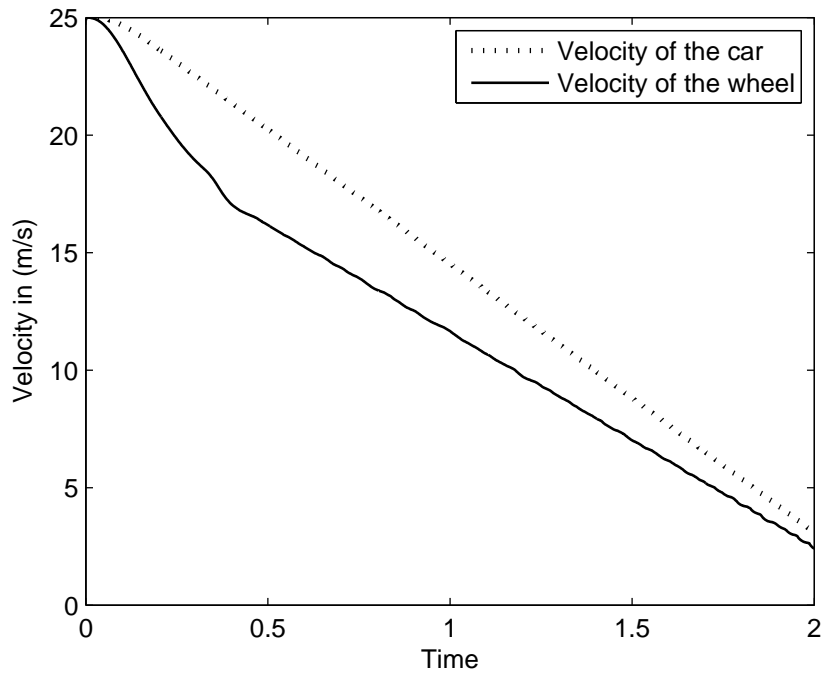


Figure 6.13. Velocity of the wheel and car with noisy input measurement.

Table 6.6. The comparison of the fuzzy algorithms with and without noise in the input measurements.

Methods	RMSE without noise	RMSE with noise	No. of parameters
T1 FNS	0.0382	0.0783	35
IT2 FNS	0.0302	0.0549	47
IT2 FNS with parameterized conjunctors	0.0358	0.0519	37

are updated based on the gradient descent algorithm, and, during the optimization process, rather than tuning the parameters of the membership functions used at the antecedent, the parameters of the parameterized conjunctors are tuned. In this way, the loss of any knowledge that is available about the system, either through expert inputs or through clustering, is prevented. The performance of the proposed approach and the traditional neuro-fuzzy structures seen in the literature are compared in modeling

a benchmark nonlinear function and in the slip regulation of a QCM without and with noisy input measurements. The results illustrate that IT2 FNS with parameterized conjunctors has satisfactory results in terms of RMSE value, as compared to other fuzzy approaches. The main advantage of the approach would show itself in applications when there is reliable expert knowledge about the system in terms of the shape of the membership functions and their placement in the input space. The tuning of the structure would still be possible for optimal performance by tuning the parameters of the conjunctors without tuning the parameters of the membership functions. It is to be noted that the proposed IT2 FNS structure has a smaller parameter set than the traditional IT2 FNS and is easier to implement.

7. RECURSIVE INTERVAL TYPE-2 FUZZY NEURAL SYSTEM

In real world applications, systems can experience many uncertainties that the traditional fuzzy logic systems may not be able to handle. In this study, the Takagi-Sugeno-Kang (TSK) fuzzy structure, which is a well-known universal approximator [60] is used in the design of a type-2 FNS. It has the following IF-THEN rule structure:

$$\text{IF } x_1 \text{ is } \tilde{A}_{1j} \text{ and...and } x_m \text{ is } \tilde{A}_{mj} \text{ THEN } z_j \text{ is } \sum_{i=1}^m a_{ij}x_i + a_{0j} \quad (7.1)$$

In this rule structure, symmetrical interval type-2 Gaussian membership functions whose lower membership functions (LMFs) are the scaled versions of the upper membership functions (UMFs) [61] are used in the antecedent parts of the fuzzy rules. An example is depicted in Figure 7.1. The consequent parts of the fuzzy rules are first order polynomials with the coefficients a_{0j} and a_{ij} .

With the traditional fuzzy c-means clustering algorithm, the standard deviation of the Gaussian membership functions are not determined, only the center values of the functions are identified. Furthermore, the traditional fuzzy c-means clustering is an off-line clustering algorithm. However, in real-time applications in which both the input and the output data change with time, a recursive approach is needed and therefore in this study, a recursive fuzzy c-means clustering algorithm in [42] is used in order to be able to update both the center and the standard deviation values of the antecedent membership functions. The algorithm has the following steps:

- (i) First of all, the number of clusters c , the fuzziness parameters η, η_m , the forgetting factors γ_v and γ_c , the fuzzy covariance matrix F_i , the center values of the membership functions v_i , the membership values μ_i and s_i for $i = 1, \dots, c$ are initialized.

(ii) The membership values μ_i are calculated as follows:

$$\mu_i(t) = \frac{1}{\sum_{j=1}^c \left(\frac{d_{i,(t)}^2}{d_{j,(t)}^2} \right)^{\frac{1}{\eta-1}}} \quad (7.2)$$

where $d_{i,(t)}^2 = (x(t) - v_i(t-1))^T(x(t) - v_i(t-1))$, ($1 \leq i \leq c$, $1 \leq t \leq N$).

(iii) Calculate s_i and $\Delta v_i(t)$:

$$s_i(t) = \gamma_v s_i(t-1) + \mu_i^\eta(t) \quad (7.3)$$

where $s_i(t-1) = \sum_{k=1}^{t-1} \mu_i^\eta(k)$.

$$\Delta v_i(t) = \frac{\mu_i^\eta(t)(x(t) - v_i(t-1))}{\gamma_v \sum_{k=1}^{t-1} \mu_i^\eta(k) + \mu_i^\eta(t)} \quad (7.4)$$

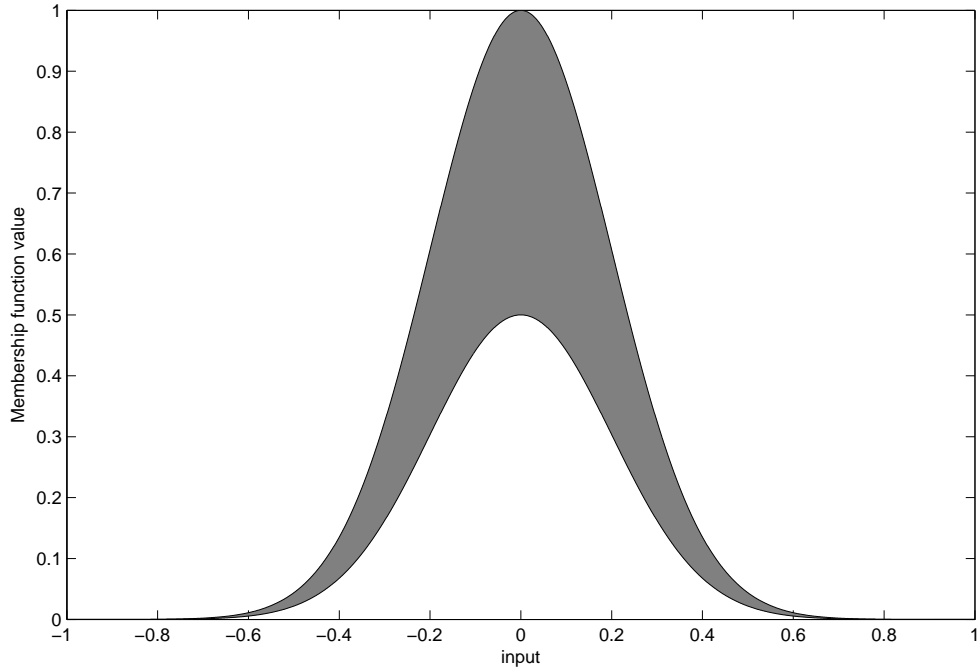


Figure 7.1. Symmetrical IT2 membership function-UMF is Gaussian and LMF is a scaled UMF.

(iv) Calculate the new centers:

$$v_i(t) = v_i(t-1) - \Delta v_i(t) \quad (7.5)$$

(v) Calculate the new fuzzy covariance matrix:

$$F_i(t) = \gamma_c \frac{s_i(t-1)}{s_i(t)} F_i(t-1) + \frac{\mu_i^\eta(t)}{s_i(t)} (x(t) - v_i(t))(x(t) - v_i(t))^T \quad (7.6)$$

$$\sigma_{i,j}^2 = \eta_m f_{i,j} \quad (7.7)$$

(vi) Gaussian membership functions are calculated by using the center value obtained in the preceding steps and the standard deviation is obtained by using the fuzzification parameter η_m and is given as follows $\sigma_{i,j} = \sqrt{\eta_m f_{i,j}}$. Here, the fuzzification parameter defines the overlapping between the membership functions. After the determination of the upper Gaussian membership functions, the height of the lower membership functions are determined by using the gradient descent learning algorithm. The upper and the lower membership functions are given in the following, respectively:

$$\bar{\mu}_j(x_i(t)) = e^{-\frac{1}{2}(\frac{x-v}{\sigma})^2} \quad (7.8)$$

$$\underline{\mu}_j(x_i(t)) = \gamma e^{-\frac{1}{2}(\frac{x-v}{\sigma})^2} \quad (7.9)$$

where γ is tuned between 0.5 and 1.

Afterwards, the lower and the upper firing strengths of each rule are calculated as follows:

$$\underline{\omega}_j = \underline{\mu}_j(x_1(t)) \cdots \underline{\mu}_j(x_n(t)) \quad (7.10)$$

$$\bar{\omega}_j = \bar{\mu}_j(x_1(t)) \cdots \bar{\mu}_j(x_n(t)) \quad (7.11)$$

The consequent part of the fuzzy rules are first order polynomials, defined as:

$$z_j = \sum_{i=1}^n a_{ij}x_i + a_{0i} \quad (7.12)$$

Subsequently, for type reduction, the Nie-Tan (NT) method [62] is used instead of the well-known Karnik and Mendel iterative algorithm, since the former has less computational burden and is easier to be utilized in real-time control applications. The output of the neuro-fuzzy structure is obtained as follows:

$$u = \frac{\sum_{j=1}^M z_j(\underline{\omega}_j + \bar{\omega}_j)}{\sum_{j=1}^M (\underline{\omega}_j + \bar{\omega}_j)} \quad (7.13)$$

7.1. Parameter Learning

After calculation of the output of the system, the gradient descent based parameter learning algorithm is used to adjust the coefficients of the consequent parts of the fuzzy rules. Initially, the output error is determined as follows:

$$E = \frac{1}{2} \sum_{i=1}^O (u_i^d - u_i)^2 \quad (7.14)$$

$$a_{ij}(t+1) = a_{ij}(t) - \lambda \frac{\partial E}{\partial a_{ij}} \quad (7.15)$$

$$a_{0i}(t+1) = a_{0i}(t) - \lambda \frac{\partial E}{\partial a_{0i}} \quad (7.16)$$

where

$$\frac{\partial E}{\partial a_{ij}} = \frac{\partial E}{\partial u} \frac{\partial u}{\partial z_j} \frac{\partial z_j}{\partial a_{ij}} \quad (7.17)$$

$$\frac{\partial E}{\partial a_{0j}} = \frac{\partial E}{\partial u} \frac{\partial u}{\partial z_j} \frac{\partial z_j}{\partial a_{0j}} \quad (7.18)$$

In above

$$\frac{\partial E}{\partial u} = u(t) - u^d(t) \quad (7.19)$$

$$\frac{\partial u}{\partial z_j} = \frac{\omega_j + \bar{\omega}_j}{\sum_{j=1}^M (\omega_j + \bar{\omega}_j)} \quad (7.20)$$

$$\frac{\partial z_j}{\partial a_{ij}} = x_i \quad (7.21)$$

$$\frac{\partial z_j}{\partial a_{0j}} = 1 \quad (7.22)$$

The parameters of the lower bound of the membership functions are tuned as follows:

$$\gamma(t+1) = \gamma(t) - \lambda \frac{\partial E}{\partial \gamma} \quad (7.23)$$

where

$$\frac{\partial E}{\partial \gamma} = \frac{\partial E}{\partial u} \frac{\partial u}{\partial \omega_j} \frac{\partial \omega_j}{\partial \mu_{ij}} \frac{\partial \mu_{ij}}{\partial \gamma} \quad (7.24)$$

$$\frac{\partial u}{\partial \underline{\omega}_j} = \frac{z_j - u}{\sum_{j=1}^N (\underline{\omega}_j + \bar{\omega}_j)} \quad (7.25)$$

$$\frac{\partial \underline{\omega}_j}{\partial \underline{\mu}_{ij}} = \prod_{k=1, k \neq i}^{N1} \underline{\mu}_{kj} \quad (7.26)$$

$$\frac{\partial \underline{\mu}_{ij}}{\partial \gamma} = \bar{\mu}_{ij} \quad (7.27)$$

The proposed method is validated by testing it on a 2-DOF helicopter for tracking a desired trajectory and on a servo system for speed control and the performances obtained are compared with those obtained by the use of a traditional T1FNS. The details of the systems are given in the following subsections.

7.2. Description of the 2-DOF Helicopter System

Helicopters are used in many areas, such as transportation, air traffic, fire-fighting, etc. [63]. Their control is a challenging task due to their highly nonlinear dynamics, their instability and the cross-coupling effects between its axes. Fuzzy logic and neural-networks are commonly used for the control of helicopters or twin rotor MIMO (multi-input-multi-output) systems (TRMS) that resembles a helicopter system. In [64], two adaptive fuzzy controllers are designed for the pitch and the yaw axes of a TRMS with 2-DOF to track desired trajectories. The performance of the algorithm is compared with non-adaptive fuzzy and PID controllers. The results obtained indicate that the adaptive fuzzy controller is more robust against external disturbances and has less steady-state error and overshoot. In [63], two different decentralized discrete-time neural network approaches; neural backstepping and neural sliding mode control methods are deployed for trajectory tracking of a 2-DOF helicopter system. The neural sliding mode controller is seen to have a better performance as compared to the neural backstepping control. It is stated that neural network methods do not need a

priori information about the system and the proposed structure is trained on-line by using an extended Kalman filter based algorithm. In [65], a fuzzy-sliding controller and a fuzzy-integral sliding controller (FSFISC) are designed for the horizontal and the vertical subsystems respectively of a twin-rotor multi-input-multi-output system. The performance of the proposed approach is compared with the methods from the literature and it is seen that the proposed approach has better tracking performance and is more robust to external disturbances. The performance of the approach proposed in this study is also validated on a 2-DOF helicopter for trajectory tracking. Subsequently, it is used for speed control a servo system.

The proposed method is tested on the 2-DOF helicopter shown in Figure 7.2, which is a highly nonlinear multi-input-multi-output (MIMO) system with strong cross-couplings between the pitch and the yaw axes. It is attached to a fixed base and its pitch and yaw (the front and the back) propellers are driven by DC motors. The front propeller controls the vertical motion of the helicopter about the pitch axis. This angle is defined as positive when the front propeller causes a motion in the upward direction. When the propeller motors are not excited, i.e. when the helicopter is at rest, the pitch angle is about -40.5° and its motion is restricted between -40.5° and 40.5° . The propeller at the back controls the horizontal motion about the yaw axis. The helicopter is able to rotate 360° in the yaw axis. The yaw angle is defined as positive in the clockwise direction. The thrust forces F_p and F_y shown in Figure 7.2 are generated at the distances r_p and r_y from the pitch and the yaw axes, respectively [66]. The voltages applied to the front and the back propeller motors are the inputs of the system and the pitch (θ) and the yaw (ψ) angles in radians are the outputs. The aim is to design a controller to track the desired trajectories in the pitch and the yaw axes. The dynamic nonlinear equations of the system obtained by using Lagrangian

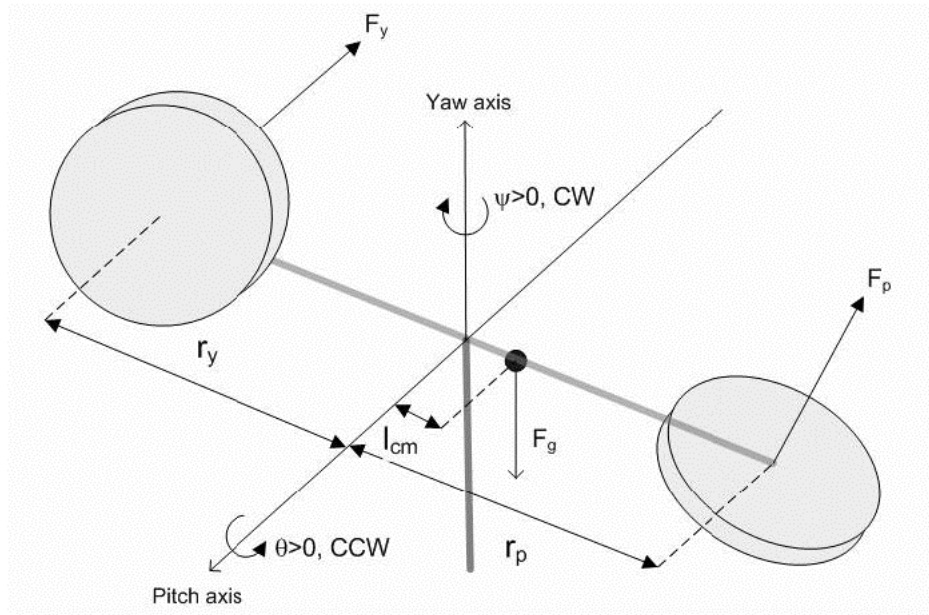


Figure 7.2. Simple free body diagram of 2-DOF helicopter [66].

mechanics are given for the pitch and the yaw axes as follows, respectively [66]:

$$\begin{aligned}
 (J_{eq,p} + m_{heli}l_{cm}^2)\ddot{\theta} &= K_{pp}V_{m,p} + \\
 &K_{py}V_{m,y} - m_{heli}gl_{cm}\cos\theta - \\
 &B_p\dot{\theta} - m_{heli}l_{cm}^2\sin\theta\cos\theta\dot{\psi}^2 \\
 (J_{eq,y} + m_{heli}l_{cm}^2\cos^2\theta)\ddot{\psi} &= K_{yp}V_{m,p} + \\
 &K_{yy}V_{m,y} - B_y\dot{\psi} + \\
 &2m_{heli}l_{cm}^2\sin\theta\cos\theta\dot{\psi}\dot{\theta}
 \end{aligned} \tag{7.28}$$

The descriptions of the variables in Equation 7.28 are given in Table 7.1.

7.2.1. Simulation Studies

The recursive interval type-2 fuzzy neural system (RIT2FNS) and the type-1 fuzzy neural system (T1FNS) are both tested on the 2-DOF helicopter shown in Figure 7.2 by a series of simulation studies [67]. The sampling time is chosen as 10ms. Two RIT2FNS controllers are designed for each axis. The block diagram of the neuro-fuzzy control structure is depicted in Figure 7.3. The pitch angle (*rad*) error (e_p), its derivative

Table 7.1. Description of the nonlinear model parameters.

Parameters	Description	Values
$J_{eq,p}$	Total moment of inertia about pitch axis	$0.0384kg.m^2$
l_{cm}	Center of mass length along helicopter body from pitch axis	$0.1855m$
$J_{eq,y}$	Total moment of inertia about yaw axis	$0.0431kg.m^2$
K_{pp}	Thrust torque constant acting on pitch axis from pitch propeller	$0.2041N.m/V$
K_{py}	Thrust torque constant acting on pitch axis from yaw propeller	$0.0068N.m/V$
K_{yp}	Thrust torque constant acting on yaw axis from pitch propeller	$0.0219N.m/V$
K_{yy}	Thrust torque constant acting on yaw axis from yaw propeller	$0.072N.m/V$
g	Gravitational constant	$9.81m/s^2$
B_p	Viscous damping about pitch axis	$0.8N/V$
B_y	Viscous damping about yaw axis	$0.318N/V$
m_{heli}	Total moving mass of the helicopter	$1.3872kg$
$V_{m,p}$	Voltage apply to pitch motor	$\pm 24V$
$V_{m,y}$	Voltage apply to yaw motor	$\pm 15V$

(Δe_p) and its integral ($\sum e_p$) are given as the inputs to the RIT2FNS controller for the pitch axis. Similarly, the yaw angle (*rad*) error (e_y), its derivative (Δe_y) and its integral ($\sum e_y$) are given as the inputs to the RIT2FNS controller for the yaw axis. In both RIT2FNSs, three symmetrical Gaussian membership functions whose LMFs are the scaled versions of the UMFs are used for each input. In the application of

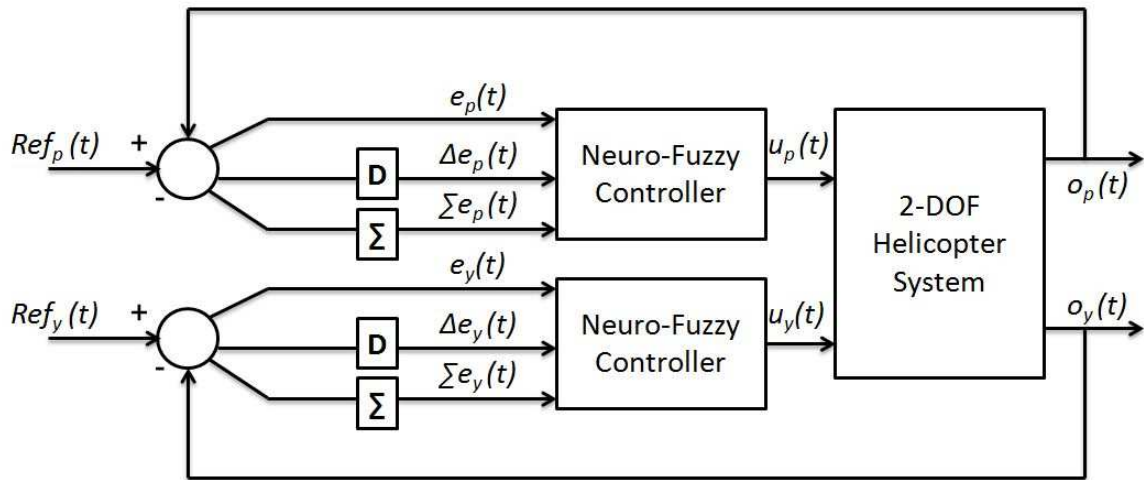


Figure 7.3. Block diagram of the neuro-fuzzy control system.

T1FNS, the number of type-1 Gaussian membership functions used for each input is also three to have a fair basis for comparison. The membership functions are randomly initialized. In the proposed approach, the center and the standard deviation of the membership functions are determined by using the recursive fuzzy c -means clustering algorithm described. The parameters at the consequent part of the fuzzy rules and γ are tuned based on a gradient descent learning algorithm. In T1FNS approach, both the antecedent and the consequent parameters of the fuzzy rules are tuned with the gradient descent approach. The initial values of the parameters at the consequent parts are chosen randomly. The initial γ values are chosen as 0.8 and they are tuned between 0.5 and 1. For the learning rate λ , a small value is chosen between 0 and 1. The learning rate is adapted according to the magnitude of the error. When the derivative of the error is negative, the learning rate is increased, and when the rate is positive it is decreased. The simulation results obtained for three different experiments are given in Figures 7.4-7.6. In the third experiment, as shown in Figure 7.6, a sudden step disturbance with a 0.1 magnitude is applied to both axes between 15 and 17 seconds. The root mean square error values of the tracking error obtained in the three experiments for each axis and the number of design parameters are given in Table 7.2, showing the robustness of both neuro-fuzzy approaches.

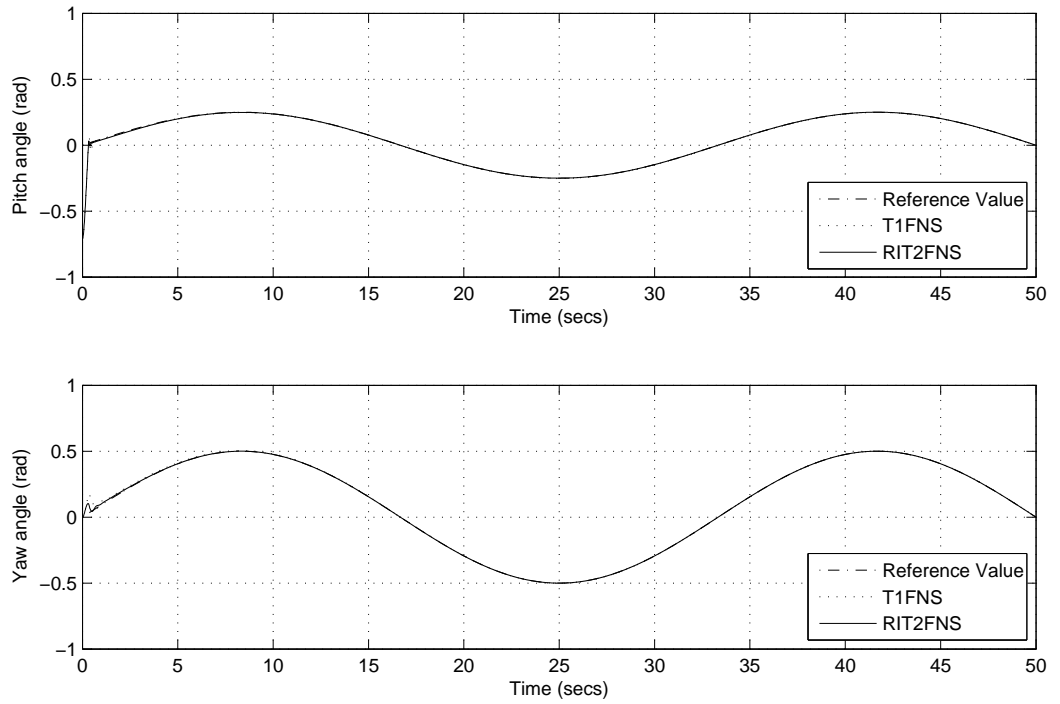


Figure 7.4. Simulation 1: The results obtained for sinusoidal reference trajectory.

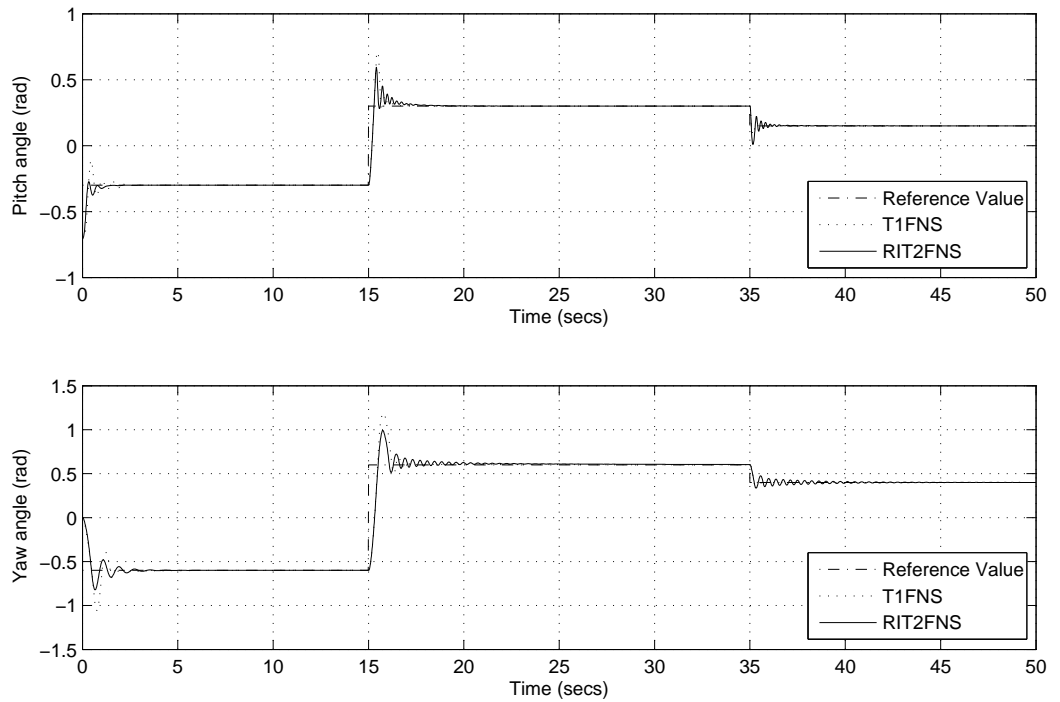


Figure 7.5. Simulation 2: The results obtained for square wave reference trajectory.

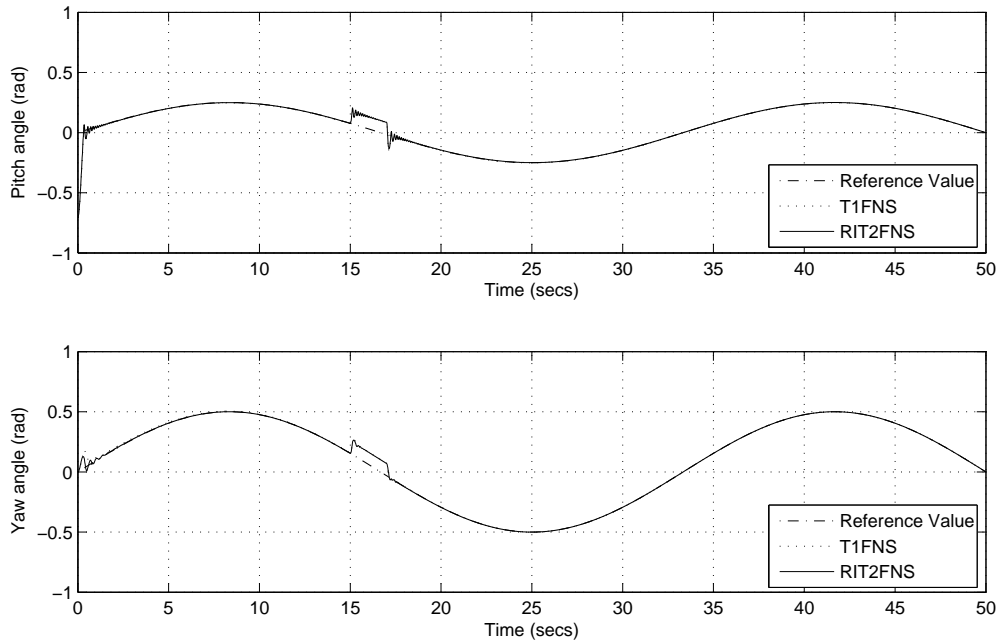


Figure 7.6. Simulation 3: The results obtained for sinusoidal reference trajectory with a sudden disturbance.

7.3. Description of the Servo System

Servo systems are commonly used in industrial processes and fuzzy neural systems are commonly deployed in the control of such systems. In [68], a fuzzy neural network (FNN) proportional-integral (PI)-/proportional-derivative (PD)-like controller with on-line learning is presented for speed trajectory tracking of a brushless drive system. It is seen that the adaptive control via the Extended Kalman Filter (EKF) learning of the FNN is superior to fuzzy logic systems (FLSs) and the experimental results obtained under various operational conditions indicate remarkable tracking performance. In [69], an adaptive self-organizing Takagi-Sugeno-Kang type fuzzy network control (ASTFNC) is deployed on a DC motor drive. The performance of the ASTFNC system with a PI-type learning algorithm is compared with some methods from the literature. The experimental studies verify the expectations that the proposed approach is more advantageous as compared to the other methods.

The proposed method is tested on the experimental setup AMIRA DR300 [70]

Table 7.2. Comparison of obtained RMSE values of 2-DOF Helicopter.

	T1FNS	RIT2FNS
Simulation 1: RMSE value in <i>rad</i> for pitch axis	0.0388	0.0385
Simulation 1: RMSE value in <i>rad</i> for yaw axis	0.0104	0.0049
Simulation 2: RMSE value in <i>rad</i> for pitch axis	0.0493	0.0430
Simulation 2: RMSE value in <i>rad</i> for yaw axis	0.1122	0.1008
Simulation 3: RMSE value in <i>rad</i> for pitch axis	0.0406	0.0393
Simulation 3: RMSE value in <i>rad</i> for yaw axis	0.0121	0.0085
Design parameters	30	39

shown in Figure 7.7. It is a nonlinear servo system. In [70], the theoretical and the mathematical background of the ideal permanently excited DC motor is given. The block scheme of the plant is presented in Figure 7.8. The plant consists of two identical permanently excited DC motors M1 and M2. The free shaft of the first motor (M1) is coupled to the second motor (M2) with a mechanical clutch. The second motor (M2) is used as a generator to create nonlinear load conditions. The block diagram of the permanently excited DC motor with a load is seen in Figure 7.9. The transfer function

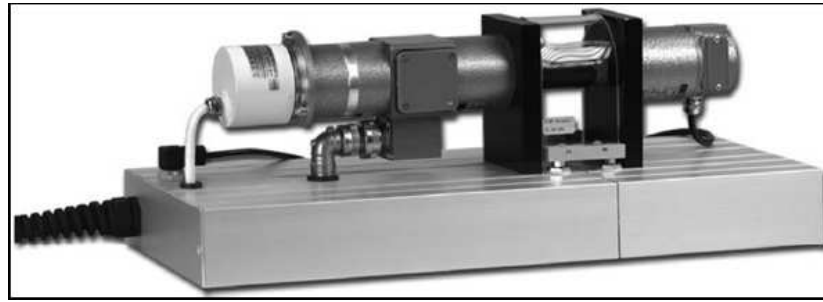


Figure 7.7. The experimental setup.

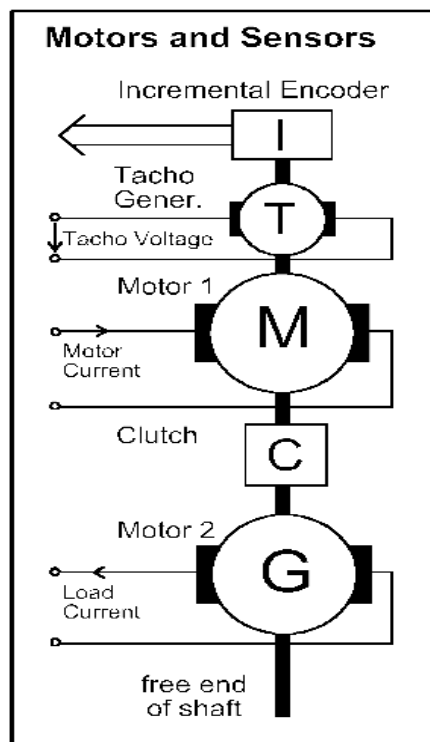


Figure 7.8. Block scheme of the plant.

of the system is given below:

$$\omega(s) = \frac{1}{C\phi} \frac{1}{1 + T_M s + T_M T_A s^2} U_A(s) - \frac{R_A}{K_M C \phi} \frac{1 + T_A s}{1 + T_M s + T_M T_A s^2} M_L(s) \quad (7.29)$$

where ω is the speed of the rotor, U_A is the armature voltage, C is the motor constant, ϕ is the magnetic excitation, K_M is the motor constant, M_L is the sum of all load torques, T_A is the armature time constant and T_M indicates the time behavior of the

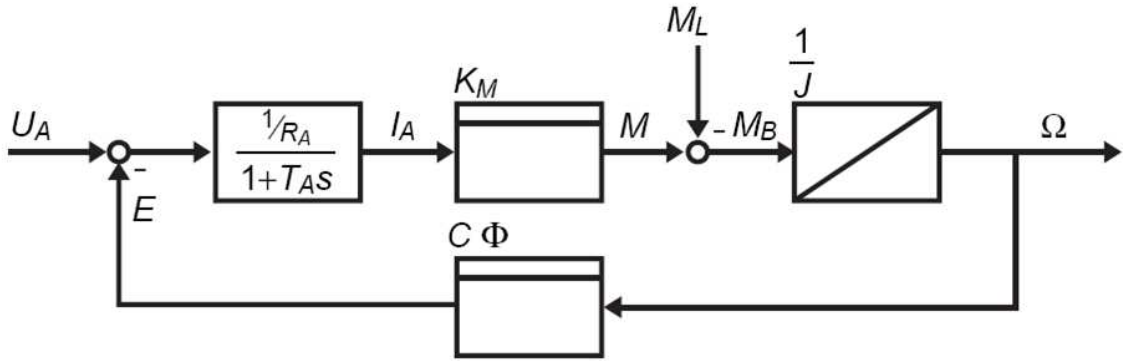


Figure 7.9. Block diagram of the constantly excited DC motor with load.

system. T_A and T_M are given as follows:

$$T_A = \frac{L_A}{R_A} \quad (7.30)$$

and

$$T_M = \frac{J R_A}{K_M C \phi} \quad (7.31)$$

The first part of the transfer function Equation 7.29 describes the reference whereas the disturbance is described by the second part. The system parameters and the numerical values that are used in the experiments are given in Table 7.3.

7.3.1. Experimental Studies

The recursive interval type-2 fuzzy neural system and the type-1 fuzzy neural system are both tested experimentally on the set up that is shown in Figure 7.7. The block diagram of the neuro-fuzzy structure is given in Figure 7.10. In the experimental studies, the sampling time is chosen as $10ms$ and the tacho speed and the applied load voltage are normalized between -1 and 1. The same initial values of the parameters and the same number of fuzzy rules are used in both NFSs as in the previous application. The experimental results obtained with varying reference and load conditions are given in Figures 7.11-7.13. In Figure 7.14, the control input signal for the second experiment is given. For the first two experiments, a sinusoidal load shown in Figure 7.15 is applied

Table 7.3. The technical data of the laboratory setup.

	Description	Value
Motor	Nominal Voltage	24 V
	Nominal Current	2 A
	Nominal Speed	3000 rpm
	Nominal Torque	0.096 Nm
	Moment of Inertia	$17.7 \cdot 10^{-6} \text{ Kg}m^2$
	Torque Constant	0.06 Nm/A
	Armature Resistance (R_A)	2.6 Ω
	Armature Inductance (L_A)	3 mH
	emf constant	6.27 mV/rpm
Mechanical clutch	Moment of Inertia	$33 \cdot 10^{-6} \text{ Kg}m^2$
Tacho	Output Voltage	5 mV/rpm
	Moment of Inertia	$10.6 \cdot 10^{-6} \text{ Kg}m^2$

to the system. In the first experiment, the reference is changed as shown in Figure 7.11. In the second experiment, the reference speed is changed as shown in Figure 7.12. In the third experiment, the load applied changes from 0.3 pu to 0.6 pu at $t = 5$ seconds and decreases to 0.5 pu at $t = 8$ seconds. The adaptation of the membership functions takes place throughout the experiments and the final membership functions for only the first experiment are given in Figures 7.16 and 7.17 for the T1FNS and the RIT2FNS respectively. The root mean square error values and the number of design parameters are given in Table 7.4.

7.4. Conclusion

In this study, an interval type-2 fuzzy neural system, the membership functions of which are determined with a recursive fuzzy c-means clustering algorithm is presented.

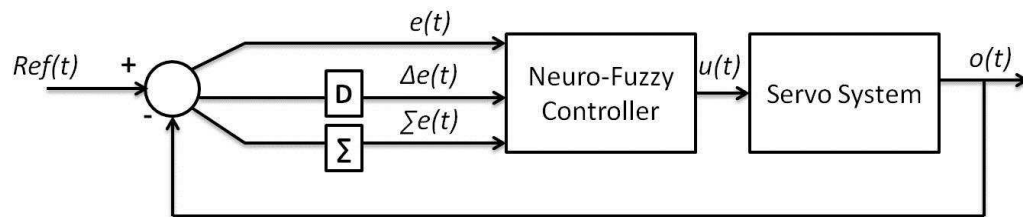


Figure 7.10. Block diagram of the neuro-fuzzy control system.

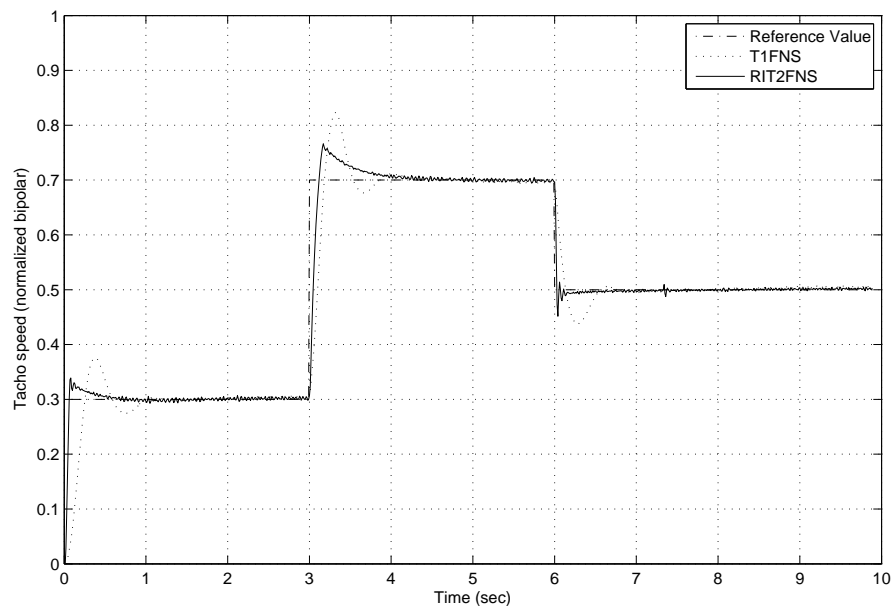


Figure 7.11. Experiment 1: The results obtained for changing reference under sinusoidal load.

As compared to the traditional fuzzy c-means clustering algorithm, in the recursive approach not only the center values of the membership functions but also the standard deviation values are identified. Another contribution of this study is that the recursive fuzzy c-means clustering algorithm is used with interval type-2 fuzzy neural system and it is applied in control applications.

The performance of the proposed approach and a traditional T1 neuro-fuzzy structure adopted from the literature are tested on a 2-DOF helicopter (a benchmark system since there exists a strong cross coupling relation between its axes) for trajectory tracking. The results obtained illustrate the effectiveness of the proposed approach. It is concluded that both algorithms are able to track time-varying reference signals

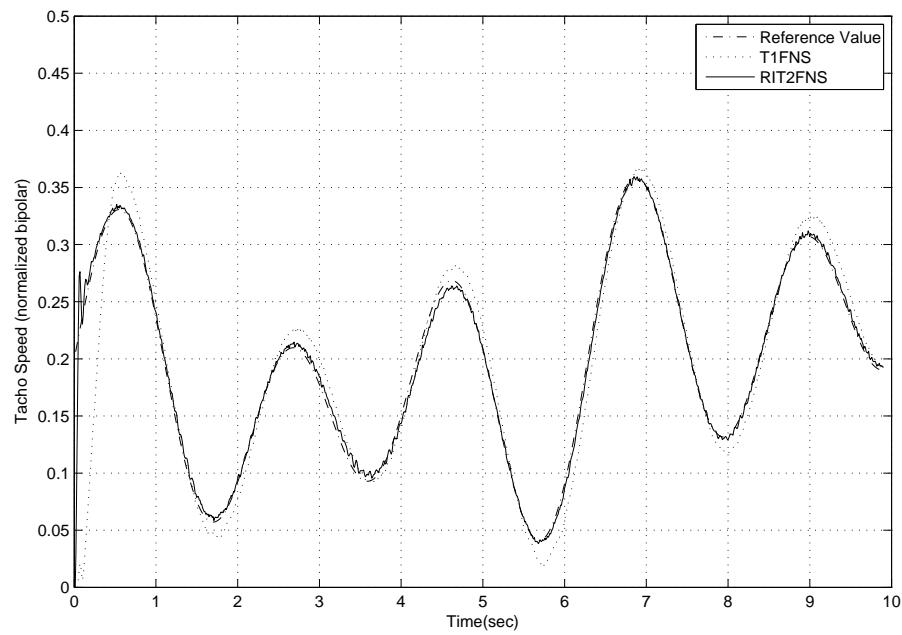


Figure 7.12. Experiment 2: The results obtained for changing reference under sinusoidal load.

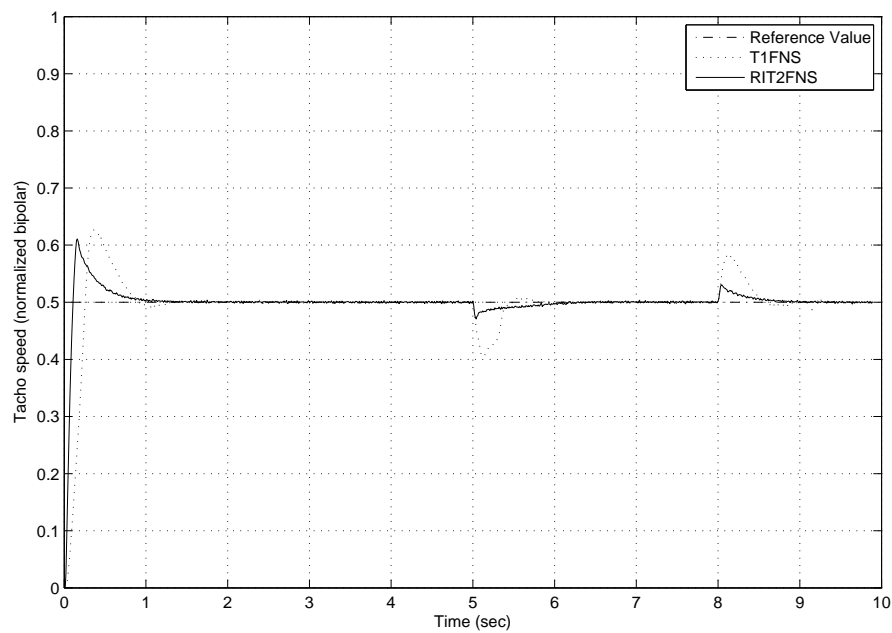


Figure 7.13. Experiment 3: The results obtained for constant reference under varying step load.

and are robust against external disturbances. However, the proposed approach has less RMSE value and less overshoot as compared to the T1FNS. The performances

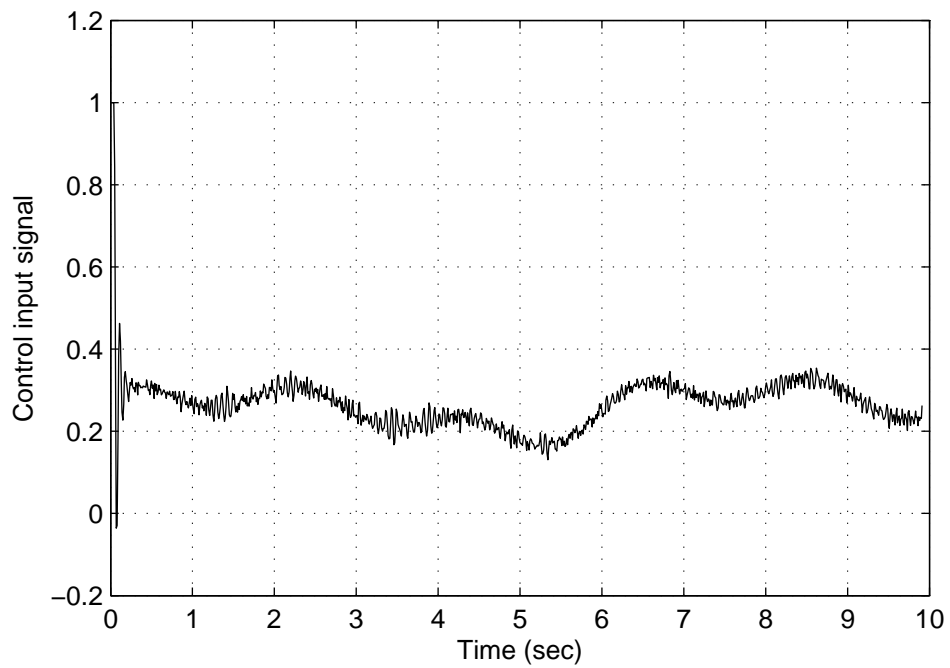


Figure 7.14. Control input signal for the second experiment (changing reference under sinusoidal load).

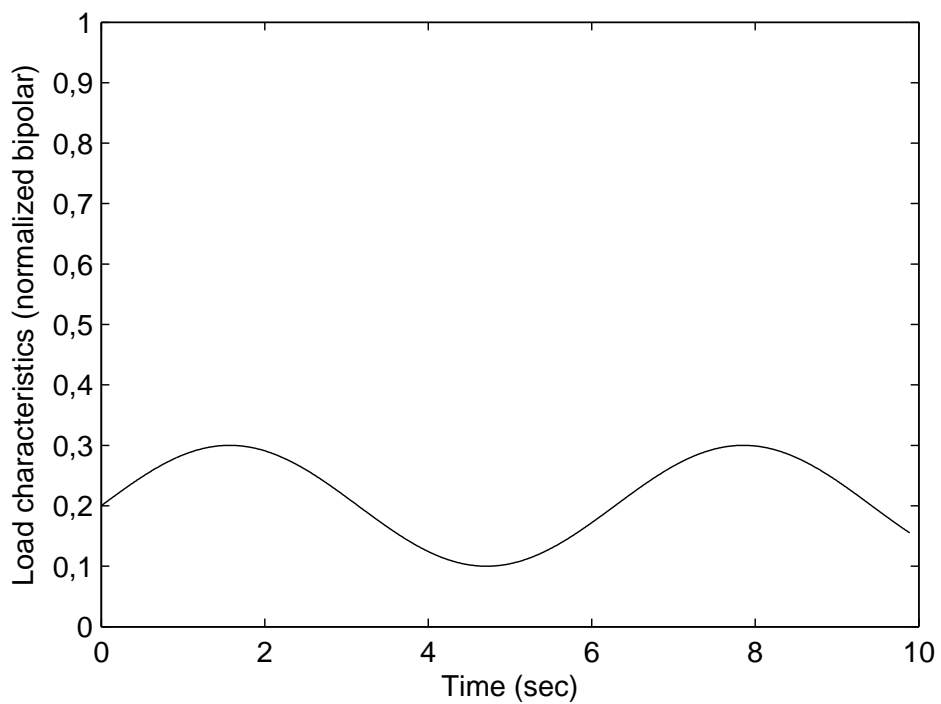


Figure 7.15. Sinusoidal load.

of both approaches are tested experimentally too on a laboratory servo system. It is observed that especially under the condition of a time varying reference signal with a

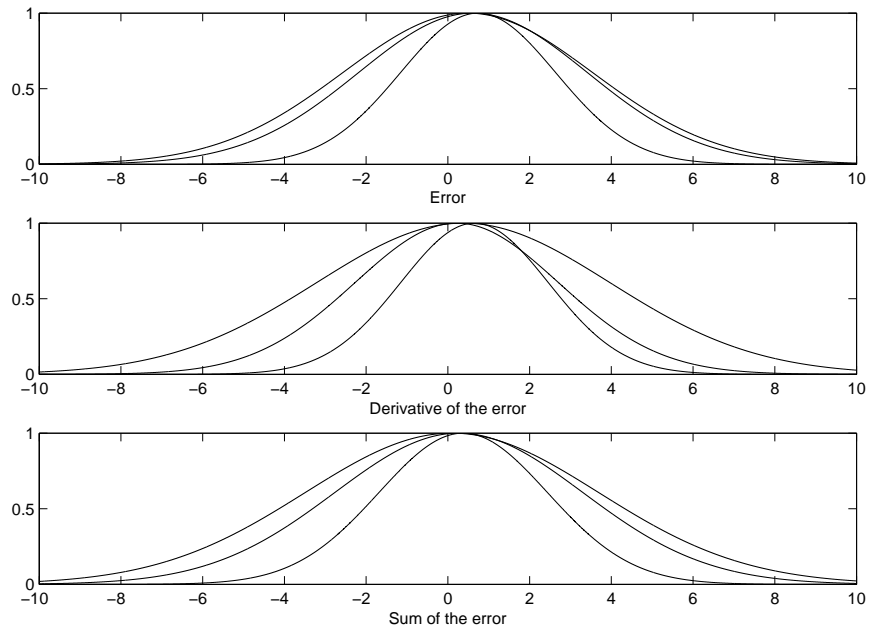


Figure 7.16. Experiment 1: The final membership functions of T1FNS.

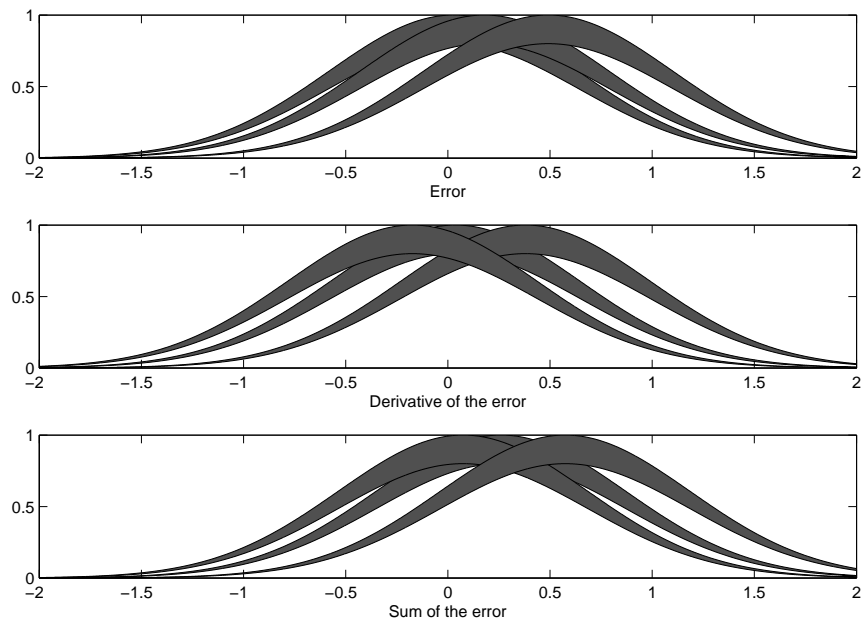


Figure 7.17. Experiment 1: The final membership functions of RIT2FNS.

nonlinear load, the proposed approach is able to track the reference signal better than the T1FNS. In addition, it is seen that the proposed approach is able to converge faster than the T1FNS and it results in smaller RMSE values in all experiments.

Table 7.4. Comparison of obtained RMSE values of real-time servo system.

	T1FNS	RIT2FNS
Experiment 1: RMSE value in <i>pu</i> (changing reference under sinusoidal load)	0.0542	0.0332
Experiment 2: RMSE value in <i>pu</i> (changing reference under sinusoidal load)	0.0366	0.0128
Experiment 3: RMSE value in <i>pu</i> (constant reference under varying step load)	0.0623	0.0375
Design parameters	30	39

7.5. Recursive Interval Type-2 Neuro Fuzzy System with Elliptical Membership Functions

As mentioned in the previous section, today, most of the systems are non-linear and time-varying. The control of these kind of processes should be realized, recursively. In this part of the study, interval type-2 neuro-fuzzy system is used with recursive fuzzy c-means clustering with elliptical membership functions. Type-2 fuzzy systems are able to handle the environmental and the inner uncertainties of the systems better than their type-1 counter part. In [71], it is shown that type-2 fuzzy logic system (T2 FLS) with interval type-2 elliptical membership functions have better noise reduction property as compared to type-1 fuzzy systems and the detailed information can be found in [71].

The interval type-2 TSK FLS is used with the integration of neural-networks. The fuzzy IF-THEN rule structure is given as follows [17]:

$$\begin{aligned}
 R^i &= \text{IF } X_1 \text{ is } \tilde{A}_{i1} \text{ and } \dots \text{ and } X_n \text{ is } \tilde{A}_{in}, \\
 &\text{THEN } z^i = a_n^i x_n + a_{n-1}^i x_{n-1} + \dots + a_0^i
 \end{aligned}$$

where X_n 's are the inputs and A_{in} 's ($i=1, \dots, n$) are the interval type-2 fuzzy sets indi-

cated with tildes. z^i is the output of the each rule. a_n^i 's are the coefficients of the first order polynomial at the consequents of the each rule. i ($i = 1, 2, \dots, M$) indicates the number of rules and n is the number of the antecedent parameters.

At the antecedents of the fuzzy IF-THEN rules, interval type-2 elliptical membership functions are used as seen in Figure 7.18. The kernel and the both support end points of these membership functions are precise and the other parts of the support are fuzzy.

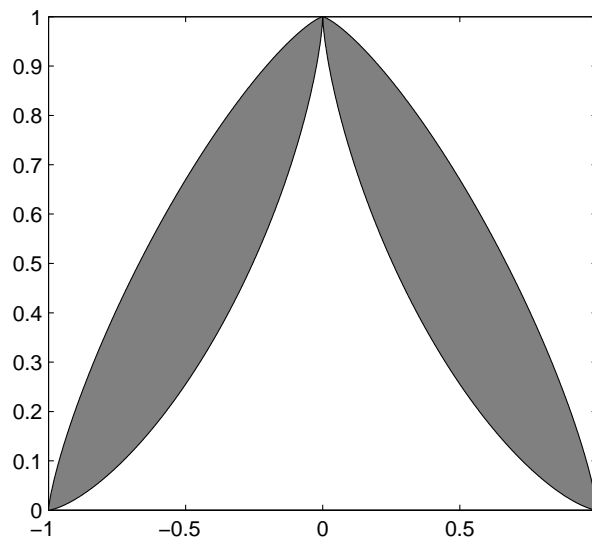


Figure 7.18. Interval type-2 elliptical membership function.

In traditional fuzzy c-means clustering algorithms, the center values are determined offline. However, for time-varying processes that the input-output data changes over time, recursive approaches should be used. In this study, recursive fuzzy c-means clustering approach [42] is used to determine the center values of the elliptical membership functions. In this clustering approach, the centers of the elliptical membership functions are determined recursively. The approach is given as in the following [42]:

- The following parameters are initialized: c (number of clusters), η (fuzziness parameter), γ_v (forgetting factor), v_i (center values of the membership functions), μ_i (membership values), and s_i for $i = 1, \dots, c$.

- The membership values μ_i are calculated as follows:

$$\mu_i(t) = \frac{1}{\sum_{j=1}^c \left(\frac{d_{i,(t)}^2}{d_{j,(t)}^2} \right)^{\frac{1}{\eta-1}}} \quad (7.32)$$

where $d_{i,(t)}^2 = (x(t) - v_i(t-1))^T(x(t) - v_i(t-1))$, ($1 \leq i \leq c$, $1 \leq t \leq N$).

- s_i and $\Delta v_i(t)$ are calculated as follows:

$$s_i(t) = \gamma_v s_i(t-1) + \mu_i^\eta(t) \quad (7.33)$$

where $s_i(t-1) = \sum_{k=1}^{t-1} \mu_i^\eta(k)$.

$$\Delta v_i(t) = \frac{\mu_i^\eta(t)(x(t) - v_i(t-1))}{\gamma_v \sum_{k=1}^{t-1} \mu_i^\eta(k) + \mu_i^\eta(t)} \quad (7.34)$$

- The new center values are determined as in the following:

$$v_i(t) = v_i(t-1) - \Delta v_i(t) \quad (7.35)$$

- The center values of the elliptical membership functions are determined by using the recursive fuzzy c-means clustering algorithm. The parameters that present the width and the width of the uncertainty of the membership functions are determined by gradient based learning approach.

The upper and the lower part of the elliptical membership functions are given in the following, respectively [71]:

$$\bar{\mu}_{ij} = \begin{cases} \left(1 - \left| \frac{x_i - v_{ij}}{d_{ij}} \right|^{b_{1ij}}\right)^{1/b_{1ij}} & , \text{ if } v_{ij} - d_{ij} < x < v_{ij} + d_{ij} \\ 0, & \text{ else} \end{cases}$$

$$\underline{\mu}_{ij} = \begin{cases} (1 - \left| \frac{x_i - v_{ij}}{d_{ij}} \right|^{b_{2ij}})^{1/b_{2ij}} & , \text{ if } v_{ij} - d_{ij} < x < v_{ij} + d_{ij} \\ 0, & \text{ else} \end{cases}$$

where b_1 and b_2 determines the width of the uncertainty of the elliptical membership functions and they are chosen as $b_1 > 1$, $0 < b_2 < 1$. v_{ij} and d_{ij} are the center and the width of the membership functions, respectively. Subsequently, the lower and the upper firing strengths of each rule are calculated as follows:

$$\underline{\omega}_j = \underline{\mu}_j(x_1(t)) \cdots \underline{\mu}_j(x_n(t)) \quad (7.36)$$

$$\bar{\omega}_j = \bar{\mu}_j(x_1(t)) \cdots \bar{\mu}_j(x_n(t)) \quad (7.37)$$

The consequent part of the fuzzy rules are first order polynomials, defined as:

$$z_j = \sum_{i=1}^n a_{ij}x_i + a_{0i} \quad (7.38)$$

Nie-Tan (NT) method [62] is used as the type-reduction procedure. This method has less computational burden and is easier to be utilized. The output of the interval type-2 neuro-fuzzy system is given as follows:

$$u = \frac{\sum_{j=1}^M z_j(\underline{\omega}_j + \bar{\omega}_j)}{\sum_{j=1}^M (\underline{\omega}_j + \bar{\omega}_j)} \quad (7.39)$$

7.5.1. Parameter Learning

In this study, gradient descent based learning approach is used to obtain an optimal neuro-fuzzy model. The width and the width of the uncertainty of the membership functions at the antecedents and the coefficients at the consequents of the fuzzy rules

are adjusted. The objective function is given as follows:

$$E = \frac{1}{2} \sum_{i=1}^O (u_i^d - u_i)^2 \quad (7.40)$$

$$a_{ij}(t+1) = a_{ij}(t) - \lambda \frac{\partial E}{\partial a_{ij}} \quad (7.41)$$

$$a_{0i}(t+1) = a_{0i}(t) - \lambda \frac{\partial E}{\partial a_{0i}} \quad (7.42)$$

$$b_{1ij}(t+1) = b_{1ij}(t) - \lambda \frac{\partial E}{\partial b_{1ij}} \quad (7.43)$$

$$b_{2ij}(t+1) = b_{2ij}(t) - \lambda \frac{\partial E}{\partial b_{2ij}} \quad (7.44)$$

$$d_{ij}(t+1) = d_{ij}(t) - \lambda \frac{\partial E}{\partial d_{ij}} \quad (7.45)$$

where

$$\frac{\partial E}{\partial a_{ij}} = \frac{\partial E}{\partial u} \frac{\partial u}{\partial z_j} \frac{\partial z_j}{\partial a_{ij}} \quad (7.46)$$

$$\frac{\partial E}{\partial a_{0j}} = \frac{\partial E}{\partial u} \frac{\partial u}{\partial z_j} \frac{\partial z_j}{\partial a_{0j}} \quad (7.47)$$

$$\frac{\partial E}{\partial b_{1ij}} = \sum_j \frac{\partial E}{\partial u} \frac{\partial u}{\partial \bar{\omega}_j} \frac{\partial \bar{\omega}_j}{\partial \bar{\mu}_{ij}} \frac{\partial \bar{\mu}_{ij}}{\partial b_{1ij}} \quad (7.48)$$

$$\frac{\partial E}{\partial b_{2ij}} = \sum_j \frac{\partial E}{\partial u} \frac{\partial u}{\partial \underline{\omega}_j} \frac{\partial \underline{\omega}_j}{\partial \underline{\mu}_{ij}} \frac{\partial \underline{\mu}_{ij}}{\partial b_{2ij}} \quad (7.49)$$

$$\frac{\partial E}{\partial d_{ij}} = \sum_j \frac{\partial E}{\partial u} \left[\frac{\partial u}{\partial \underline{\omega}_j} \frac{\partial \underline{\omega}_j}{\partial \underline{\mu}_{ij}} \frac{\partial \underline{\mu}_{ij}}{\partial d_{ij}} + \frac{\partial u}{\partial \bar{\omega}_j} \frac{\partial \bar{\omega}_j}{\partial \bar{\mu}_{ij}} \frac{\partial \bar{\mu}_{ij}}{\partial d_{ij}} \right] \quad (7.50)$$

In above

$$\frac{\partial E}{\partial u} = u(t) - u^d(t) \quad (7.51)$$

$$\frac{\partial u}{\partial z_j} = \frac{\omega_j + \bar{\omega}_j}{\sum_{j=1}^M (\omega_j + \bar{\omega}_j)} \quad (7.52)$$

$$\frac{\partial z_j}{\partial a_{ij}} = x_i \quad (7.53)$$

$$\frac{\partial z_j}{\partial a_{0j}} = 1 \quad (7.54)$$

$$\frac{\partial u}{\partial \bar{\omega}_j} = \frac{z_j - u}{\sum_{j=1}^N (\omega_j + \bar{\omega}_j)} \quad (7.55)$$

$$\frac{\partial \bar{\omega}_j}{\partial \bar{\mu}_{ij}} = \prod_{k=1, k \neq i}^{N1} \bar{\mu}_{kj} \quad (7.56)$$

$$\frac{\partial u}{\partial \underline{\omega}_j} = \frac{z_j - u}{\sum_{j=1}^N (\underline{\omega}_j + \bar{\omega}_j)} \quad (7.57)$$

$$\frac{\partial \underline{\omega}_j}{\partial \underline{\mu}_{ij}} = \prod_{k=1, k \neq i}^{N1} \underline{\mu}_{kj} \quad (7.58)$$

$$\begin{aligned} \frac{\partial \bar{\mu}_{ij}}{\partial b_{1ij}} &= -\frac{1}{b_{1ij}^2} \ln \left(1 - \left| \frac{x_i - v_{ij}}{d_{ij}} \right|^{b_{1ij}} \right) \left(1 - \left| \frac{x_i - v_{ij}}{d_{ij}} \right|^{b_{1ij}} \right)^{\frac{1}{b_{1ij}}} \\ &\quad - \frac{1}{b_{1ij}} \ln \left| \frac{x_i - v_{ij}}{d_{ij}} \right| \left| \frac{x_i - v_{ij}}{d_{ij}} \right|^{b_{1ij}} \left(1 - \left| \frac{x_i - v_{ij}}{d_{ij}} \right|^{b_{1ij}} \right)^{\frac{1}{b_{1ij}} - 1} \end{aligned} \quad (7.59)$$

where $v_{ij} - d_{ij} < x_i < v_{ij} + d_{ij}$

$$\begin{aligned} \frac{\partial \underline{\mu}_{ij}}{\partial b_{2ij}} &= -\frac{1}{b_{1ij}^2} \ln \left(1 - \left| \frac{x_i - v_{ij}}{d_{ij}} \right|^{b_{2ij}} \right) \left(1 - \left| \frac{x_i - v_{ij}}{d_{ij}} \right|^{b_{2ij}} \right)^{\frac{1}{b_{2ij}}} \\ &\quad - \frac{1}{b_{1ij}} \ln \left| \frac{x_i - v_{ij}}{d_{ij}} \right| \left| \frac{x_i - v_{ij}}{d_{ij}} \right|^{b_{2ij}} \left(1 - \left| \frac{x_i - v_{ij}}{d_{ij}} \right|^{b_{2ij}} \right)^{\frac{1}{b_{2ij}} - 1} \end{aligned} \quad (7.60)$$

where $v_{ij} - d_{ij} < x_i < v_{ij} + d_{ij}$

$$\frac{\partial \bar{\mu}_{ij}}{\partial d_{ij}} = \frac{1}{|d_{ij}|^2} \text{sign}(d_{ij}) |x_i - v_{ij}| \left| \frac{x_i - v_{ij}}{d_{ij}} \right|^{b_{1ij} - 1} \left(1 - \left| \frac{x_i - v_{ij}}{d_{ij}} \right|^{b_{1ij}} \right)^{\frac{1}{b_{1ij}} - 1} \quad (7.61)$$

where $v_{ij} - d_{ij} < x_i < v_{ij} + d_{ij}$

$$\frac{\partial \underline{\mu}_{ij}}{\partial d_{ij}} = \frac{1}{|d_{ij}|^2} \text{sign}(d_{ij}) |x_i - v_{ij}| \left| \frac{x_i - v_{ij}}{d_{ij}} \right|^{b_{2ij} - 1} \left(1 - \left| \frac{x_i - v_{ij}}{d_{ij}} \right|^{b_{2ij}} \right)^{\frac{1}{b_{2ij}} - 1} \quad (7.62)$$

where $v_{ij} - d_{ij} < x_i < v_{ij} + d_{ij}$

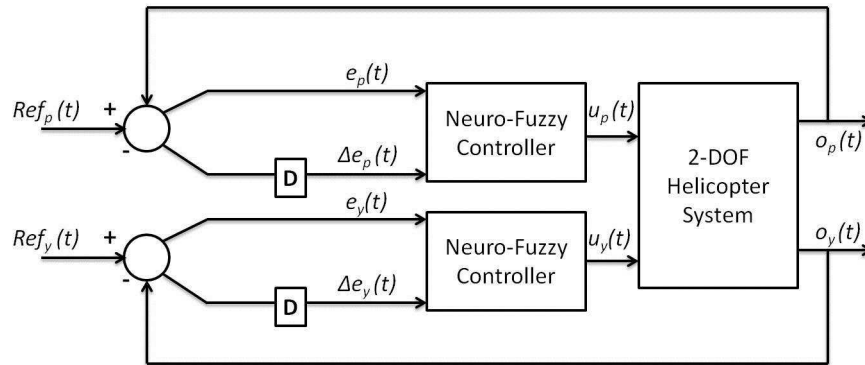


Figure 7.19. The block diagram of the system.

7.5.2. Simulation Results

The position tracking of a 2-DOF helicopter is realized through interval type-2 neuro-fuzzy system with recursive fuzzy c-means clustering algorithm with elliptical membership functions [72]. The block diagram of the system is given in Figure 7.19. 2-DOF helicopter is a coupled non-linear MIMO (multi-input-multi-output) system. For each axis; the pitch and the yaw axes, an interval type-2 neuro-fuzzy system with elliptical membership functions is designed. The inputs for the each controller are the error (e) and the derivative of the error (Δe). Two elliptical membership functions are used for each input and they are initialized randomly. The center of the membership functions are determined by recursive fuzzy c-means clustering algorithm. The number of clusters determines the number of fuzzy rules used in the neuro-fuzzy system. Gradient based learning approach is used to adapt the width and the width of the uncertainty parameters of the antecedent membership functions and the coefficients at the consequents of the fuzzy rules. The initial values of these parameters are chosen randomly. The learning rate λ is chosen between 0 and 1 and it is adapted according to the magnitude of the error. Its magnitude is increased, when the derivative of the error is negative. It is decreased, when the rate is positive.

Three simulation studies are realized and the obtained the pitch and the yaw trajectory tracking results are given in Figures 7.20-7.22. In the third application, a small step disturbance with a 0.1rad magnitude is applied between the *20th* and *20.5th* seconds. The final membership functions obtained for the pitch and the yaw axes in

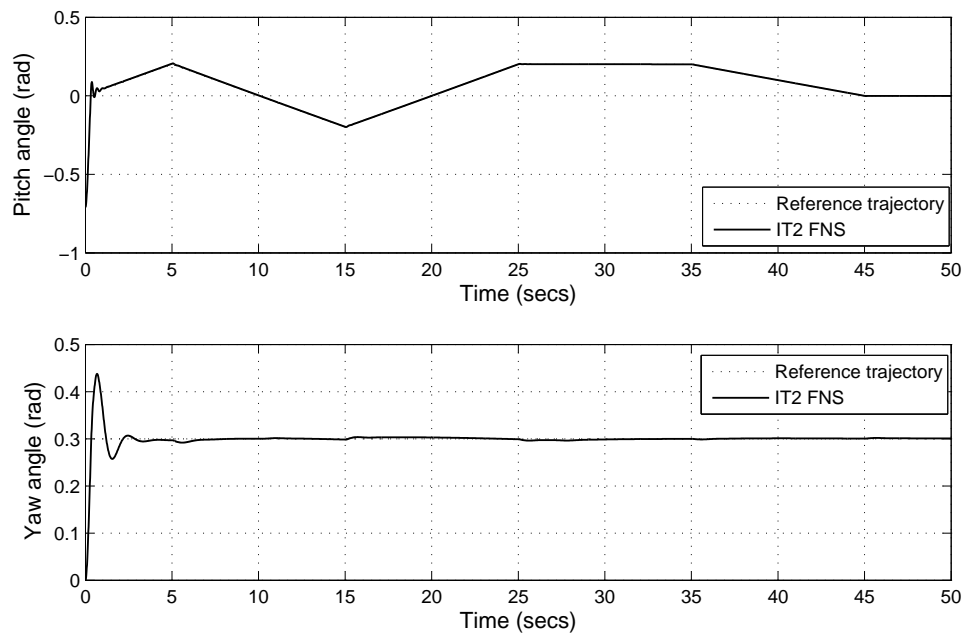


Figure 7.20. First simulation study, changing reference trajectory for the pitch axis and step reference trajectory for the yaw axis of a 2-DOF helicopter.

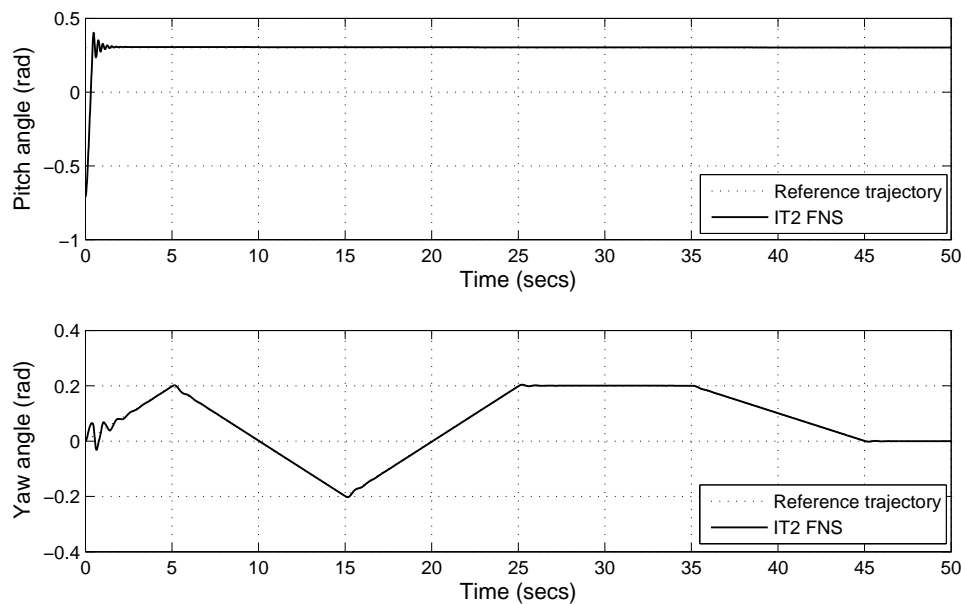


Figure 7.21. Second simulation study, step reference trajectory for the pitch axis and changing reference trajectory for the yaw axis of a 2-DOF helicopter.

the third application are given respectively in Figure 7.23 and 7.24. The root mean square error (RMSE) values for each axes are given in Table 7.5.

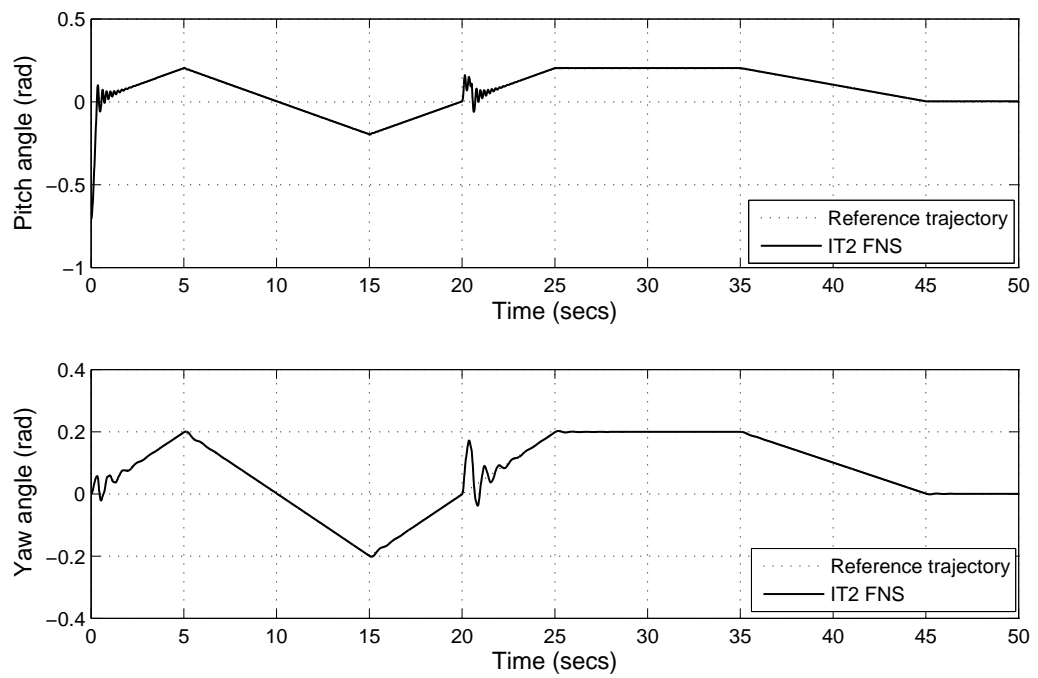


Figure 7.22. Third simulation study, changing reference trajectory with a disturbance for both axes of a 2-DOF helicopter.

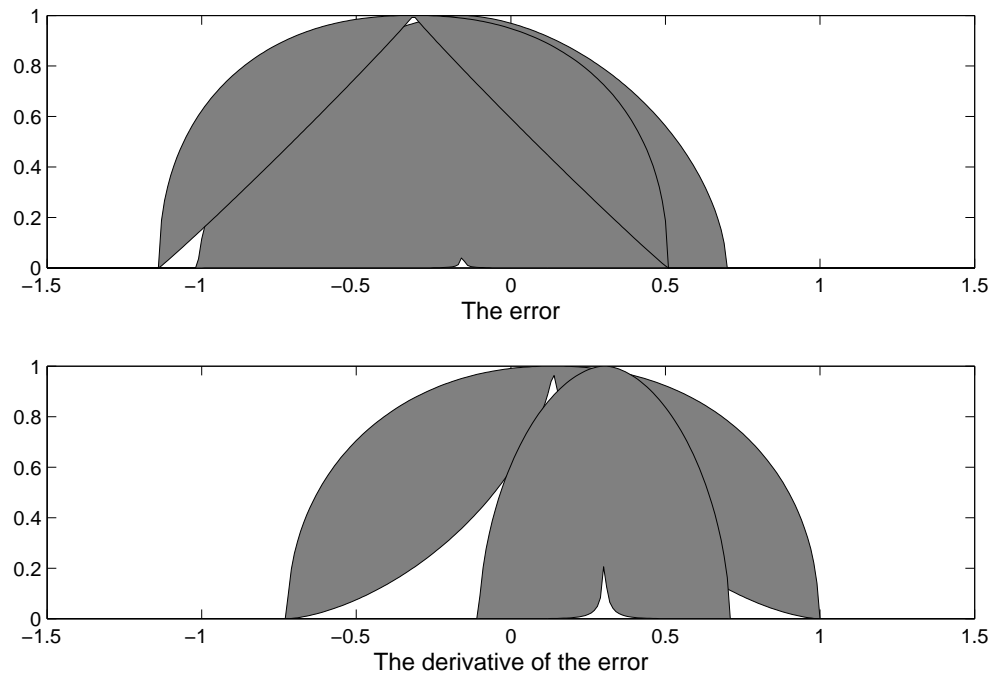


Figure 7.23. The final membership functions of the third simulation study for the pitch axis.

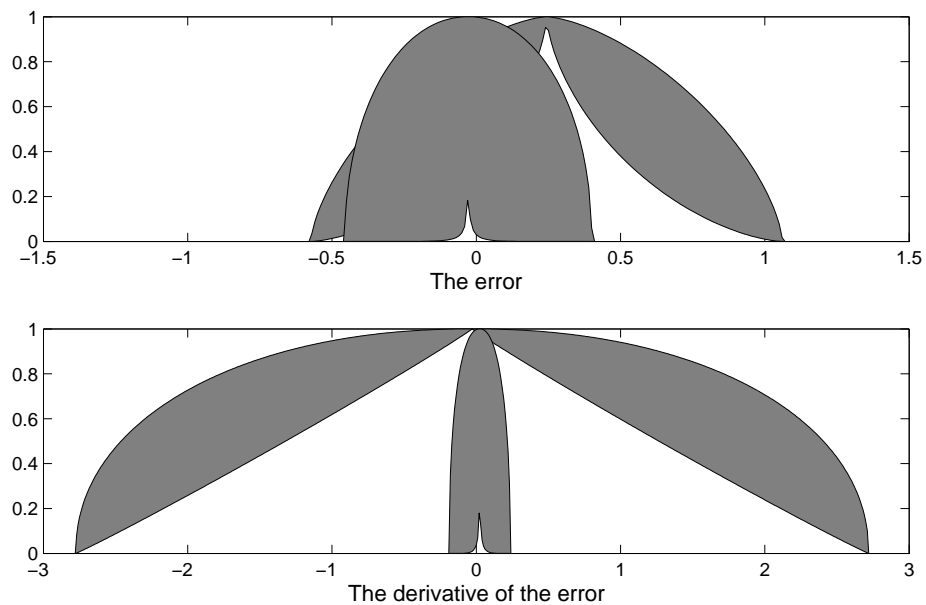


Figure 7.24. The final membership functions of the third simulation study for the yaw axis.

7.5.3. Conclusion

Desired position tracking of a 2-DOF helicopter is performed by interval type-2 neuro-fuzzy system with recursive fuzzy c-means clustering algorithm with elliptical membership functions. The centers of the elliptical membership functions are determined by using recursive fuzzy c-means clustering algorithm. The width and the width of the uncertainty parameters and the parameters at the consequents of the fuzzy rules are obtained by using gradient descent based learning approach. When the results are analyzed in detail, it is seen that the neuro-fuzzy controller is able to track the reference trajectory well even under disturbance.

Table 7.5. The obtained RMSE values.

	RIT2FNS
Simulation 1: RMSE value in <i>rad</i> for pitch axis	0.0385
Simulation 1: RMSE value in <i>rad</i> for yaw axis	0.0216
Simulation 2: RMSE value in <i>rad</i> for pitch axis	0.0612
Simulation 2: RMSE value in <i>rad</i> for yaw axis	0.0055
Simulation 3: RMSE value in <i>rad</i> for pitch axis	0.0395
Simulation 3: RMSE value in <i>rad</i> for yaw axis	0.0098

8. CONCLUSION

The focus of this dissertation is to contribute into the design of interval type-2 neuro-fuzzy system for modeling and control applications. For this aim, first of all, type-1 and type-2 fuzzy logic systems are used with parameterized conjunctors in modeling benchmark nonlinear functions. In these fuzzy logic systems, the linguistic information is obtained by using fuzzy c-means clustering algorithms. The obtained knowledge is kept fixed and the parameters of the parameterized conjunctors are tuned instead of membership functions at the antecedents. It is observed that interval type-2 fuzzy logic system gives better RMSE value especially with noise in the input measurements as compared to type-1 counterpart.

Subsequently, a novel approach to the use of neuro-fuzzy structures, which is interval type-2 neuro-fuzzy system with parameterized conjunctors is proposed and it is used in modeling a benchmark nonlinear function and in slip regulation of a QCM without and with noisy input measurements. The linguistic information about the systems that are considered is obtained by using interval type-2 FCM clustering algorithm. In FCM clustering algorithms, one of the disadvantages is that the number of clusters need to be given in advance. However, the input data sets cannot be always well-separable. Validity indices are used to alleviate this problem. In this study, a validity index is proposed and the result of this validity index is used to determine the number clusters and the number of fuzzy rules of the neuro-fuzzy structure. The performance of the proposed approach is compared with the type-1 neuro-fuzzy system and interval type-2 neuro-fuzzy system without parameterized conjunctors. The results obtained indicate the efficacy of the approach.

Another contribution of this study is the implementation of IT2 FNS with recursive FCM clustering algorithm. Today, most of the processes that have been encountered are time-varying and in the control of these processes a recursive approach is needed. In this part of the study, the centers and the standard deviation values of the membership functions at the antecedents are determined by using recursive fuzzy

c-means clustering algorithm. The designed approach is implemented in trajectory tracking of a 2-DOF helicopter and in speed control of a real-time servo system. The results obtained is compared with type-1 neuro-fuzzy system. It is seen that the interval type-2 fuzzy neural system with recursive FCM clustering algorithm has less RMSE value and converges faster than type-1 fuzzy neural system. Subsequently, the same interval type-2 neuro-fuzzy structure is used with elliptical membership functions. These membership functions have the noise reduction property. The neuro-fuzzy structure is applied in the position tracking of a 2-DOF helicopter and it is seen that it is able to track the reference trajectory well even under noise in the measurements.

APPENDIX A: LABORATORY SETUP: SERVO SYSTEM

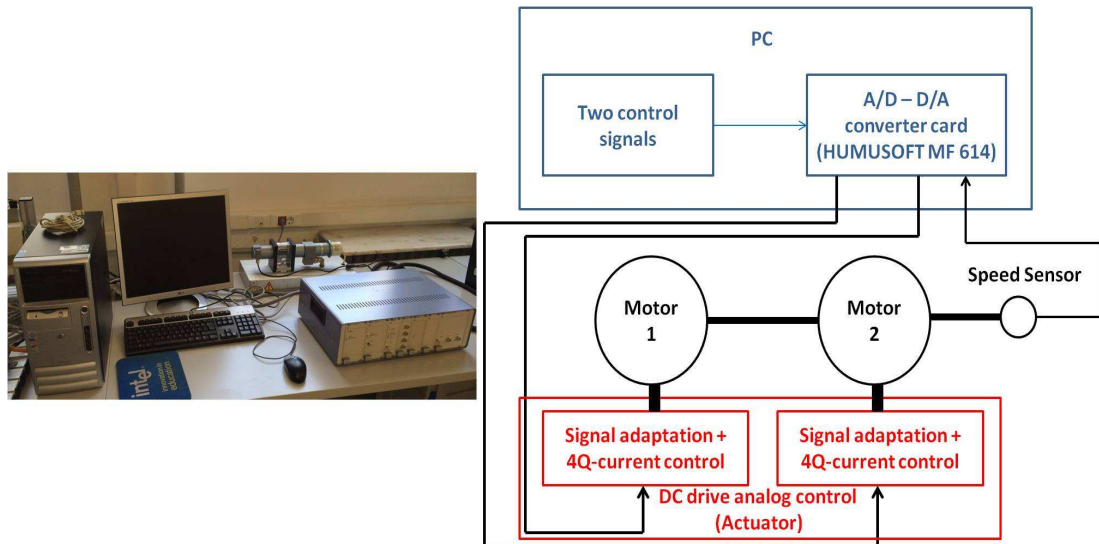


Figure A.1. The schematic view of the hardware station.

The schematic view of the hardware station is seen in Figure A.1. The hardware station is mainly composed of the following elements; plant, actuator unit, PC with the A/D converter card.

The plant consists of two identical permanently excited DC motors M1 and M2. The free shaft of the first motor (M1) is coupled to the second motor (M2) with a mechanical clutch, K. The second motor (M2) is used as a generator to create nonlinear load conditions. The output sensors are; a tacho generator and an incremental encoder.

The actuator unit is composed of four quadrant (4Q) current controllers for each motor, signal adaptation unit, output sensors, and power supplies, (Mains: 220-240 V, 50 Hz, 200 W). The technical data for the actuator with signal adaption unit is given in Table A.2. The direction of the current can be arbitrarily adjusted with the use of 4Q-current controller. As a result, the rotation of the motor is also adjustable in arbitrary directions [70] and [73].

The designed algorithm is deployed for the speed control of the DC motor and it is digitally implemented by using an A/D converter card, namely HUMUSOFT MF

614 [74]. PC is connected to the real-time servo system by this card. The input/output features of the Humusoft MF614 are given in the following Table A.1 [73].

Table A.1. The input/output features of the Humusoft MF614.

Inputs	Outputs
3 sensor signals ± 10 V at 12 Bit A/D converter for tacho voltage and current monitors	2 control signals for the servo amplifiers ± 10 V from 12 Bit D/A-converter
Input for 4Q-incremental encoder signal	Digital enable/disable for servo amplifiers

This card is used for standard data acquisition and control applications. It is compatible with Real-Time Workshop for MATLAB[®]. This Real-Time Workshop for MATLAB[®] gives ability the designer to deploy a control algorithm using MATLAB/Simulink. It converts Simulink models into C code. Subsequently, the code is compiled and an executable code is created with .rwd extension and it is implemented in real-time.

Table A.2. The technical data for the actuator with signal adaption unit.

	Description	Value
Inputs servo amplifiers	Supply voltages	$\pm 35 V, 50 W$
	Control signal	$\pm 10 V (0.23 A/V)$
Outputs servo amplifiers	Armature current for the motor/generator	max. $\pm 2.0 A (\pm 8.0 A, 10 ms)$
	Current monitor	$0.2 V/A$
Inputs signal adaption unit	2 control signals, range	$\pm 10 V (*)$
	Servo amplifier enabled/disabled	
	Speed	$5 V/1000 rpm, V=0.5$
	Monitor of motor current	$0.2 V/A, V=22.0$
	Monitor of generator current	$0.2 V/A, V=22.0$
Outputs signal adaption unit	2 control signals range	$\pm 10 V$
	Speed	$2.5 V/1000 rpm, \text{max. } \pm 10 V (*)$
	Motor current	$2.0 V/A, \text{max. } \pm 10 V (*)$
	Generator current	$4.4 V/A, \text{max. } \pm 10 V (*)$

(*) = Measurement output at the front

APPENDIX B: PUBLICATIONS RELATED TO THE THESIS

In the course of the PhD studies, the following papers have been published, submitted, or presented:

- (i) Aras, A.C. and O. Kaynak, “Interval Type-2 Fuzzy Neural System Based Control with Recursive Fuzzy C-Means Clustering”, *International Journal of Fuzzy Systems*, accepted for publication, 2014.
- (ii) Aras, A.C. and O. Kaynak, “Fuzzy Interval Tsk Type-2 Modeling with Parameterized Conjunctors,” *Asian Journal of Control*, accepted for publication, 2014.
- (iii) Aras, A.C. and O. Kaynak, “Position Tracking Control of a 2-DOF Helicopter based on Interval Type-2 Neuro-Fuzzy System with Elliptical Membership Functions”, *the 40th Annual Conference of the IEEE Industrial Electronics Society, IECON 2014*, 2014, submitted.
- (iv) Aras, A.C. and O. Kaynak, “Trajectory Tracking of a 2-DOF Helicopter System using Neuro-Fuzzy System with Parameterized Conjunctors”, *2014 IEEE/ASME International Conference on Advanced Intelligent Mechatronics*, 2014, accepted.
- (v) Aras, A.C., O. Kaynak, and I.Z. Batyrshin, “Nonlinear Function Approximation based on Fuzzy Algorithms with Parameterized Conjunctors,” *IEEE International Conference on Mechatronics, ICM 2013*, pp. 81-86, 2013.
- (vi) Aras, A.C., O. Kaynak, and R. Abiyev, “Slip Control of a Quarter Car Model Based on Type-1 Fuzzy Neural System with Parameterized Conjunctions,” *the 38th Annual Conference of the IEEE Industrial Electronics Society, IECON 2012*, pp. 2488-2493, 2012.
- (vii) Kayacan, E., Y. Oniz, A.C. Aras, O. Kaynak, and R. Abiyev, “A Servo System Control with Time-Varying and Nonlinear Load Conditions Using Type-2 TSK Fuzzy Neural System,” *Applied Soft Computing*, Vol. 11, pp. 5735–5744, 2011.
- (viii) Oniz Y., A.C. Aras, O. Kaynak, and R. Abiyev, “Experimental Evaluation of a Type-2 Fuzzy Control Algorithm on an Anti-Lock Braking System,” *the 37th*

Annual Conference of the IEEE Industrial Electronics Society, IECON 2011, pp. 564 - 568, 2011.

- (ix) Aras, A.C., Y. Oniz, O. Kaynak, and R. Abiyev, "Type-1 and Type-2 Fuzzy Control of an Anti-Lock Breaking System (ABS) and Evaluation of Its Performances," *the 8th International Conference on Informatics in Control, Automation and Robotics, ICINCO*, pp. 503-508, 2011.
- (x) Oniz Y., E. Kayacan, A.C. Aras, O. Kaynak, and R. Abiyev, "A Servo System Control with Time-Varying Load Using Type-2 Fuzzy Neural System," *Proceedings of the 36th Annual Conference on IEEE Industrial Electronics Society, IECON 2010*, pp. 35-40, 2010.
- (xi) Aras, A.C., E. Kayacan, Y. Oniz, O. Kaynak, and R. Abiyev, "An Adaptive Neuro-Fuzzy Architecture for Intelligent Control of a Servo System and Its Experimental Evaluation," *Proceedings of the IEEE International Symposium on Industrial Electronics*, pp. 68-73, 2010.

REFERENCES

1. Zadeh, L. A., "Soft Computing and Fuzzy Logic," *IEEE Software*, Vol. 11, No. 6, pp. 48-56, 1994.
2. Chu, T.-C. and P. Charnsethikul, "Ordering Alternatives under Fuzzy Multiple Criteria Decision Making via a Fuzzy Number Dominance based Ranking Approach," *International Journal of Fuzzy Systems*, Vol. 15, No. 3, pp. 263-273, 2013.
3. Aras, A.C., O. Kaynak, and I. Batyrshin, "A Comparison of Fuzzy Methods for Modeling," *Proceedings of 34th Annual Conference of IEEE Industrial Electronics Conference IECON 2008*, pp. 43-48, 2008.
4. Wang, H. and H. Gu, "A Fuzzy Clustering Method for Generating Fuzzy Models," *Asian Journal of Control*, Vol. 10, No. 6, pp. 687-697, 2008.
5. Cao, H., G. Si, Y. Zhang, X. Ma, and J. Wang, "Load Control of Ball Mill by a High Precision Sampling Fuzzy Logic Controller with Self-Optimizing," *Asian Journal of Control*, Vol. 10, No. 6, pp. 621-631, 2008.
6. Al-Hadithi, B.M., A. Jiménez, and F. Matia, "Variable Structure Control with Chattering Reduction of a Generalized T-S Model," *Asian Journal of Control*, Vol. 15, No. 1, pp. 155-168, 2013.
7. Al-Gallaf, E. A., "Clustered based Takagi-Sugeno Neuro-Fuzzy Modeling of a Multivariable Nonlinear Dynamic System," *Asian Journal of Control*, Vol. 7, No. 2, pp. 163-176, 2005.
8. Ma, T.-T., "A Direct Control Scheme based on Recurrent Fuzzy Neural Networks for the UPFC Series Branch," *Asian Journal of Control*, Vol. 11, No. 6, pp. 657-668, 2009.

9. Atanassov, K. T., "Intuitionistic Fuzzy Sets Past, Present and Future," *EUSFLAT 2003 Proceedings*, pp. 12-19, 2003.
10. Liang, Y.-W., C.-C. Chen, and S. Sheng-Dong Xu, "Study of Reliable Design Using T-S Fuzzy Modeling and Integral Sliding Mode Control Schemes," *International Journal of Fuzzy Systems*, Vol. 15, No. 2, pp. 233-243, 2013.
11. Chang, W.-J., P.-H. Chen, and C.-T. Yang, "Robust Fuzzy Congestion Control of TCP/AQM Router via Perturbed Takagi-Sugeno Fuzzy Models," *International Journal of Fuzzy Systems*, Vol. 15, No. 2, pp. 203-213, 2013.
12. Zdesar, A., D. Dovzan, and I. Skrjanc, "Self-Tuning of 2 DOF Control based on Evolving Fuzzy Model," *Applied Soft Computing*, Vol. 19, pp. 403-418, 2014.
13. Abiyev, R., O. Kaynak, and, E. Kayacan, "A Type-2 Fuzzy Wavelet Neural Network for System Identification and Control," *Journal of the Franklin Institute*, Vol. 350, No. 7, pp. 1658-1685, 2013.
14. Wang, C.-H. and K.-N. Hung, "Intelligent Adaptive Law for Missile Guidance Using Fuzzy Neural Networks," *International Journal of Fuzzy Systems*, Vol. 15, No. 2, pp. 182-191, 2013.
15. Mon, Y.-J. and C.-M. Lin, "Supervisory Fuzzy Gaussian Neural Network Design for Mobile Robot Path Control," *International Journal of Fuzzy Systems*, Vol. 15, No. 2, pp. 142-148, 2013.
16. Mendel, J. M., *Uncertain Rule-Based Fuzzy Logic Systems: Introduction and New Directions*, Upper Saddle River, NJ: Prentice Hall, 2001.
17. Liang, Q. and J. M. Mendel, "An Introduction to Type-2 TSK Fuzzy Logic Systems," *IEEE International Fuzzy Systems Conference Proceedings (Volume:3)*, pp. 1534-1539, 1999.

18. Ren, Q., M. Balazinski, and L. Baron, "Type-2 TSK Fuzzy Logic System and Its Type-1 Counterpart," *International Journal of Computer Applications (0975-8887)*, Vol. 20, No. 6, pp. 8-13, 2011.
19. Fadali, M. S., S. Jafarzadeh, and A. Nafeh, "Fuzzy TSK Approximation Using Type-2 Fuzzy Logic Systems and Its Application to Modeling a Photovoltaic Array," *American Control Conference (ACC)*, pp. 6454-6459, 2010.
20. Jafarzadeh, S., M. S. Fadali, and C.Y. Evrenosoglu, "Solar Power Prediction Using Interval Type-2 TSK Modeling," *IEEE Transactions on Sustainable Energy*, Vol. 4, No. 2, pp. 333-339, 2013.
21. Lee, C.-H., F.-Y. Chang, and C.-M. Lin, "On-Line Adaptive Interval Type-2 Fuzzy Controller Design via Stable SPSA Learning Mechanism," *International Journal of Fuzzy Systems*, Vol. 14, No. 4, pp. 489-500, 2012.
22. Kayacan, E., Y. Oniz, A.C. Aras, O. Kaynak and R. Abiyev, "A Servo System Control with Time-Varying and Nonlinear Load Conditions Using Type-2 TSK Fuzzy Neural System," *Applied Soft Computing*, Vol. 11, No. 8, pp. 5735-5744, 2011.
23. Wang, L., Z. Liu, Y. Zhang, C. L. P. Chen, and X. Chen, "Type-2 Fuzzy Logic Controller Using SRUKF-based State Estimations for Biped Walking Robots," *International Journal of Fuzzy Systems*, Vol. 15, No. 4, pp. 423-434, 2013.
24. Jang, J. -S. R., C.-T. Sun, and E. Mizutani, *Neuro-Fuzzy and Soft Computing: A Computational Approach to Learning and Machine Intelligence*, Upper Saddle River, NJ: Prentice Hall, 1997.
25. Batyrshin, I. and O. Kaynak, "Parametric Classes of Generalized Conjunction and Disjunction Operations for Fuzzy Modeling," *IEEE Transactions on Fuzzy Systems*, Vol. 7, No. 5, pp. 586-596, 1999.
26. Batyrshin, I., O. Kaynak, and I. Rudas, "Fuzzy Modeling based on Generalized

- Conjunction Operations,” *IEEE Transactions on Fuzzy Systems*, Vol. 10, No. 5, pp. 678-683, 2002.
27. Jain, A. K., R. P. W. Duin, and Jianchang Mao, “Statistical Pattern Recognition: A Review,” *IEEE Transactions on Pattern Analysis and Machine Intelligence*, Vol. 22, No. 1, pp. 4-37, 2000.
28. Meyer-Baese, A., O. Lange, A. Wismueller, and M. K. Hurdal, “Analysis of Dynamic Susceptibility Contrast MRI Time Series based on Unsupervised Clustering Methods,” *IEEE Transactions on Information Technology in Biomedicine*, Vol. 11, No. 5, pp. 563-573, 2007.
29. Vesanto, J. and E. Alhoniemi, “Clustering of the Self-Organizing Map,” *IEEE Transactions on Neural Networks*, Vol. 11, No. 3, pp. 586-600, 2000.
30. Jain, A. K., M. N. Murty, and P. J. Flynn, “Data Clustering: A Review,” *ACM Computing Surveys*, Vol. 31, No. 3, pp. 264-323, 1999.
31. Liao, T. W., “Clustering of Time Series Data-a Survey,” *Pattern Recognition*, Vol. 38, No. 11, pp. 1857-1874, 2005.
32. Xu, Rui and D. Wunsch, “Survey of Clustering Algorithms,” *IEEE Transactions on Neural Networks*, Vol. 16, No. 3, pp. 645-678, 2005.
33. Hwang, C. and F. C.-H. Rhee, “Uncertain Fuzzy Clustering: Interval Type-2 Fuzzy Approach to C-Means,” *IEEE Transactions on Fuzzy Systems*, Vol. 15, No. 1, pp. 107-120, 2007.
34. Wang, W. and Y. Zhang, “On Fuzzy Cluster Validity Indices,” *Fuzzy Sets and Systems*, Vol. 158, No. 19, pp. 2095-2117, 2007.
35. Bezdek, J. C., *Pattern Recognition with Fuzzy Objective Function Algorithms*, Plenum, NY, 1981.

36. Trauwaert, E., "On the Meaning of Dunn's Partition Coefficient for Fuzzy Clusters," *Fuzzy Sets and Systems*, Vol. 25, No. 2, pp. 217-242, 1988.
37. Bezdek, J.C., "Cluster Validity with Fuzzy Sets," *Journal of Cybernetics and Systems*, Vol. 3, No. 3, pp. 58-73, 1974.
38. Bezdek, J.C., "Numerical Taxonomy with Fuzzy Sets," *Journal of Mathematical Biology*, Vol. 1, pp. 57-71, 1974.
39. Xie, X. L. and G. Beni, "A Validity Measure for Fuzzy Clustering," *IEEE Transactions Pattern Analysis and Machine Intelligence*, Vol. 13, No. 8, pp. 841-847, 1991.
40. Fukuyama, Y. and M. Sugeno, "A New Method of Choosing the Number of Clusters for the Fuzzy C-Means Method," *Proceedings of Fifth Fuzzy Systems Symp.*, pp. 247-250, 1989.
41. Pakhira, M.K., S. Bandyopadhyay, and U. Maulik, "Validity Index for Crisp and Fuzzy Clusters," *Pattern Recognition*, Vol. 37, No. 3, pp. 487-501, 2004.
42. Dovzan, D. and I. Skrjanc, "Recursive Fuzzy C-Means Clustering for Recursive Fuzzy Identification of Time-Varying Processes," *ISA Transactions*, Vol. 50, pp. 159-169, 2011.
43. Liang, Q. and J. M. Mendel, "Interval Type-2 Fuzzy Logic Systems: Theory and Design", *IEEE Transactions on Fuzzy Systems*, Vol. 8, No. 5, pp. 535-550, 2000.
44. Hagrass, H., "Type-2 FLCs: A New Generation of Fuzzy Controllers", *IEEE Computational Intelligence Magazine*, Vol. 2, No. 1, pp. 30-43, 2007.
45. Aras, A.C., "A Comparison of Fuzzy Methods for Modeling", *MS. Thesis, Bogazici University*, 2008.
46. Mendel, J.M. and R.I.B. John, "Type-2 Fuzzy Sets Made Simple," *IEEE Transac-*

- tions on Fuzzy Systems*, Vol. 10, No. 2, pp. 117-127, 2002.
47. Mendel, J. M., "Type-2 Fuzzy Sets and Systems: An Overview", *IEEE Computational Intelligence Magazine*, Vol. 2, No. 1, pp. 20-29, 2007.
 48. Dunn, J. C., "A Fuzzy Relative of the ISODATA Process and Its Use in Detecting Compact Well Separated Clusters," *Journal of Cybernetics*, Vol. 3, pp. 32-57, 1973.
 49. Choi, B.-I. and F. C.-H. Rhee, "Interval Type-2 Fuzzy Membership Function Generation Methods for Pattern Recognition," *Information Sciences*, Vol. 179, No. 13, pp. 2102-2122, 2009.
 50. Liang, Q. and J. M. Mendel, "Equalization of Nonlinear Time-Varying Channels Using Type-2 Fuzzy Adaptive Filters," *IEEE Transactions on Fuzzy Systems*, Vol. 8, No. 5, pp. 551-563, 2000.
 51. Biglarbegan, M., W. W. Melek and J. M. Mendel, "On the Stability of Interval Type-2 TSK Fuzzy Logic Control Systems," *IEEE Transactions on Systems, Man, and Cybernetics, Part B: Cybernetics*, Vol. 40, No. 3, pp. 798-818, 2010.
 52. Aras, A.C., O. Kaynak, and I.Z. Batyrshin, "Nonlinear Function Approximation based on Fuzzy Algorithms with Parameterized Conjunctors," *IEEE International Conference on Mechatronics, ICM 2013*, pp. 81-86, February, 2013.
 53. Weijun li and Z. Liu, "A Method of SVM with Normalization in Intrusion Detection," *Procedia Environmental Sciences*, Vol. 11, Part A, pp. 256-262, 2011.
 54. Aras, A.C. and O. Kaynak, "Fuzzy Interval TSK Type-2 Modeling with Parameterized Conjunctors," *Asian Journal of Control*, *accepted for publication*, 2014.
 55. Frank, A. and A. Asuncion, "*UCI Machine Learning Repository* [<http://archive.ics.uci.edu/ml>]," Irvine, CA: University of California, School of

Information and Computer Science.

56. Abiyev, R. and O. Kaynak, "Fuzzy Wavelet Neural Networks for Identification and Control of Dynamic Plants-A Novel Structure and A Comparative Study," *IEEE Transactions on Industrial Electronics*, Vol. 55, No. 8, pp. 3133-3140, 2008.
57. Johansen, T.A., I. Petersen, J. Kalkkuhl, and J. Ludemann, "Gain-Scheduled Wheel Slip Control in Automotive Brake Systems," *IEEE Transactions on Control Systems Technology*, Vol. 11, No. 6, pp. 799- 811, 2003.
58. Aras, A.C., O. Kaynak, and R. Abiyev, "Slip Control of a Quarter Car Model based on Type-1 Fuzzy Neural System with Parameterized Conjunctions," *IECON 2012 - 38th Annual Conference on IEEE Industrial Electronics Society*, pp. 2488-2493, 2012.
59. Burckhardt, M., *ABS und ASR, Sicherheitsrelevantes, Radschlupf-Regel System*, Lecture Scriptum, University of Braunschweig, Germany, 1987.
60. Castro, J. L., "Fuzzy Logic Controllers Are Universal Approximators," *IEEE Transactions on SMC*, Vol. 25, No.4, pp. 629-635, 1995.
61. Mendel, J.M. and Hongwei Wu, "Type-2 Fuzzistics for Symmetric Interval Type-2 Fuzzy Sets: Part 1, Forward Problems," *IEEE Transactions on Fuzzy Systems*, Vol. 14, No. 6, pp. 781-792, 2006.
62. Wu, D., "Approaches for Reducing the Computational Cost of Interval Type-2 Fuzzy Logic Systems: Overview and Comparisons," *IEEE Transactions on Fuzzy Systems*, Vol. 21, No. 1, pp. 80-99, 2013.
63. Hernandez-Gonzalez, M., A.Y. Alanis, E.A. Hernandez-Vargas, "Decentralized Discrete-Time Neural Control for a Quanser 2-DOF Helicopter," *Applied Soft Computing*, Vol. 12, No. 8, pp. 2462-2469, 2012.

64. Jahed, M. and M. Farrokhi, "Robust Adaptive Fuzzy Control of Twin Rotor MIMO System," *Soft Computing*, Vol. 17, No. 10, pp. 1847-1860, 2013.
65. Tao, C.-W., J.-S. Taur, Y.-H. Chang, and C.-W. Chang, "A Novel Fuzzy-Sliding and Fuzzy-Integral-Sliding Controller for the Twin-Rotor Multi-Input-Multi-Output System," *IEEE Transactions on Fuzzy Systems*, Vol. 18, No. 5, pp. 893-905, 2010.
66. Quanser Inc., Quanser 2-DOF Helicopter Manual, *Tech. rep.*, Quanser 2010.
67. Aras, A.C. and O. Kaynak, "Interval Type-2 Fuzzy Neural System Based Control with Recursive Fuzzy C-Means Clustering", *International Journal of Fuzzy Systems*, *accepted for publication*, 2014.
68. Rubaai, A. and P. Young, "EKF-Based PI-/PD-Like Fuzzy-Neural-Network Controller for Brushless Drives," *IEEE Transactions on Industry Applications*, Vol. 47, No. 6, pp. 2391-2401, 2011.
69. Hsu, C.-F., "Intelligent Tracking Control of a DC motor Driver Using Self-Organizing TSK-Type Fuzzy Neural Networks," *Nonlinear Dynamics*, Vol. 67, No. 1, pp. 587-600, 2012.
70. AMIRACorp., DR300 Laboratory Setup Speed Control with Variable Load, *Tech. rep.*, AMIRA 2000.
71. Khanesar, M.A., E. Kayacan, M. Teshnehlab, and O. Kaynak, "Analysis of the Noise Reduction Property of Type-2 Fuzzy Logic Systems Using a Novel Type-2 Membership Function," *IEEE Transactions on Systems, Man, and Cybernetics, Part B: Cybernetics*, Vol. 41, No. 5, pp. 1395-1406, 2011.
72. Aras, A.C. and O. Kaynak, "Position Tracking Control of a 2-DOF Helicopter based on Interval Type-2 Neuro-Fuzzy System with Elliptical Membership Functions", *The 40th Annual Conference of the IEEE Industrial Electronics Society, IECON 2014*, 2014, submitted.

73. AMIRA, *DR300 Speed Control with Variable Load*, Catalogue Amira, 2004.
74. HUMUSOFT, MF 614 Multifunction I/O Card, *User's Manual*, HUMUSOFT 2002.